

**Geochemical Modelling
in the Near-Field of a
HLW Repository in a
High-Saline Environment**

Geochemical Modelling in the Near-Field of a HLW Repository in a High-Saline Environment

Helge Moog
Ulrich Noseck
Sven Hagemann
Jens Wolf
Dieter Buhmann

September 2018

Remark:

This R&D report was prepared under funding reference No. 02E10719 and No. 02E9954 of the Federal Ministry of Economics and Energy (BMWi).

The work was conducted by the Gesellschaft für Anlagen- und Reaktorsicherheit (GRS) gGmbH.

The authors are responsible for the content of the report.

Keywords:

ChemApp, Geochemical modelling, HLW Repository, Near Field, Radionuclide Solubility, Salt Rock

Preface

The overall objective of the R&D projects ISIBEL and ISIBEL-II was to summarise the state of the art in disposal of heat-generating radioactive waste in salt formations and to evaluate whether a demonstration of technical feasibility and repository safety was possible. For the first time, a concept that took full credit of the favourable properties of salt formations, reflecting the concept of safe containment, was developed and tested. Geochemical modelling is an important input into the development of a comprehensive safety case for a waste repository. Based on laboratory experiments it provides the solubility limits or concentration limits of every considered element as the major parameter to represent its mobility in the geochemical environment after mobilization. In order to be conservative, this parameter should be derived from the maximum expected concentration of the considered element. In order to demonstrate conservatism, a key objective of the safety assessment is to obtain a thorough knowledge of the geochemical processes, especially in the near field. For a high saline environment a dataset of solubilities for the long-term safety analyses for a repository for heat-generating waste was documented in the long-term safety assessment "Sicherheitsanalyse Mischkonzept (SAM, /BUH 91/)". Significant progress in the development of numerical tools, its underlying databases and their application for geochemical modelling has been made in the last 25 years. Dozens of research projects were carried out in this period improving the thermodynamic databases. What is lacking is a comprehensive analysis of the expected species in a high-saline environment and the maximum expected concentration of the relevant radionuclides for the long-term safety. This report is a fundamental part for this kind of analysis summarizing available thermodynamic data and assessing geochemical calculations performed at GRS. Due to the high complexity of the geochemistry in a repository the work described in this report cannot give the comprehensive picture but intends to start a process aiming at an appropriate set of solubility data for high saline environments. According to the envisaged time frame of the site selection process in Germany /KOM 16/ this process has to be initiated immediately.

Contents

1	Introduction.....	1
2	Thermodynamic framework	5
3	Fundamental requirements for geochemical modelling	9
3.1	Relevant Elements.....	9
3.1.1	Radionuclides contributing to calculated dose	10
3.1.2	Chemical elements determining the geochemical environment.....	12
3.2	Expected solutions in a repository in salt	17
3.3	Thermodynamic databases.....	21
3.3.1	The seven-component seawater system.....	21
3.3.2	Geotechnical materials	22
3.3.3	THEREDA	22
3.4	Geochemical codes	23
3.4.1	EQ3/6	23
3.4.2	Geochemist's Workbench	24
3.4.3	ChemApp	24
3.4.4	PHREEQC.....	24
3.4.5	Capabilities and features of geochemical codes	24
4	Evolution of the geochemical conditions	27
4.1	General description.....	27
4.2	Composition of solutions.....	28
4.3	Composition of vitrified waste	28
4.4	Composition of spent fuel	29
4.5	Calculation of the geochemical evolution	30
5	Geochemical conditions and element solubilities	33
5.1	The six-component seawater system.....	33
5.2	Matrix elements	34
5.2.1	Aluminium and Silicon	34

5.2.2	Barium	36
5.2.3	Boron	36
5.2.4	Iron	37
5.2.5	Lithium	39
5.2.6	Phosphorus	40
5.3	Activation and fission products.....	41
5.3.1	Carbon.....	41
5.3.2	Chlorine, Iodine	42
5.3.3	Caesium, Rubidium	43
5.3.4	Molybdenum	44
5.3.5	Nickel.....	46
5.3.6	Niobium	48
5.3.7	Palladium.....	48
5.3.8	Samarium	49
5.3.9	Selenium	50
5.3.10	Strontium	52
5.3.11	Technetium.....	54
5.3.12	Tin	55
5.3.13	Zirconium.....	55
5.4	Actinides and decay products	56
5.4.1	Americium and curium	57
5.4.2	Neptunium	59
5.4.3	Protactinium.....	60
5.4.4	Plutonium	61
5.4.5	Radium	63
5.4.6	Thorium	64
5.4.7	Uranium.....	66
6	Summary and conclusions	69
7	References	75
A	Appendices	91

A 1	Calculation of the composition of model solutions	93
A 2	Pitzer coefficients for actinides and Tc.....	126
	List of Figures	141
	List of Tables	143

1 Introduction

The main focus of the safety concept for a repository for heat-generating radioactive waste in Germany is on the safe containment of the waste within the containment-providing rock zone (CRZ) /BMU 10/, /BUH 08/, /MOE 12/. This rock zone is part of the repository system which, in conjunction with the technical seals, ensures containment of the waste. In order to demonstrate the safe containment in the CRZ, the key elements of the long-term safety assessment are the demonstration of the integrity of the geotechnical barriers (shaft and drift seals in combination with the compacted backfill) and of the geological barrier (in a salt rock e. g. a salt rock formation). By demonstrating the integrity of all these barriers, the safe containment shall be accomplished by preventing intrusion of brine to the waste forms /MOE 12/.

According to the safety concept described in /MOE 12/ the geological barrier has to provide the permanent containment of the radioactive waste. The characteristics of the salt rock within the CRZ are essential for the containment. Thereto the integrity of the salt rock within the CRZ must be ensured, which is governed by the rock properties. Perforations of the geological barrier are inevitable upon mine construction and result in a hydraulic bypass of the geological barrier. Creep processes promoted by visco-plastic-elastic properties of the salt rock will lead eventually to the closure of such mine openings, thus restoring the original properties of the geological barrier. Since this process requires some time, engineered high-performance shaft seals and drift seals will be built, that exhibit dedicated sealing properties immediately upon construction. The remaining mine openings in the emplacement areas are backfilled with crushed salt as a long-term stable material. Due to the compaction of the crushed salt that is driven by the salt creep a very low permeability of the crushed salt will develop with time. Evidence must be provided that the sealing by the compacted backfill material is fully developed at the times, when the performance of the engineered barriers can no longer be demonstrated. The safety concept in salt thus aims at preventing a contact between brines and the emplaced waste.

Owing to the uncertainty in predicting the real evolution of the repository system, plausible scenarios have to be developed. According to the German safety requirements the safety of the repository has to be demonstrated for probable and less probable developments (scenarios) of the site over the demonstration period of 1 million years /BMU 10/. This kind of an analysis implies scenarios of the repository system for which an impairment of the barrier integrity and therefore the development of a pathway for brines to the

waste cannot be excluded a priori /BEU 12/. Such scenarios include processes that describe a contact between brines and emplaced waste and thus the mobilization and migration of radioactive nuclides. The assessment of these processes is a fundamental part of the consequence analysis.

For the analysis of the scenarios, well-advanced integrative models are available for the numerical assessment of the near field and its processes, e. g. the RepoTREND near field model LOPOS /BUH 99/. Basic principle of near field models such as LOPOS is to use the solubility or concentration limits of every considered element as the major parameter to represent its mobility in the geochemical environment after mobilization. In order to be conservative, this parameter should be derived from the maximum expected concentration of the considered element. In order to demonstrate conservatism, a key objective of the safety assessment is to obtain a thorough knowledge of the geochemical processes, especially in the near field. For a repository for HLW this includes an adequate understanding of their long-term behaviour. To model the geochemical environment and to determine solubility limits in the geochemical environment, the following fundamental requirements have to be fulfilled /MOO 15/:

- an assumption on the initial composition of the system under consideration,
- an assumption as to the relevant aqueous (or gaseous) species and solid phases,
- a thermodynamic database which contains thermodynamic data for all relevant aqueous (and gaseous) species and solid phases, and
- a suitable code, which upon input of initial system composition and database calculates its composition at thermodynamic equilibrium.

Conceptually, the definition of geochemical boundary conditions for a particular system (the “input” for the code), the thermodynamic database (implying assumptions as to the aqueous speciation model and the phases, which can be formed), and the geochemical code itself constitute the “model”, which is used to predict the chemical behaviour of a system

This report aims at assessing the existing thermodynamic data needed for a geochemical modelling whose results can be applied in long-term safety assessment for a HLW repository in a high saline environment. Chapter 1 describes the thermodynamic framework needed for the understanding of the further chapters. For the assessment of the concentration limits of radionuclides, it is mandatory to define the system under study,

and the conditions under which the concentration limits are recommended. The concentration limits of the radionuclides will be assessed for the direct environment in the vicinity of spent nuclear fuel and vitrified waste from reprocessing. Chapter 3 describes the fundamental requirements for geochemical modelling summarizing relevant elements and solutions that have to be considered for a HLW repository in salt. It also summarizes existing thermodynamic databases and numerical codes used in geochemical analysis. Chapter 4 describes the boundary conditions for all model calculations for the geochemical evolution in the considered systems. Chapter 5 evaluates the existing database for relevant elements and the results of geochemical modelling of brines in HLW repository system in salt. For all relevant elements an assessment of its database and the consequences for performance assessment are given.

2 Thermodynamic framework

As stated in the introductory section performance assessment for repositories for radioactive waste requires an evaluation of the maximum likely solubility of contaminants in an aqueous solution in the geochemical environment of the repositories near field. A wide variety of chemical reactions can occur in such a multicomponent electrolyte mixture leading to complex solution chemistry. One important aspect of the expected electrolyte systems in a repository's near field in high saline environment is the strong thermodynamic non-ideality due to interionic and intermolecular interactions among the various ionic and molecular species.

Numerical models describing geochemical reactions are based on stoichiometric and thermodynamic equations that consider mass, charge, and energy balances for the components in the system. Whereas the formulation of mass and charge balance is straightforward, the formulation of the energy balance needs some explanations regarding the thermodynamic framework. The calculation of the energy balance is based on the available energy or Gibbs free energy G_i of each component. According to the laws of thermodynamics the Gibbs free energy can be derived from the entropy and the enthalpy of a thermodynamic system. It is a function of pressure p and the temperature T and in a closed system in the state of equilibrium with constant pressure and temperature the change in the Gibbs free energy is zero.

As for every thermodynamic property a standard state G_i^0 can be defined for the Gibbs free energy at specified conditions of temperature, pressure for an infinite dilution:

$$G_i = G_i^0 + G_i^{\text{ex}} \quad (2.1)$$

where

G_i^0 Gibbs free energy of component i at standard state

G_i^{ex} excess Gibbs free energy of component i

The standard state is a continuous function of temperature and pressure, but not of the composition. The standard state for 298.15 K and 1 bar is called reference state. The excess term G_i^{ex} is the departure of the Gibbs free energy from the standard state and thus a function of temperature, pressure and composition. It represents the actual free

energy minus the free energy of an ideal solution of the same composition. This term is related directly to the activity a_i as follows:

$$G_i^{\text{ex}} = RT \ln(a_i) \quad (2.2)$$

where

- R Gas constant
- T temperature
- a_i activity of component i

For a system in equilibrium the free energy balances and G_i equals zero. Equation (2.2) can then be related to the standard state of the Gibbs free energy

$$-G_i^0 = G_i^{\text{ex}} = RT \ln(a_i) \quad (2.3)$$

For a reaction equation with several components a_i equation (2.3) can be written as

$$-\Delta G_R^0 = RT \sum_i \ln(a_i) \quad (2.4)$$

where

- ΔG_R^0 standard state Gibbs free energy for the reaction R

Using the law of mass action equation (2.4) can be formulated as

$$-\Delta G_R^0 = RT \ln(K_R) \quad (2.5)$$

where

- K_R equilibrium constant of reaction R

With equation (2.5) it is possible to calculate equilibrium constants from the standard state Gibbs free energy. It is nevertheless necessary to evaluate the components activities in order to calculate the mass and energy balances and to predict solubility limits of species in an aqueous solution.

The activity of a species depends on its interionic and intermolecular interactions with other species in the solution and is related to the concentration by the activity coefficient:

$$a_i = \gamma_i m_i \quad (2.6)$$

where

- γ_i activity coefficient of component i
- m_i molality of component i

The key to predicting the excess (nonideal) contribution to the thermodynamic properties of species in solution are the activity coefficients. The activity coefficient strongly depends on the salinity of the solution: In infinitely dilute solutions the molality of a species equals its activity. With an increasing salinity, the activity coefficient is decreasing.

Since activity coefficient cannot be directly measured, several theoretical and empirical models have been developed to predict the activity in electrolyte solutions. The most common model is the Debye-Hückel approach /STU 81/:

$$\log \gamma_i = \frac{-Az^2\sqrt{I}}{1+Br_0\sqrt{I}} \quad (2.7)$$

where

- A first Debye-Hückel parameter, see /STU 81/
- B second Debye-Hückel parameter, see /STU 81/
- I ionic strength
- r_0 parameter that represents the distance of closest approach of ions

The Debye-Hückel equation has been successfully applied to aqueous system at low salinities /STU 81/. But some of the assumptions of the Debye-Hückel theory become invalid at high ionic strengths. Since the expected brines in the near field of a repository in salt are of high ionic strengths, the correct determination of the ion's activities is of high importance. For the thermodynamic modelling of high saline solutions Pitzer developed an approach to extend the classical Debye-Hückel formulation for activity coefficients with terms for specific interactions between the species in the system /PAB 87/, /PIT 73a/, /PIT 73b/, /PIT 74a/, /PIT 74b/, /PIT 75/, /PIT 91/. These terms content specific parameters for considered combination of species (Pitzer coefficient). The theory is

based on a semi-empiric equations system for describing the non-ideal behaviour of electrolyte solutions. Pitzer obtained a general expression for the excess free energy of the mixed electrolyte:

$$\frac{G^{ex}}{RT} = W_w[f(I) + \sum_i \sum_j \lambda_{ij}(I)m_i m_j + \sum_i \sum_j \sum_k \mu_{ijk} m_i m_j m_k] \quad (2.8)$$

where

- W_w kilograms of water
- $f(I)$ term related to ionic strength I (Debye-Hückel term)
- $\lambda_{ij}(I)$ term to account for short range interaction between ion pairs
- μ_{ijk} term to account for triple ion interaction at high ionic strengths

Comparing equation (2.8) and equation (2.2) and combining terms relating to single, double and triple ion interactions different expressions can be derived for the activity coefficients of electrolytes, cations, anions and neutral species /PIT 91/.

Pitzer equations include terms for both electrostatic and short-range forces. The Pitzer coefficients can be determined by laboratory experiments. /HAR 84/ developed a set of Pitzer coefficients for the geochemical modelling of the solubility in the system of oceanic salt. The Pitzer theory has been successfully applied to the activity coefficients calculation of many salts of different valences, in aqueous solutions with ionic strength up to near saturation. The determination of Pitzer coefficients is one of the fundamental requirements for the geochemical modelling of high saline solutions.

It should be noted, however, that a perfect thermodynamic equilibrium in nature is rather the exception than the rule. Dissolution and precipitation processes may be governed by kinetic effects resulting in different reaction products than anticipated on the grounds of pure chemical thermodynamics. Metastable solid phase phases may persist even for geologic time frames, and a system may follow different reaction paths depending on system composition and temperature. To lend credit to the predicting potential of geochemical modeling a thermodynamic database must be supplemented by additional experimental evidence from laboratory tests or in-situ-experiments.

3 Fundamental requirements for geochemical modelling

The associated risk of the disposal system depends not only on the quantity of radioactive elements stored in a repository, but also on whether and to what extent these elements can be mobilized. Waste containers and primary waste forms become corroded by high saline water, and radionuclides are leached. New solid reaction products will be formed, which are thermodynamically favoured under given geochemical conditions. These secondary phases may incorporate or otherwise retain a certain quantity of specific radioelements. Other processes like radiolysis, colloid formation, and sorption may also affect radionuclide migration.

3.1 Relevant Elements

Independent of the results of a detailed scenario analysis for a specific site, geochemical reactions for a repository in a saline environment can be divided in four groups (Fig. 3.1):

1. Interaction of deep groundwaters already present in the host rock or intruding from the outside the host rock formation with salt rock minerals yielding high saline solutions,
2. reaction of high saline solutions with technical barrier materials,
3. reaction of high saline solutions with the container materials, e. g. cast iron and
4. reaction of waste matrix materials, e. g. borosilicate glass and mobilisation of radionuclides, generation of secondary minerals.

Secondary reactions of mobilized waste components with the containment, backfill, and seals were not considered.

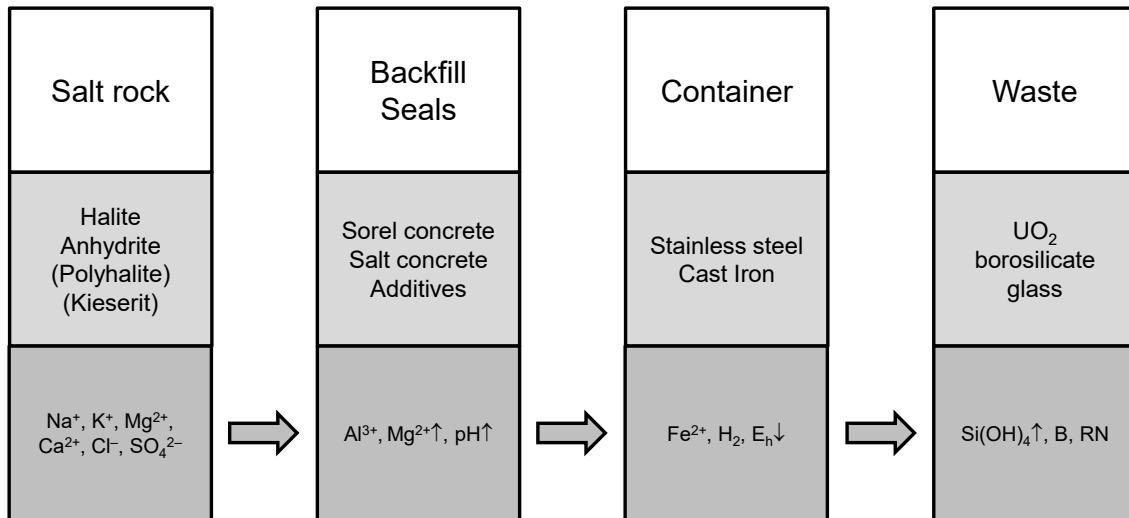


Fig. 3.1 Schematic concept for the evolution of solutions intruding into the emplacement area of a repository for heat-generating waste in salt

Taking these reactions into account the question arises which elements should be considered for the geochemical modelling of the repository's near field. There are two straightforward high-level criteria to determine whether an element is of potential significance:

- Radioisotopes of the element may significantly contribute to the dose as calculated in integrated models for performance assessment.
- The element may influence significantly the geochemical environment or contribute to the retention¹ in the near field of a repository.

3.1.1 Radionuclides contributing to calculated dose

For the long-term safety analysis those radionuclides are relevant, that contribute to the considered safety indicators. According to the German safety requirements this safety indicator is a dose calculated for the biosphere or in the context of the simplified radiological statement at the boundary of the CRZ /BMU 10/. The assessment period for HLW

¹ The term "retention" may refer to enrichment of radionuclides and other hazardous substances on the surface of primary and secondary phases (sorption), co-precipitation, solid solution formation or direct precipitation.

is one million years. Criteria for radionuclides that have to be considered in performance assessment are not specified but at least the following aspects should be considered:

- the radionuclide’s inventory in the considered waste types,
- the half-life, and
- the dose conversion factor.

A selection of radionuclides relevant for performance assessment was carried out for vitrified waste in /HOS 85/. Based on selected radiological criteria the fission and activation products were categorized in four priority classes (Tab. 3.1).

Tab. 3.1 Priority classes of fission and activation products according to /HOS 85/

Priority class	Radionuclides
I	Ni-59, Se-79, Zr-93, Nb-94, Tc-99, Pd-107, Sn-126, I-129, Cs-135
II	C-14, Ni-63, Rb-87, Sr-90, Mo-93, Cs-137, Sm-147, Sm-151
III	Be-10, Cl-36, Cd-113m, Nd-144, Ho-166m
IV	H-3, Ag-108m, Sn-121m, La-138, Eu-152

The actinides disposed with the waste have also to be taken into account. /HOS 85/ screened the four decay chains of the actinides by different radiological criteria taking into account specific effects in the decay chains (Tab. 3.2).

Tab. 3.2 Considered actinides and decay products according to /HOS 85/

Decay series	Radionuclides
Thorium (4n)	U-232, Th-232, U-236, Pu-240, Cm-244, Pu-244, Cm-248
Neptunium (4n+1)	Th-229, U-233, Np-237, Am-241, Pu-241, Cm-245
Uranium (4n+2)	Ra-226, Th-230, U-234, Pu-238, U-238, Pu-242, Am-242m, Cm-246
Americium (4n+3)	Pa-231, U-235, Pu-239, Am-243, Cm-247

In the project SPIN a comprehensive analysis of safety and performance indicators were carried out on an international level /BEC 03/. In order to calculate these indicators as realistic as possible a list of radionuclides that have to be considered in the calculation is provided in /BEC 03/. The list comprises all radionuclides of priority class I and II in Tab. 3.1 and Cl-36 and Ho-166m of priority class III. The only additional listed radionuclide is Ca-41.

Based on the comparison of the analyses in /HOS 85/ and /BEC 03/, it is concluded to consider the following elements as important for geochemical modelling:

- Fission and activation products: Cs, Rb, Sr, Tc, Sn, Sm, Nb, Ni, Se, I, Mo, Cl, C, Pd, and Zr.
- Actinides and decay products: Th, Pa, U, Np, Pu, Am, Cm, Ra.

Besides the radionuclides that are disposed of in a repository for HLW and can contribute to the calculated dose, those elements have to be included in geochemical modelling that have a significant influence on the geochemical environment (chapter 5).

Lead is an end product of three decay chains and was not considered in the calculations, as no long-term relevant radio-isotopes exist. However, the formation of lead might be relevant in terms of chemical toxicity.

3.1.2 Chemical elements determining the geochemical environment

A key parameter of the chemical environment is the hydrogen concentration $p\text{H}^2$. After the beginning of corrosion processes at the surface of containers or barrier materials it is determined by the corrosion process and the presence of solid corrosion phases.

Other important elements form sparingly soluble compounds with a main component of aqueous solution (like sulphate) or particular species able to form complexes with dose-relevant nuclides.

The initial bulk composition of solution and major features like $p\text{H}$ and the overall redox state in a repository are primarily determined by the minerals constituting the host rock and the geotechnical material. However, the genesis of solutions also plays an important role, as the same solution components may be the result of ancient seawater evaporation processes and earlier contact with minerals that are not actually present near the emplacement area. Especially trace elements (e. g. Br, B, Li, Rb, Sr, Fe) as well as potash constituents (Mg, K, SO_4) are often found in concentrations that are not related to the mineral or elemental composition of the host rock.

² $p\text{H}$ refers to the negative logarithm of the hydrogen (H^+) concentration – $\log c\text{H}$, a more useful parameter than the $p\text{H}$ to describe the acidity or alkalinity of concentrated salt solutions

The elements from the salt host rock which are relevant for the geochemical environment are described in Chapter 3.1.2.1 and those from the emplaced geotechnical materials are described in Chapter 3.1.2.2.

3.1.2.1 Salt rock

Salt rock is composed of different minerals (evaporates) originally precipitated from a saturated surface or near-surface brine driven by evaporation. Salt deposits occur in sedimentary basins that are present world-wide often many hundreds of meters thick. The ocean is the primary source of almost all salt deposits. The evaporation of seawater leads to the sedimentation of an evaporitic sequence. Given the standard composition of sea water the expected evaporation cycle can be investigated in laboratory experiments leading to the evaporitic sequence described in many textbooks. Nevertheless, in reality, there is a broad range of hydrological and geological conditions leading to a much higher variety of salt minerals found in natural evaporitic sediments. Dependent on the sea water availability, inflow of other sediments, and temperature regime the evaporitic cycle can become quite complex. As a result of evaporation of a solution metastable mineral phases could develop under manifold conditions. Moreover, interaction of remaining solutions with previously precipitated salt minerals as well as pressure and temperature may transform primarily formed minerals into different mineral compositions.

Evaporation yields a crystallization sequence of various salts, salt hydrates, double salts, and salt phases of higher complexity, e. g. chlorides and sulphates of sodium, potassium, calcium, and magnesium, carbonates of sodium and magnesium either with or without calcium, and nitrates of sodium and potassium. Subordinate in quantity are admixtures of bromides, iodides, borates, and a few other complex salts, such as iron chlorides /SON 84/. A comprehensive overview on minerals of the evaporitic sequence is given in /BRA 71/. Tab. 3.3 gives an overview of the minerals and their chemical composition.

Tab. 3.3 Stable crystallizing salts in the hexary oceanic salt system; after /BRA 71/ and /EUG 80/

Symbol	Mineral name	Composition	Mol weight [g/mol]
a	Anhydrite	CaSO ₄	136.15
An	Antarcticite	CaCl ₂ · 6 H ₂ O	219.08
ap	Aphthitalite ³	K ₃ Na(SO ₄) ₂	332.42
bi	Bischofite	MgCl ₂ · 6 H ₂ O	203.33
bl	Bloedite	Na ₂ Mg(SO ₄) ₂ · 4 H ₂ O	334.51
c	Carnallite	KMgCl ₃ · 6 H ₂ O	277.88
cc	Chlorocalcite	KCaCl ₃	185.54
da	D'Ansite	Na ₂₁ MgCl ₃ (SO ₄) ₁₀	1574.29
e	Epsomite	MgSO ₄ · 7 H ₂ O	246.5
g	Gypsum	CaSO ₄ · 2 H ₂ O	172.18
gb	Glauberite	Na ₂ Ca(SO ₄) ₂	278.21
goe	Goergeyite	K ₂ Ca ₅ (SO ₄) ₆ · H ₂ O	873.03
hx	Hexahydrite	MgSO ₄ · 6 H ₂ O	228.49
k	Kainite	KMgClSO ₄ · 3 H ₂ O	244.48
ks	Kieserite	MgSO ₄ · H ₂ O	138.41
lg	Langbeinite	K ₂ Mg ₂ (SO ₄) ₃	415.04
lh	Leonhardtite	MgSO ₄ · 4 H ₂ O	192.45
le	Leonite	K ₂ Mg(SO ₄) ₂ · 4 H ₂ O	366.71
loe	Loeweite	1/7[Na ₁₂ Mg ₇ (SO ₄) ₁₃ · 15 H ₂ O]	280.76
m	Mirabilite	Na ₂ SO ₄ · 10 H ₂ O	322.22
5h	Pentahydrite	MgSO ₄ · 5 H ₂ O	210.47
p	Polyhalite	Ca ₂ K ₂ Mg(SO ₄) ₄ · 2 H ₂ O	602.98
sh	Schoenite ⁴	K ₂ Mg(SO ₄) ₂ · 6 H ₂ O	420.75
n	Rock salt (Halite)	NaCl	58.45
sy	Sylvite	KCl	74.55
sg	Syngenite	K ₂ Ca(SO ₄) ₂ · H ₂ O	328.43
ta	Tachydrite	CaMg ₂ Cl ₆ · 12 H ₂ O	517.65
t	Thenardite	Na ₂ SO ₄	142.06
vh	Vanthoffite	Na ₂ Mg(SO ₄) ₄	546.57

³ /BRA 71/ uses the old name glaserite (gs)

⁴ Other common name: picromerite

3.1.2.2 Geotechnical materials

In addition to the geological host rock also the emplaced geotechnical materials will impact the potentially inflowing solution. These materials are used for backfilling and sealing, as container material and as waste matrix, which is schematically shown in Fig. 3.1. On its way into the emplacement areas the solution is modified by reactions with concrete and other materials from sealings, iron and other metals from the container and after container failure by reaction with the waste matrix.

In the following the main elements with highest impact on the geochemical conditions are considered.

The elements Si and Al are relevant since they are major constituents of the glass matrix, in cementitious materials and also relevant if other alumino-silicate-minerals are considered. While reaction path calculations with cementitious waste forms were not within the scope of the present study, alumino-silicate-minerals may precipitate as a result of reaction between vitrified waste and solution.

Barium is a minor component in the glass matrix and in SNF. However, it is of importance due to its low solubility in the presence of sulphate, and because of that affecting the concentration of radionuclides like Ra and Sr, which co-precipitate with BaSO_4 .

Boron is also a major component of vitrified nuclear waste and has to be considered in the dissolution reaction of R7T7 (see chapter 4.3). The significance of boron lies with its capability to influence the solution pH, to form tetraborate complexes with actinides /BOR 10/. Due to its rather high solubility, boric acid and borate may become a major component of the solution phase with a potential impact on the activity coefficient of all dissolved species.

Lithium is a minor component of the glass matrix and very mobile. Therefore, it is used as an indicator for the congruent reaction progress of the glass matrix.

Phosphate, also a minor component of the glass matrix has a potential for complex formation and precipitation with actinides.

Iron is a constituent of the glass matrix but it's major source is represented by the container materials. The composition of container materials of a steel cask for HLW and the inner and outer container of a Pollux cask used for spent fuel are listed in Tab. 3.4.

Ferric and ferrous iron (Fe^{3+}/Fe^{2+}) dominate the overall redox state of the nearfield once the corrosion of the containers has started. In a later stage it will be superseded by the couple Fe^{2+}/H_2 , at the time remaining oxygen is consumed.

It is also of relevance with respect to corrosion products, which are formed upon the contact of waste containment and aqueous solution and might provide a sorption barrier for many other cations. Furthermore, steel-based containments contain other elements such as Cr and Mn. While thermodynamic data and even Pitzer coefficients are available /HAG 15/ and the preparation of a thermodynamic database would be possible, these elements were not considered in our calculations.

Tab. 3.4 Selected components in container materials for HLW and Pollux cask in wt.-% /KTA 88/

Element	1.4403 steel ¹	GGG 40.3 ²	15 MnNi 63 ³
Fe	>58.8	>91.5	>96.33
Cr	22.0 – 24.0	<0.1	<0.2
Ni	12.0 – 14.0		0.5 – 0.9
Cu		<1	<0.07
Mo			<0.05
Mn	<2.0	0.1 – 0.6	1.15 – 1.7
Al			0.015 – 0.065
N	0.08		<0.016
P			<0.017
Si	<0.1	2.0 – 3.0	0.15 – 0.37
C	<0.15	3.4 – 3.8	0.1 – 0.2

¹ HLW cask, ² Pollux outer cask, ³ Pollux inner cask

Based on the discussion in Chapter 3.1.2.1 and 3.1.2.2 it is concluded to consider the following additional elements as important for geochemical modelling:

- Salt minerals: Na, K, Ca, Mg, Cl and SO_4 .
- Geotechnical materials: Al, Ba, B, Fe, Li (indicator for reaction progress), PO_4 and Si.

3.2 Expected solutions in a repository in salt

Different types of sediments in the German Zechstein basin may be distinguished with regard to their composition in terms of some stoichiometric defined mineral phases, e. g.: 1. **halite** and **anhydrite**, 2. **polyhalite** and 3. potassium and magnesium minerals such as **carnallite**, **sylvite**, **kainite** and **kieserite** /HER 00/. Solutions that have long been in contact with these salt minerals will be in equilibrium with them. However, the composition of a solution reflects not only the actual mineral phases present, but to some extent also the salt rocks which it was historically exposed to. This is especially true for solutions that are stored in porous anhydrite layers. The composition of naturally occurring salt solutions varies greatly, but some solution types may be identified that are typical for a wide range of situations.

Graphical methods are used to represent possible compositions of solutions in evaporate systems (or seawater system). These methods are based on the Gibbs' phase rule that defines the stability fields of possible phases in a system of several components. The number of components is the number of chemically independent constituents of the system, i.e. the minimum number of independent species necessary to define the composition of all phases of the system. In a phase diagram there is a limited number of points on where all phases coexist in equilibrium. This point is also referred to as an invariant point (IP), because p and T are uniquely specified.

The considered system is a six-component system based on the ions Na^+ , K^+ , Mg^{2+} , Ca^{2+} , Cl^- and SO_4^{2-} . In earlier studies calcium was considered as a less important constituent because of its relatively low concentrations. These studies focused on the Ca-free five-component sea water system /BRA 71/. But it could be proven in several studies that Ca-bearing evaporates can have a significant influence on an evaporitic system. Despite its limitations the five-component system has the advantage that it can be easier illustrated. It is a valuable tool to discuss expected solutions in a repository in salt. Since salt brines are saturated with halite the relationship between the stability fields of the five-component salt system can be illustrated in a Jänecke representation (Fig. 3.2).

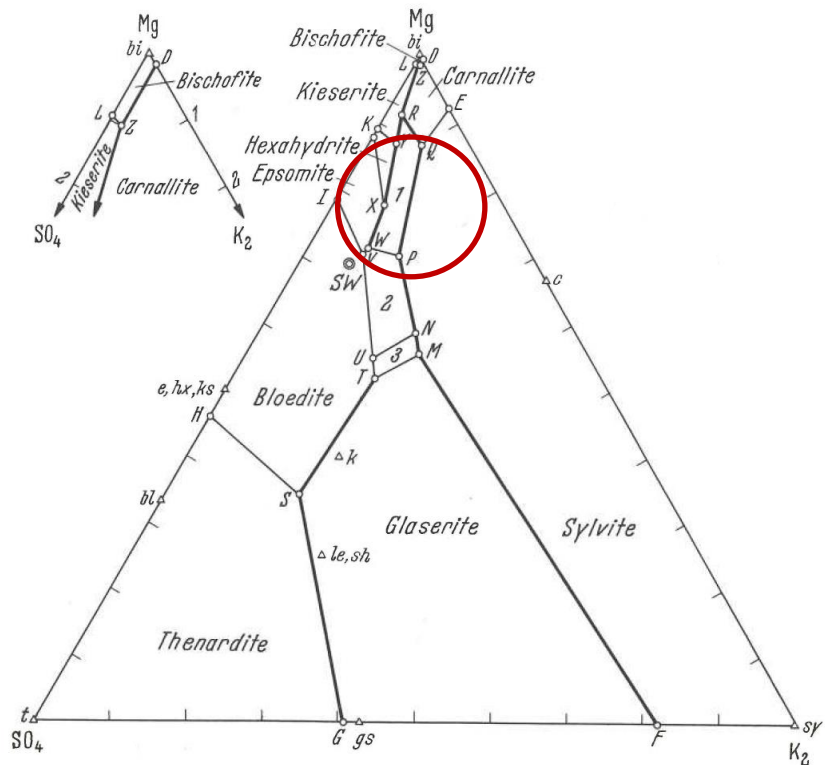


Fig. 3.2 The five-component system NaCl-KCl-MgCl₂-Na₂SO₄-H₂O at 25 °C and 1 bar at NaCl saturation /BRA 71/

Stability fields 1 = kainite + halite, 2 = leonite + halite, 3 = schoenite + halite. Abbreviations of the minerals are explained in Tab. 3.3). Invariant points are explained in Tab. 3.5, SW = seawater). Red circle shows area of composition of most brines found in the German Zechstein formations.

According to /HER 07/ solutions naturally occurring in salt and potash mines may be classified into six types according to their formal content of MgCl₂ (concentration of Mg minus concentration of sulphate) and CaCl₂:

- Type A: Solutions with a MgCl₂ content of more than 400 g/l and a NaCl content below 12 g/l. They are or were in contact with the salt rock carnallite. Depending on its subtype different equilibrium solution result
 - carnallite/ kieserite/ tachhydrite or carnallite/ kieserite/ bischofite: near equilibrium solution Z (Ca system: IP20),
 - carnallite/ kieserite/ kainite: near equilibrium solution R (IP19),
 - carnallite/ sylvite: near equilibrium solution Q (IP21).

- Type B: Solutions with a MgCl_2 content between 320 and 400 g/l and a NaCl content around 19 g/l, resulting from a contact with sylvinitic, kieseritic or polyhalitic hartsalz: between equilibrium solution P and Q.
- Type C: solutions with a MgCl_2 content between 150 and slightly over 320 g/l, The NaCl content may rise up to 100 g/l resulting from langbeinitic hartsalz: between equilibrium solutions M and P.
- Type D: MgCl_2 content below 150 g/l, NaCl content between 100 and 300 g/l, resulting from contact with sylvinitic, anhydritic hartsalz or impoverished hartsalz. Solutions of this type may have been in contact with cap rock solutions. To this group belongs the equilibrium solution IP9 that results from the dissolution of polyhalitic rock salt as well as fluids that are generated if polyhalitic rock salt is heated.
- Type E: Solutions with a varying MgCl_2 content between 320 and 0 g/l with contact cap rock solutions. The initial MgCl_2 concentration is high but will decrease following intensive inflow. The NaCl concentrations typically rises at first (dissolution of NaCl but will decrease afterwards due to admixing of low salinity cap rock water.
- CaCl_2 bearing solutions that are the result of interaction of MgSO_4 brines with calcite or sulphate reducing processes during or after the genesis of the salt formation. Unlike solutions A to E their sulphate concentration is very low

It should be noted that incomplete metamorphosis of salt rocks or mixing of solutions with higher and lower MgCl_2 content may lead to solutions that cannot be directly linked to specific mineral compositions. In /KIE 01/ the composition of potentially occurring solutions were documented in order to have standard solutions for corrosion experiments:

- Solution 1 represents a $\text{NaCl-KCl-MgCl}_2\text{-Na}_2\text{SO}_4$ solution at points Q and R (Q- brine⁵).
- Solution 2 represents a $\text{MgCl}_2\text{-CaCl}_2\text{-(NaCl-KCl)}$ solution (CaCl_2).
- Solution 3 represents a $\text{NaCl-CaSO}_4\text{-(KCl-MgCl}_2)$ solution (Gipshut⁶-solution).

⁵ Most experiments show no significant difference between Q and R brines. Therefore Q-brine is standardly applied as a typical solution in the German Zechstein (IP21 for the six-component system).

⁶ In the calculations performed in this study the Mg and K content of solution 3 was neglected in order to establish a limiting case for a solution with a very low Mg content. Such a solution would be saturated with respect to anhydrite and halite only and is referred to as 'Gipshut' solution, Engl. cap rock solution

Solution 1 and 3 are derived from expected compositions explained above. Solutions with an unexpected high concentration of CaCl₂ (Solution 2) have been observed in mines in the German Zechstein. In opposite to the derivation of solution 1 and 3 the genesis of this solution is ambiguous /HER 00/, /KIE 01/. Solution 2 was therefore not considered in the model calculations described in chapter 4.

Tab. 3.5 Jänecke coordinates of invariant points (IP) in the halite saturated six-component system Na-K-Mg-Ca-SO₄-Cl-H₂O at 25°C and 1 bar /EUG 80/

IP	Mineral phases (see Tab. 3.3)	K ₂	Mg	Ca	SO ₄	a(H ₂ O)	IP (Ca-free)
1	sy + c + p + a	6.17	90.60	0.06	3.18	0.5202	-
2	c + ks + p + a	1.63	91.91	0.01	6.45	0.4569	-
3	ks + hx + p + a	1.19	87.72	0.01	11.08	0.4983	-
4	hx + e + p + a	1.45	83.27	0.02	15.27	0.5675	-
5	e + bl + p + a	1.88	75.04	0.03	23.05	0.6409	-
6	bl + gb + p + a	2.59	72.78	0.04	24.59	0.6659	-
7	bl + gb + ap + p	18.69	40.87	0.03	40.41	0.7080	-
8	ap + gb + sg + p	19.40	40.57	0.03	39.99	0.7085	-
9	gb + sg + p + a	27.49	51.85	0.37	20.29	0.7189	-
10	sy + sg + p + a	31.01	62.18	0.44	6.36	0.6870	-
11	ap + sy + sg + p	25.12	53.39	0.02	21.47	0.6804	-
12	t + ap + bl + gb	18.64	34.25	0.03	47.08	0.7137	S
13	ap + sh + bl + p	17.27	52.75	0.01	29.97	0.6831	T
14	sh + le + bl + p	14.36	58.47	0.01	27.16	0.6693	U
15	bl + le + e + p	8.71	67.83	0.00	23.46	0.6236	V
16	le + e + k + p	8.56	70.70	0.00	20.74	0.6048	W
17	e + hx + k + p	5.01	78.71	0.00	16.28	0.5675	X
18	hx + ks + k + p	2.14	86.61	0.01	11.24	0.4983	Y
19	ks + c + k + p	2.05	90.37	0.01	7.57	0.4683	R
20	bi + ks + c + a	0.19	99.56	0.12	0.14	0.3382	Z
21	k + c + sy + p	5.90	87.52	0.01	6.57	0.5174	Q
22	k + le + sy + p	10.62	71.28	0.00	18.10	0.6064	P
23	le + sh + sy + p	20.92	56.87	0.01	22.20	0.6693	N
24	sh + ap + sy + p	21.76	55.68	0.01	22.55	0.6717	M
25	c + an + sy + a	2.15	6.48	91.37	0.00	0.2053	-
26	b + c + ta + a	0.14	32.79	67.06	0.00	0.1801	-
27	ta + an + c + a	0.26	21.30	78.44	0.00	0.1589	-

In a repository in the post-closure phase the solutions that result from dissolution of salt minerals come into contact with the other components of the repository.

3.3 Thermodynamic databases

Thermodynamic databases contain data that are needed by programs for geochemical modelling for the calculation of chemical equilibria. Depending on the particular geochemical code used these data comprise equilibrium constants or other standard formation data for solid phases, gas components or aqueous species. They may also cover specific ion interaction coefficients in order to allow the calculation of species activity coefficients in saline solutions.

Thermodynamic data in such databases need to be internally consistent and must be appropriate for the geochemical system of interest – that means, they must include those solid phases and solution species that are likely to occur under the conditions of the system under investigation.

3.3.1 The seven-component seawater system

The system of oceanic salts is usually understood as comprising the primary species Na^+ , K^+ , Mg^{2+} , Ca^{2+} , Cl^- , SO_4^{2-} , and HCO_3^- in aqueous solution. The term “oceanic” indicates that this system is of relevance to understand chemical equilibria in a marine environment whose ionic strength requires the use of correction terms for the non-ideal interaction between solutes in aqueous solution. This is an additional requirement for the thermodynamic database. As discussed in chapters 3.1.2.1 and 3.2 in the context of aqueous solutions in rock salt formations (which are evaporites from a marine environment) we have to deal with saturated salt solutions with chloride concentrations ranging up to 6 to 9 M. For the geochemical modelling of high-saline solutions the Pitzer model is frequently used (see chapter 1). The first thermodynamic database published for this system was created by /HAR 84/ and was first implemented for the geochemical code EQ3/6. Implementations for other codes followed. The database was largely adopted and, in some parts, augmented in THEREDA /MOO 15/, see www.thereda.de.

3.3.2 Geotechnical materials

As discussed in chapter 3.1.2.2 plugs and backfills may contain Si- and Al-compounds (bentonite, cementitious materials). Extensive databases exist for them due to the fact, that bentonite and cementitious materials are more or less part of all concepts for nuclear disposal. One example is the database THERMOCHIMIE which is being developed by ANDRA for geochemical processes in argillaceous rock water /GIF 14/. The question if such data are applicable to high-saline conditions as they are encountered in rock salt cannot be answered straightforwardly and must be assessed separately for each system of interest.

The containment may consist of steel (essentially iron with some additions of other elements), Zircalloy rods, spent UO₂ fuel matrix or glass (“vitrified waste”). The waste itself releases primarily actinides from the spent fuel (U, Pu), decay products, fission products, activation products and other waste components. Only those chemical elements are covered in the modelling for which thermodynamic data exist, both for high-saline conditions (THEREDA) and for solutions of groundwater type (NEA thermodynamic database, THERMOCHIME, Nagra/PSI Chemical Thermodynamic Data Base /HUM 02/).

3.3.3 THEREDA

THEREDA is an ongoing joint project among five research institutions, namely

- Surface Processes Division of the Institute of Resource Ecology at the Helmholtz-Zentrum Dresden-Rossendorf (HZDR-IRE);
- Institute for Nuclear Waste Disposal at the Karlsruhe Institute of Technology (KIT-INE);
- Department for Salt Chemistry of the Institute of Inorganic Chemistry at the Technical University of Freiberg (TUBAF);
- AF Consult, Department of Groundwater Protection and Waste Disposal/Switzerland (AFC), meantime replaced by Paul-Scherrer-Institute, Laboratory for Waste Management (PSI-LES);
- Department for Process Analysis of the Final Repository Safety Research Division at the Gesellschaft für Anlagen und Reaktorsicherheit (GRS).

The main objective is to create a common thermodynamic database aiming at the calculation of solubilities relevant for nuclear waste disposal in high saline environments, which is mutually accepted by the five contributing partners. The primary product of the project is the provision for ready-to-use parameter files for altogether four supported geochemical codes, namely PHREEQC, Geochemist's Workbench, EQ3/6, and CHEMAPP. These parameter files are available free of charge for registered users from the THEREDA website⁷.

3.4 Geochemical codes

One of the fundamental requirements of geochemical modelling is the calculation of the speciation in the aqueous phase. The main assumption is local thermodynamic equilibrium. The calculations are based on finding a global thermodynamic equilibrium between all constituents in all phases of a given system. There are two major strategies to accomplish this: minimizing the global Gibbs energy of the system under consideration (Gibbs energy minimization, GEM-approach) or solving a system of equations which represent individual equilibrium reactions (law of mass action, LMA-approach). The codes listed in the following are those, which are mainly used for highly saline solutions. Databases for all these codes can be extracted from THEREDA. A more complete list of geochemical codes is compiled on a Website, managed by HZDR⁸.

3.4.1 EQ3/6

EQ3/6 is a software package for geochemical modelling. It was created in the Lawrence Livermore National Laboratory in California in the 1970s. It was originally intended for application to seawater-basalt interactions in mid-ocean ridge hydrothermal systems and since 1990 developed into a code which allowed to calculate equilibria in high-saline systems /WOL 92/, /WOL 02/ (in conjunction with the database developed by /HAR 84/). EQ3/6 follows the LMA-approach and is no longer under development.

⁷ www.thereda.de

⁸ <http://www.hzdr.de/FWR/VB/modeling.html#speciation>

3.4.2 Geochemist's Workbench

Geochemist's Workbench (GWB) is a commercial software which follows the LMA-approach /BET 08/. It features a modern graphical user interface and can account for surface complexation and reaction kinetics. Results can be presented in diagrams /BET 14a/ /BET 14b/. Another important feature of GWB is that it is able to create pH-E_H-diagrams and to model reactive transport.

3.4.3 ChemApp

ChemApp is actually a programmer's library which provides subroutines to define chemical systems, calculate thermodynamic equilibria and retrieve results /PET 07/. It follows the GEM-approach and was originally designed for metallurgical purposes. ChemApp is proprietary software. ChemApp does not feature the representation of adsorption phenomena or reaction kinetics but has some advantages when it comes to solid solutions and very complex systems. Version 5.5.3 was used.

3.4.4 PHREEQC

PHREEQC is mainly a general purpose geochemical code, including speciation and saturation-index calculations, batch-reaction and one-dimensional (1D) transport calculations with reversible and irreversible reactions, including aqueous, mineral, gas, solid-solution, surface-complexation and ion-exchange equilibria, specified mole transfers of reactants, kinetically controlled reactions, mixing of solutions, and inverse modelling /PAR 13/. PHREEQC follows the LMA approach. A feature of PHREEQC is its ability to be adapted to specific geochemical problems by modifying its database (reactions and species can be added or suppressed easily) and/or adding specific modules (programmed in BASIC) to take into account, for instance, a particular kinetic law. Results can be presented in diagrams.

3.4.5 Capabilities and features of geochemical codes

The features and capabilities of the codes considered here are summarized in the following table (Tab. 3.6).

Tab. 3.6 Capabilities and features of the described geochemical codes

Capabilities and Features	EQ3/6	GWB	ChemApp	PHREEQC
Approach	LMA	LMA	GEM	LMA
Code	FORTRAN	C++	FORTRAN	C++
Source code available	Yes	No	No	Yes
Pitzer model	Yes	Yes	Yes	Yes
SIT model	No	No	Yes	Yes
Kinetics	Yes	Yes	No	Yes
Solid solutions	Yes	Yes	Yes	Yes
Surface complexation	No	Yes	No	Yes
Transport	No	Yes	No	Yes
Graphical user interface	No	Yes	No	Yes

ChemApp was used for the present work for practical reasons. At the time when the geochemical calculations had to be conducted, no common thermodynamic database for repository-relevant systems existed in Germany. ChemApp had already been used in earlier projects and an Excel® based interface existed to administrate thermodynamic data and export them into a format compatible with ChemApp. Therefore, it was decided to use this interface and add the thermodynamic data developed by KIT-INE. Another important advantage of ChemApp is that it may calculate thermodynamic equilibria for systems with very small masses of water or even no water at all. This is an important feature for reaction path calculations with corroding metallic phases or glass, where liquid water is consumed.

4 Evolution of the geochemical conditions

4.1 General description

The evolution of the geochemical conditions in a waste emplacement area of a repository is particularly dependent on (i) the amount and composition of the inflowing solution, (ii) the composition of the waste and (iii) the interaction of the inflowing solution with the waste constituents. For the calculations performed here it is assumed that saturated brines enter the emplacement area, fill the available void volume and get into contact with the waste.

As discussed in section 3.2 the composition of the intruding brine depends on the contact of the solution with different minerals, namely on the solubility equilibria of the respective minerals in such a multicomponent system. On the basis of potential reactions which have formed Zechstein solutions /KIE 01/ proposed three standard brines (see section 3.2). Two of these solutions were considered here to account for the uncertainty of the intruding solution (see sections 3.2 and 4.2).

Two emplacement systems are considered, a borehole for vitrified HLW and a drift for POLLUX containers with spent fuel elements. The composition of vitrified glass and spent fuel is discussed in sections 4.3 and 4.4. For a borehole with HLW containers a brine filled volume of 2 m³ and for a drift with POLLUX containers a brine filled volume of 1,000 m³ is assumed.

Tab. 4.1 Principal pattern of considered systems

Solution 1	SF	Without metallic iron
	SF	With metallic iron
Solution 3	SF	Without metallic iron
	SF	With metallic iron
Solution 1	HLW	Without metallic iron
	HLW	With metallic iron
Solution 3	HLW	Without metallic iron
	HLW	With metallic iron

Beside the dissolution of the waste matrix the corrosion of the container material affects the geochemical conditions. Especially the iron corrosion process leads to strongly reducing conditions. The composition of the steel, including elements like chromium, nickel, molybdenum and others, also changes the composition of the solution but was not considered. Here, only the corrosion of iron is assumed in order to address the most

relevant effect on the geochemical conditions. Generally, two calculations are performed for every system, one with an iron component and one without the presence of iron, where the first, as a consequence, provides more reducing conditions.

4.2 Composition of solutions

Due to the uncertainty of the brine composition, which might enter the repository the calculations are performed assuming two different solutions, a NaCl-KCl-MgCl₂-Na₂SO₄ representing the invariant point Q (near IP21 in the calcium containing system) with a high magnesium content (denoted as solution 1) and saturated with respect to halite and anhydrite (denoted as solution 3). The composition of both solutions has been calculated using the data base of Harvie, Møller and Weare (HMW) and is compiled in Tab. 7.1 in A 1 . They are the basis for modelling. However, it should be mentioned, that for most invariant solutions discrepancies occur between calculated and experimental compositions. Further investigations are necessary to close the gap between model and experiment.

4.3 Composition of vitrified waste

Vitrified waste will be deposited in steel containers with a steel mass of 75 kg and a mass of the glass matrix of about 398 kg. One unit vitrified waste (one borehole) contains 238 containers summing up to 2.38 m³ iron (density = 7.5 g cm⁻³) and 35.7 m³ glass-matrix (density = 2.65 g cm⁻³). This setting is equivalent to 3.3786 mol Fe per 1 kg glass matrix. One unit vitrified waste shall react with 2 m³ solution, the supposed remaining void volume in the environment of the container. For solution 1 with a density of 1.3151 g cm⁻³ this is equivalent to 0.0278 kg solution on 1 kg R7T7 and 0.1886 kg iron or 48.6 kg R7T7 and 9.17 kg Fe on 1 kg H₂O in the initial amount of solution 1. It turned out that the calculation aborted before all R7T7 has reacted. The maximum reaction progress was 0.158 kg R7T7 and 0.0298 kg Fe on 1 kg H₂O. Therefore, the calculations have been performed with a value of 0.15 kg R7T7. For solution 3 the ratio is adapted according to its density of 1.2201 g cm⁻³. For the composition of vitrified glass it is referred to Grambow et al. /GRA 99/, see Tab. 4.2.

Tab. 4.2 Composition of R7T7 glass matrix /GRA 99/

Oxide	wt. %	mol/kg ⁹	Oxide	wt. %	mol/kg ⁹
SiO ₂	46.2	7.69	UO ₂	0.50	0.019
Al ₂ O ₃	4.9	0.96	PuO ₂	0.26	0.009
B ₂ O ₃	14.3	4.11	NpO ₂	0.00070	0.000
CaO	4.1	0.73	AmO ₂	0.019	0.001
Na ₂ O	9.7	3.13	SrO	0.33	0.0318
Li ₂ O	2.0	1.339	MoO ₃	1.7	0.1181
ZnO	2.5	0.307	CoO	0.12	0.0160
Cr ₂ O ₃	0.50	0.066	NiO	0.74	0.054
Fe ₂ O ₃	2.7	0.338	SnO ₂	0.02	0.0013
P ₂ O ₅	0.30	0.042	Sb ₂ O ₃	0.004	0.00027
MnO ₂	0.72	0.0828	TeO ₂	0.24	0.0150
Ag ₂ O	0.03	0.0026	Cs ₂ O	1.42	0.1008
CdO	0.03	0.0023	Nd ₂ O ₃	1.59	0.0945
BaO	0.61	0.0398	ThO ₂	0.0503	0.00191
La ₂ O ₃	0.9	0.0552	Cm ₂ O ₃	5.13E-08	5.13E-08
Ce ₂ O ₃	0.93	0.0567	TcO ₂	4.16E-06	3.17E-07
Pr ₂ O ₃	0.44	0.0267	ZrO ₂	2.65	0.081
Y ₂ O ₃	0.2	0.0177			

4.4 Composition of spent fuel

For drift disposal spent fuel will be disposed of in Pollux casks. One unit (emplacement drift) spent fuel waste contains 149.3 m³ metal and 9.48 m³ spent fuel. It is supposed to react with 1,000 m³ solution. Assuming a density of 7.5 g cm⁻³ for the container material and 10.35 g cm⁻³ for the spent fuel this results in 0.09 kg spent fuel and 9.87 kg iron reacting with 1 kg solution 1. In the calculations if not stated otherwise a reaction progress of 0.11 is applied. For solution 3 the ratio is adapted according to its density of 1.2201 g cm⁻³. The composition of spent fuel is based on a UO₂ fuel with 4 % enrichment and a burn-up of 50 GWd/t_{hm}. Tab. 4.3 shows the inventory of only those elements that are considered in our calculations.

⁹ Content refers to mol element/kg glass matrix

Tab. 4.3 Chemical composition of spent fuel as used for the calculations – The element content is referred to 1 kg of waste

Element	Content [mol/kg]	Element	Content [mol/kg]
Ag	0.00107	Pu	0.0445
Am	0.00790	Ra	$1.25 \cdot 10^{-7}$
Ba	0.0293	Se	0.000991
Cd	0.00154	Sr	0.00646
Cm	0.0000446	Tc	0.0113
Cs	0.01731	Th	$3.76 \cdot 10^{-7}$
I	0.00260	U	3.926
Mo	0.0523	Zr	0.0648
Nd	0.0420	O	8.38
Np	0.00421		

4.5 Calculation of the geochemical evolution

Two types of calculations have been performed:

1. reaction path calculations to characterize the evolution of the geochemical conditions and
2. batch calculations to identify the maximum concentration (solubility limit) for the respective element.

All calculations are performed for a temperature of 25 °C. The actual temperature in the emplacement area will definitely be higher (at least 35 °C, the natural temperature of the host rock at a depth of about 800 m, but could be higher, depending on the assumed time of instantaneous radionuclide release). However, thermodynamic data for temperatures other than 25 °C are only sparsely available.

For the reaction path calculations the composition of the waste type was defined according to the descriptions in chapters 4.2, 4.3 and 4.4. For the cases without iron the calculations are performed up to the reaction progress of 0.15 kg/kg H₂O for vitrified glass and 0.11 kg/kg H₂O for spent fuel, respectively. In the presence of iron, the calculations for the spent fuel systems were performed up to a reaction progress of 0.001 only because of numerical instabilities.

Tab. 4.4 shows the pH and E_H values for the eight systems (Tab. 4.1) after the calculation, where the lower E_H value in brackets describes the system with iron. The dissolution of vitrified waste in a Mg-rich solution causes a slightly acidic pH-value in the range of 5 to 6, whereas the pH for vitrified waste in a saturated NaCl brine yields a pH in the range of 9 to 10. The solution of SF for both systems evolves to slightly alkaline pH-values between 8 to 9. In the presence of iron, the pH in solution 3 rises to about 12. The E_H values in the system with vitrified waste are slightly oxidising, if iron is absent and decrease in the presence of iron. For the systems with spent fuel, the dissolution of the waste already causes a reducing environment. The values for the calculation endpoints are listed in Tab. 4.4. For these final conditions the solubilities of each element were calculated.

Tab. 4.4 pH and E_H values calculated with ChemApp for the considered systems, representing the basis for the solubility calculations; values in brackets represent systems with metallic iron

	HLW - solution1	HLW – solution3	SF - solution1	SF – solution3
pH	5-6	9-10	8-9	8-12
E_H [V]	0.0 – (-0.1)	0.3 – (-0.4)	-0.2 – (-0.3)	-0.2 – (-0.8)

5 Geochemical conditions and element solubilities

In the following for each element mentioned in chapter 3.1, available data, relevant mineral phases and species are briefly described. Each description is divided in the following parts:

1. Which thermodynamic database (Pitzer coefficients and equilibrium constants) was applied in the geochemical calculations?
2. Discussion of the results, which are the important species?
3. New available thermodynamic data, which have not been applied in the calculations.
4. R&D needs.

For the matrix elements (chapter 5.2) their impact on the radionuclide behaviour, their relevant solid phases and solution species under the calculated conditions are discussed.

For the actinides, their daughter radionuclides, the long-term relevant fission and activation products, additionally element solubilities in high saline solutions under geochemical conditions expected in the repository areas are described (chapters 5.3 and 5.4). Generally, data, which have been used in the early long-term safety assessment "Sicherheitsanalyse Mischkonzept (SAM)" /BUH 91/ are listed. Further results from speciation calculations performed at GRS and – where available – information from the recent safety assessment "Vorläufige Sicherheitsanalyse Gorleben (VSG)" /KIE 12/ are discussed.

5.1 The six-component seawater system

Equilibrium constants and Pitzer ion interaction coefficients were adopted from /HAR 84/. Applying these data and parameters it is possible to reproduce naturally encountered host rock solutions in good approximation /HER 00/. These so-called "HMW-data" own an exceptional position in that the Pitzer coefficients involved were considered, and hence: set constant, in the procedures for the determination of Pitzer coefficients and (in part) solubility constants for other systems. This means that all other Pitzer coefficients used here, including those for radionuclides are valid only in conjunction with the HMW-parameters.

5.2 Matrix elements

As matrix elements those elements are denoted, which are contained in the waste matrix or the container material and do not represent long-term relevant radionuclides. These elements might impact the geochemical conditions and therewith the maximum concentrations of the radionuclides. Elements that are also important radionuclide, e. g. Nickel, are described in chapter 5.3.

5.2.1 Aluminium and Silicon

Si along with Al plays an important role as main matrix element in vitrified waste (e. g. R7T7). Furthermore, Si and Al are also relevant if cementitious materials or clays are considered. While reaction path calculations with cementitious waste forms were not within the scope of the present study, aluminosilicate minerals may precipitate as a result of reaction between vitrified waste and solution.

Therefore, Pitzer coefficients for Si- and Al- aqueous species were included in the database. These were published by /REA 90/ in conjunction with relevant cement phases. The latter, however, were adopted from /RAR 97/.

Data for solid cement phases are taken from /RAR 97/. Other Si-/Al-phases, namely some clay minerals and zeolites, were included as recommended by Mariner /MAR 04/. Mariner's report documents the development and validation of the in-drift precipitates/salts (IDPS) model. The IDPS model is a geochemical model designed to predict the post-closure effects of evaporation and deliquescence on the chemical composition of water within the Engineered Barrier System (EBS) in support of the Total System Performance Assessment of the Yucca Mountain disposal site for radioactive waste. It should be noted, however, that the temperature-dependent Pitzer coefficients given there are not generally consistent with Pitzer coefficients from HMW at 25 °C.

At pH ~ 9.5 neutral silicic acid dissociates to give H_3SiO_3^- , relevant for the systems with solution 3. Hence, only for those systems Pitzer coefficients for H_3SiO_3^- could have any impact on the results. At lower pH values un-dissociated silicic acid $\text{SiO}_2(\text{aq})$ was the predominant species, to which no Pitzer coefficients were assigned at all.

Two significant developments can be identified with respect to thermodynamic modelling of cementitious materials.

As to the modelling in highly concentrated salt solutions a literature review combined with own experiments was carried out /MEY 09/. The survey contains solubility constants and equilibrium constants for numerous solid phases and aqueous species. Literature data on solubility and own isopiestic measurements allowed the calculation of temperature dependent Pitzer coefficients for interactions hitherto uncovered in existing databases. Further effort is needed to derive consistent thermodynamic data from this report for the purpose of geochemical modelling.

Real cementitious systems have been addressed by EMPA (Eidgenössische Materialprüfungs- und Forschungsanstalt) in Switzerland. They developed a thermodynamic database covering a temperature range of 0 – 100 °C /MAT 07/. It is available for the geochemical codes GEMS and PHREEQC. Not only pure solid phases but also solid solutions (both ideal and non-ideal) are included.

It is clear, that the database used in the calculations for this project does not reflect the present state of knowledge but needs to be updated. E. g., both of the above-mentioned approaches are complementary.

In comparison to the database used for this study knowledge about reaction kinetics, the nature of neo-formed minerals, and processes contributing to radionuclide retention (precipitation, solid solution formation, ion exchange) has significantly improved meanwhile. Higher attention should therefore be paid to the kinetics of glass corrosion and the identification of secondary minerals. This has not only consequences for the evolution of the near-field pH-conditions, but also affects the mobility of radionuclides. Precipitation kinetics can be modelled in dependence on its saturation status in aqueous solution /VER 92/, which in turn requires knowledge about solubility constants and interaction coefficients. /GIN 94/ studied the combined effect of temperatures up to 90 °C and the presence of organic ligands on the corrosion of R7T7.

For integrated models, conservative assumptions for the glass dissolution could be applied, supplemented with thermodynamic data for the most stable secondary minerals. Absence of a colloidal contribution should be proofed in experiments with high saline solutions.

5.2.2 Barium

Barium is relevant as it is a component of vitrified waste and spent fuel and might particularly form low soluble mineral phases with sulphate, incorporating radionuclide cations like strontium or radium.

At the time when the calculations were conducted no Pitzer coefficients for Ba^{2+} were present in the database. It was considered to be present as Ba^{2+} in aqueous solution.

With respect to solid phases Ba was allowed to precipitate as pure Barite (BaSO_4) /HUM 02/, BaSeO_3 /MOM 05a/, BaSeO_4 /MOM 05a/ or as part of an ideal solid solution formed with Strontianite (SrSO_4) and RaSO_4 .

In the meantime, a polythermal Pitzer database for Sr, Ba, and Ra was presented in /MOO 14/ used in conjunction with the calculation of earth alkaline sulphate solubilities in high saline hydrothermal systems. This database should be integrated in THEREDA for future model calculations. However, data gaps persist for some high saline systems, e. g. concentrated MgCl_2 -solutions.

5.2.3 Boron

Boron along with Al and Si plays an important role as matrix element in vitrified waste (e. g. R7T7). The significance of boron chemistry lies with its capability to influence the solution pH and to form tetraborate complexes with actinides /BOR 10/.

Boron under conditions relevant to this study is primarily encountered with the oxidation number +III. Various types of metal borates, e. g. with transition elements or lanthanides, are known. Boron oxide B_2O_3 upon contact with free water readily forms boron acid. It was therefore not included in the database as solid phase. The only solid phase considered for boron was $\text{Na}_2[\text{B}_4\text{O}_5(\text{OH})_4]\cdot 8\text{H}_2\text{O}$ (Borax), being defined by reaction using an equilibrium constant from /WAG 82/. No reference is given for this phase in the documentation for the IDPS-model /MAR 04/. As to aqueous species, for boron only $\text{B}(\text{OH})_3(\text{aq})$ was considered.

Speciation of boron is, besides pH, highly dependent upon its total concentration. At higher concentrations, boron forms a multitude of oligomeric species. For concentrations

up to 10^{-2} M, however, boron is dissolved predominantly as monomeric boric acid $B(OH)_3$ (aq) and tetraborate ($HB_4O_7^-$ or $B_4O_7^{2-}$) /CRA 11/. As a general trend, boron tends to form simpler species with increasing temperature /SCH 05/. Thus, the decision as to which boron species future investigations should focus on depends on the question on its maximum likely total concentration in solution.

There is a potential for boron to form sparingly soluble borates (or tetraborates) with actinides in aqueous solution, but for the present study no efforts were undertaken to explore this possibility in depth.

Only few studies exist, which give information on boron concentration as a result of leaching experiments.

/ADV 01/ reported about the leaching of a SON68-type borosilicate glass and found a total of 0.01 M boron dissolved after 2500 days, but it remains dubious which type of solution was used. /VER 01/ detected a total of 0.005 M of boron with pure water and a granite-type solution. /PIE 10/ presented graphical results only from leaching experiments with pure water and a variety of glasses. Due to the logarithmic scaling it is difficult to tell the maximum boron concentration, which is well between 0.01 M and 0.1 M.

The work of /BOR 10/ has special significance for the disposal of nuclear waste in Germany because their experiments were conducted in highly mineralized solutions.

Summarizing it seems necessary to create a reliable model for the speciation of boron in highly mineralized solutions, and to determine Pitzer coefficients accordingly. But prior to such efforts it is essential to determine the maximum possible concentration of boron after leaching experiments in highly mineralized solutions and with the particular glass in question for nuclear waste disposal. This will help to focus lab work on boron species of relevance.

5.2.4 Iron

Fe is the major component of the steel container materials. Equilibria with ferrous iron (Fe^{3+}/Fe^{2+} or Fe^{2+}/H_2) are the predominant redox couples in the near field of repository. Therefore, the standard potential between both oxidation states of iron is of high interest. Moreover, as most iron will be found in direct vicinity to the waste containment, high-

temperature data are of relevance. For the calculation of the redox state, as referencing to the partitioning of iron into Fe^{2+} and Fe^{3+} , it is necessary to calculate the respective activity coefficients. For high saline solutions this requires the knowledge of Pitzer coefficients.

The speciation model for iron in this work consisted of Fe^{2+} and Fe^{3+} only. While it is acknowledged that the real speciation especially of ferric iron follows a far more complicated pattern, no reliable database was available to calculate the pertinent reactions in high saline media. Pitzer coefficients for Fe(II) and Fe(III) for the interaction with Na, K, Mg, Ca, Cl, and SO_4 were determined in /MOO 04/ and /RUM 04/. Iron-bearing Si/Al-phases, two iron oxides (goethite and hematite), and Na- and K-jarosite were adopted from the IDPS-model.

For conditions considered here Fe^{3+} was of minor importance; total molalities ranged from 10^{-26} and 10^{-56} mol/kg.

At present the experimental basis for binary Pitzer coefficients for the interaction between Fe^{2+} and SO_4^{2-} is poor. Only four publications altogether, the first one from 1937, report about direct measurements of water activity, which are precisely those data which are most relevant for the calculations of ferrous iron activity coefficients. One possibility to mend this situation could be to include data from sulfuric acid FeSO_4 -systems which are available at greater numbers and also for different temperatures.

As to ferric iron, the main interest rests on the stability constants of hydroxo-complexes as the most important species at relevant pH conditions. The question is whether and to which extent the formation of these complexes will be altered by the presence of other electrolytes, namely sodium chloride. /XUE 99/ investigated the solubility of iron hydroxide in up to 5 M NaCl solutions at temperatures up to 50 °C and calculated conditional stability constants. However, with regard to the low solubility of ferric iron (down to 10^{-10} M and below) it remains unclear whether Pitzer coefficients for ferric iron species are relevant or not.

Ferric iron speciation may be further complicated by the presence of $\text{CO}_2(\text{g})/\text{HCO}_3^-$ due to the formation of mixed hydroxo-carbonato- or carbonato-complexes (see the very interesting discussion between /BRU 92a/, /BRU 92b/, /BRU 00/ and /HUM 00/). However, this matter is of no relevance for the calculations in this study which were done under the assumption that no carbon was present.

As to the model calculations undertaken in this project it remains unclear whether a refined database for iron would have changed the results noticeably. Two reasons for this are that neither the corrosion of containment material, nor the retention of radionuclides on corrosion products, were of interest in this study. Another issue of interest not covered by this study is the kinetics of metallic corrosion, and the accompanying generation of H₂-gas¹⁰. As to the speciation of iron the hydrolysis of ferric iron in high saline solutions poses severe problems for the modeller. However, in more reducing conditions (as with metallic iron present in the calculation) ferric iron is likely to appear in negligible concentrations only (see above).

Another field of interest is, which corrosion products are formed upon the contact of waste containment and aqueous solution. Along with ferrous and ferric hydroxides, hematite, magnetite, and goethite, some corrosion experiments indicated towards the formation of alkaline chlorides such as Hibbingite (Fe,Mg)(OH)₃Cl in high saline solutions. Recently, the solubility for the pure-iron end-member Fe₂(OH)₃Cl was investigated in NaCl- and Na₂SO₄ solutions /NEM 11/. But it is unclear up to which Mg-content this phase would be stable, because at room temperature the pure-magnesium end-member Mg₂(OH)₃Cl occurs as hydrous phase only.

For future advancements it should be considered to employ a stepwise approach for the creation of a thermodynamic database for iron. Due to the rather high number of potentially present species in neutral and alkaline solution a simplifying approach should be chosen that focusses on those species that are most relevant and dominating in the expected pH range.

5.2.5 Lithium

Lithium was used as an indicator for the reaction progress. No solid phase was included for Li and only Li⁺ as aqueous species.

As to Li⁺ Pitzer coefficients for this work were adopted from /KIM 88a/, /KIM 88b/. Meanwhile comprehensive studies were conducted to determine solubilities and vapour pressures in Li-containing aqueous solutions, e. g. /JOR 09/, /MOR 10/, /RAR 07/. The latter

¹⁰ For reactive transport modelling the solubility of H₂(g) might also be important.

work contains Pitzer coefficients for the interaction between Li^+ and SO_4^{2-} , which are missing in the database used for this work. In the calculations with R7T7 Li^+ attained a maximum concentration of 0.2 M. Although this value is well below any solubility limit for Lithium, Li^+ could still contribute to the activities of other aqueous species. It is therefore recommended to extend the database for the most important interactions with the main components of high saline solutions.

5.2.6 Phosphorus

Phosphorous is relevant as a minor constituent in the HLW glass matrix. It might affect the pH value, act as complexing ligand for radionuclide cations and form low soluble minerals.

Gibbs energies of formation for the following aqueous species were directly adopted from /MOM 05a/: $(\text{H}_2\text{P}_2\text{O}_7)^{2-}$, $(\text{H}_2\text{PO}_4)^-$, $(\text{H}_3\text{P}_2\text{O}_7)^-$, $(\text{HP}_2\text{O}_7)^{3-}$, $(\text{HPO}_4)^{2-}$, $(\text{P}_2\text{O}_7)^{4-}$, $(\text{PO}_4)^{3-}$, $\text{H}_3\text{PO}_4(\text{aq})$, $\text{H}_4\text{P}_2\text{O}_7(\text{aq})$. Phosphorus is also present in some aqueous species and solid phases with Pu, Th, U, and Zn.

The database used for this work did not contain Pitzer coefficients for phosphate species. Thus, it cannot be excluded that hydrolysis equilibria between the various phosphate species were not modelled correctly.

In some of our calculations for vitrified waste Pu(III)-, Am(III)- or Np(IV) formed solid phases with phosphate. While the underlying solubility constants may be uncertain and no information about complex formation with actinides were available when the calculations were done, these results indicate that solid phase formation with phosphate could be a relevant retention mechanism for actinides.

For the most relevant phosphate species available data had been worked through and experiments were conducted in a research project that aimed at the development of a comprehensive set of Pitzer coefficients. This way and for the first time a comprehensive database for the systems Na, K – Cl, SO_4 – PO_4 , HPO_4 , H_2PO_4 – H_2O could be established /SCH 13/, /SCH 15/. For systems containing Mg and Ca, however, data gaps persist, and probably will remain so until some principal problems with regard to emf-measurements in high-saline solutions will be solved. It is planned to go for this in a future project.

The release of some actinides and rare earths was investigated in /MEN 98/. With phosphate containing glasses, retention of radionuclides was greatly enhanced by the neo-formation of phosphates. The experiments were conducted in low saline solutions, and more than 90 % of lanthanides and Th were associated with colloids. The potentially significant impact of phosphate had been recognized by the US Department of Energy which funded a project on corrosion rate modelling of iron phosphate glasses /SCH 11/.

Phosphate has a potential for complex formation and precipitation with actinides. In our calculations with R7T7 it attained a concentration of 10^{-3} M. Therefore, it cannot be excluded that with the new database for phosphates results would change significantly. Furthermore (and for the modelling of vitrified waste dissolution only) a closer look on phosphate complexes and phosphate containing solid phases with radionuclides would be worthwhile.

5.3 Activation and fission products

Based on the discussion in chapter 3.1 the description here is focussed on the elements important for geochemical modelling.

5.3.1 Carbon

Carbon is an activation product forming impurities in the fuel, and it is also present in the structural elements of the fuel assembly. Its only radioactive isotope is C-14, which represents a minor proportion of carbon in terms of mass. An estimated 5 % of carbon is present both in the gap and in the grain boundaries /WER 04/, /BIS 16/.

The chemical form of carbon in the metal parts and the spent fuel matrix is very likely carbide. Investigations of C-14 leaching from hull waste identified inorganic and organic carbon being released from the metallic samples /KAN 02/, /TAN 07/. Such small organic molecules can be very mobile but can also undergo microbial degradation to methane or carbon dioxide. However, radionuclide release data under disposal conditions are not available /KIE 12/ and is a research topic in the running European project CAST /SCO 14/. Therefore, carbon was not considered in the GRS calculations. Data used in the SAM study are compiled in Tab. 5.1.

Tab. 5.1 Solubility data for C at different geochemical conditions derived from previous studies

Study	Solubility limit [Mol/l]			Remark
	BE	Min	Max	
SAM				
-acid	10 ⁰	10 ⁰	10 ⁰	emplacement sites with vitrified glass and SNF (not applied)
-neutral	10 ⁻²	10 ⁻⁴	10 ⁰	
-alkaline	10 ⁻⁶	10 ⁻⁸	10 ⁻⁴	emplacement sites with cementitious material drifts; mixing of different brine compositions
-unknown	10 ⁻⁴	10 ⁻⁸	10 ⁰	

BE = best estimate

5.3.2 Chlorine, Iodine

The long-term relevant Cl-36 as activation product and the isotopes of iodine as I-129 as fission product occur in spent fuel and to a lesser extent in vitrified HLW, since the major part of them is cut off during the reprocessing process.

Iodine is to some extent sensitive on redox conditions. At reducing conditions iodine is present predominantly as iodide, but under certain conditions it can also be found in elemental form with a solubility much lower than with its compounds with components of the system of oceanic salts. This form, however, tends to be stable only at rather acid conditions of ~ pH = 3-5. Furthermore, chlorine is the predominant anion in the high mineralised solutions considered here.

Pitzer coefficients for the interaction of aqueous species of iodine with the oceanic system were adopted from an earlier research project /HAG 12/, /BIS 15/. Species and phases taken into account were I⁻, NaI·2H₂O, KI, MgI₂·8H₂O. An additional solid phase was adopted from /MOM 05b/: I₂(cr).

Under conditions relevant for repositories chlorine is present in a single oxidation state only (-I). In the database chloride was not only accounted for as single species Cl⁻ but also in a number of complexes (heavy metal, actinides). Pitzer coefficients for chloride were adopted from the HMW-database.

Chlorine and Iodine are assumed to be very mobile under the conditions expected in the repository. Therefore, no solubility limit is assumed in long-term safety analysis. However, in one near field chemical model the formation of almost insoluble silver iodide, AgI is considered, /BER 14a/, /BER 14b/. Whether or not AgI may be a solubility limiting

phase depends on the availability of at least equimolar quantities of Ag^+ . If silver is instead reduced to metallic silver, retardation of iodide would not occur.

According to calculations in this study iodine attained a concentration in the order of 10^{-4} M, before the calculation terminated. For iodides, this is still well below relevant solubility limits. This includes heavy metal iodides such as PbI_2 or CdI_2 . Thus at the present state of knowledge iodine can be regarded as not limited by solubility.

Future efforts for iodine and chloride should focus on other retention mechanisms like surface complexation on secondary phase surfaces or co-precipitation. For Cl-36 incorporation into solid halides could be considered. For iodine it should be established whether elemental iodine $\text{I}_2(\text{cr})$ is formed on the surface of corrosion phases, e. g. by oxidation of iodide under conditions where $\text{I}_2(\text{cr})$ is thermodynamically stable.

5.3.3 Caesium, Rubidium

Isotopes of caesium and rubidium occur as fission products in vitrified HLW and spent fuel. The aqueous speciation in solution is dominated by the free cations Rb^+ and Cs^+ in most natural groundwaters, with no influence of the main variables of the system, pH and carbonate content, in the range of conditions of interest for this work. For Cs no solubility limit was regarded at SAM. In SAM a solubility limit of 1 mol/l for all geochemical conditions was used.

Thus, for Rb and Cs no solid phases were considered for the calculations presented here. Assumed aqueous species were Rb^+ and Cs^+ . Being part of the assumed composition of R7T7-glass and/or spent fuel this means that the solubility of these element is considered unlimited.

Though Pitzer coefficients for Cs were established by /NEC 98/ and are part of the database used, they are not likely to have an effect on the calculations presented here because of the rather low Cs-concentrations (see below). The same can be said for Rb. However, Pitzer coefficients for both Cs and Rb might become important, if their retention by surface complexation modelling is of interest, because in that case their activity is needed rather than their concentration.

/ALT 11/ had conducted an extensive literature review on all available data for Cs with regard to the determination of Pitzer coefficients. For Cs these efforts have resulted in two publications /SCH 12/, /SCH 13a/ and a complete set of Pitzer coefficients is available for the system Na, K, Mg, Ca – Cl, SO₄ – H₂O which is available from THEREDA.

With R7T7 a maximum concentration of 10⁻² M for Cs was calculated. This is well below the solubility of solid phases Cs forms with chloride or sulphate. However, with regard to its radiological potential, the retention of Cs by secondary phases formed by glass alteration may be significant. /INA 06/ studied the retention of Cs on a Japanese simulated waste glass. The mechanism for retention can be incorporation/co-precipitation, in which case it is irreversible, or cation exchange, in which case it is reversible (and, as might be assumed, strongly affected by a high background concentration of salt minerals). There is no general model available for Cs-retention. Further efforts in this direction should be aimed towards an understanding of glass alteration and the nature of secondary minerals.

/ALT 11/ conducted an extensive literature review on all available data with regard to the determination of Pitzer coefficients for Rb. No data are available for CaCl₂ containing solutions. For systems with MgCl₂ or MgSO₄ experimental data are questionable. However, as with Cs, retention of Rb due to solid phase formations is not likely and should therefore not be in the focus of future efforts. However, there are some indications for the incorporation of Rb in carnallite /SCH 71/ and sylvite /MCI 68/. Such mechanisms should be investigated in more detail. As to the retention on glass alteration products the same applies as for Cs.

5.3.4 Molybdenum

The isotope Mo-93 is a fission product and contained in spent fuel and HLW. It is a redox sensitive element. In the presented calculations the species MoO₄²⁻ (molybdate) was considered only. Pitzer coefficients were adopted from /GRA 92/. Considered solid phases were powellite (CaMoO₄), MgMoO₄·5H₂O(s), and Na_{0.5}Nd_{0.5}MoO₄(s).

In our calculations the maximum concentration in the systems with pH values between 8 and 10 is in the range between 10⁻⁵ and 10⁻⁶ mol/l and one to two orders of magnitude higher in HLW in solution 1 at pH 5 to 6 (Tab. 5.2). Solubility is always controlled by the

mineral phase powellite (CaMoO_4). An exception is the system of spent fuel with solution 1, where no Ca is present at all.

Tab. 5.2 Solubility data for Mo at different geochemical conditions

Study	Solubility limit [Mol/l]			Remark	
	BE	Min	Max		
-acid	10^{-2}	10^{-3}	10^{-1}	emplacement sites with vitrified glass and SNF (not applied) emplacement sites with cementitious material drifts; mixing of different brine compositions	
-neutral	10^{-4}	10^{-7}	10^{-1}		
-alkaline	10^{-4}	10^{-7}	10^{-1}		
-unknown	10^{-4}	10^{-7}	10^{-1}		
GRS	Range			Mineral phase	Relevant species
HLW, sol. 1	$10^{-3} - 10^{-5}$			CaMoO_4	MoO_4^{2-}
HLW, sol. 3	$10^{-5} - 10^{-6}$			CaMoO_4	MoO_4^{2-}
SF, sol. 1	10^{-3}			n.l.	MoO_4^{2-}
SF, sol. 3	$10^{-5} - 10^{-6}$			CaMoO_4	MoO_4^{2-}

n.l. = not limited, no Ca present in system, BE = best estimate

These values are slightly lower than those used in the SAM study. /FEL 92/ determined its solubility to be in the order of magnitude of 10^{-5} M in CaCl_2 solutions and recommended some Pitzer coefficients. Nevertheless, no conclusive statements can be made as to the impact of Mo on secondary phase formation with radionuclides. It is assumed that Mo could contribute to the retention of radionuclides, especially with rare earth elements.

Its impact on the radionuclide concentration evolving in the near-field of an underground waste repository at the present time cannot be assessed conclusively. Mo features an extraordinary manifold chemical versatility. It has oxidation states ranging from II to VI and coordination numbers from 4 to 8. It may form poly-molybdates or hetero-poly-molybdates with other ligands such as PO_4^{3-} or SiO_4^{4-} in aqueous solution, to mention just a few ones /BAR 85/.

Under reducing conditions Mo(III) and Mo(IV) have been observed. Reduction of Mo(VI) by reducing agents such as metallic zinc/ hydrogen directly leads to the formation of Mo(III) /HOE 41/. However, metallic molybdenum is not formed this way, so it may be assumed that reduction by metallic iron does not lead to elemental molybdenum either. The oxidation state Mo(IV) may only be achieved by mixing Mo(III) and Mo(V) solutions. Currently, there are only few thermodynamic data on Mo(III) and Mo(IV) solids and

species available /WAN 10/. A calculation of Mo solubility in NaCl brines under conditions where Mo(III) is predominant is presently not possible.

5.3.5 Nickel

Nickel is a relevant matrix element, since it is present in several steels used, but the isotopes Ni-59 and Ni-63 are also important radionuclides in HLW and spent fuel originating from activation in the reactor.

Nickel is mainly found in the oxidation state +2 in aqueous and solid states. The aqueous nickel speciation is dominated by hydrolysis complexes at neutral pH range. Pitzer coefficients for the interaction between Ni^{2+} and components of the oceanic system were determined within the frame of a research project located at the Bergakademie Freiberg. Pitzer coefficients and solid phases were adopted from the final report for this project /BRE 99/. Elementary Ni, and solubility constants for $\text{NiSeO}_4 \cdot 6\text{H}_2\text{O}$ and $\text{NiSeO}_3 \cdot 2\text{H}_2\text{O}$ /MOM 05b/ were added.

In our calculations hydroxo- and sulphate species are the most important aqueous complexes from pH 6 to 9 under the conditions considered here (Tab. 5.3). In the calculations it is assumed that $\alpha\text{-NiS}$ is the mineral phase, which determines the Ni concentration, except in less reducing systems with pH in the range 8 to 10, where $\beta\text{-Ni(OH)}_2$ is considered. It should be noted that in other geochemical near-field models, NiO is considered as the solubility limiting phase. Nickel oxide is much more stable than Ni(OH)_2 but it does not form even at elevated temperatures /PAL 11/.

At pH values between 5 and 6 the solubility reaches the highest values between 10^{-2} and 10^{-4} mol/l. The solubility decreases with increasing pH and evolution to more reducing conditions, where the availability of sulfide increases. As a consequence, the maximum concentration range for systems with spent fuel at pH-values between 8 and 9 is calculated to be between 10^{-5} and 10^{-9} mol/l. In the system of HLW with solution 3, with pH values between 9.5 and 10 the solubility range is even lower with values ranging between 10^{-7} and 10^{-11} mol/l.

Tab. 5.3 Solubility data for Ni at different geochemical conditions

Study	Solubility limit [Mol/l]					
SAM	BE	Min	Max	Remark		
-acid	10 ⁻²	10 ⁻³	10 ⁻¹	emplacement sites with vitrified glass and SNF (not applied) emplacement sites with cementitious material drifts; mixing of different brine compositions		
-neutral	10 ⁻⁴	10 ⁻⁷	10 ⁻¹			
-alkaline	10 ⁻⁵	10 ⁻⁷	10 ⁻³			
-unknown	10 ⁻⁴	10 ⁻⁷	10 ⁻¹			
GRS	Range		Mineral phase (+Fe)	Mineral phase	Relevant species (+Fe)	Relevant species
HLW, sol. 1	10 ⁻² – 10 ⁻⁴		α-NiS	α-NiS	Ni ²⁺	NiSO ₄ , Ni ²⁺
HLW, sol. 3	10 ⁻⁷ – 10 ⁻¹¹		α-NiS	β-Ni(OH) ₂	Ni(OH) ₃ ⁻ , Ni(OH) ⁺	Ni(OH) ₃ ⁻ , Ni ²⁺ , NiSO ₄
SF, sol. 1	10 ⁻⁵ – 10 ⁻⁹		α-NiS	α-NiS	NiSO ₄ , Ni ²⁺ , Ni(OH) ⁺	NiSO ₄ , Ni(OH) ⁺ , Ni ²⁺
SF, sol. 3	10 ⁻⁶ – 10 ⁻⁹		α-NiS	β-Ni(OH) ₂	Ni(OH) ₃ ⁻	Ni ²⁺ , NiSO ₄ , Ni(OH) ⁺

The database for Ni, as applied in the model calculations is valid for moderately acid solutions only. Other solid phases of interest, however, relate to sulphides or oxides, where other aqueous species such as hydroxo complexes or Ni(HS)⁺ may be important. In solutions equilibrated with CO₂(g) complexes with carbonate are known. For all these species standard thermodynamic data are known. However, Pitzer coefficients for them are largely missing in the literature. The applied database contains Pitzer coefficients for the basis species Ni²⁺ only, which leaves the activities of all other Ni-species uncorrected with regard to high ionic strengths. This might lead to erroneous results for solubilities. With regard to the (assumed) stable phase NiS with R7T7 it is furthermore problematic that Pitzer coefficients for HS⁻ are missing in the database.

For a further development of the database it is recommended to have a specific look onto the solubility of Ni-oxides and –carbonates in brine solutions and to extend the database for HS⁻ Pitzer coefficients. As to the latter a decision would have to be made, whether the gas phase should be included in the database or not. If so, one is left with the additional problem to create an equation of state for H₂S(g) accounting for non-ideal conditions in the gas phase and at the same time consistent with a Pitzer model for the

aqueous solution. Some advances have been made recently to determine the solubility of $H_2S(g)$ in aqueous solutions /SAV 12, /XIA 00/.

It should also be noted that due to the similar chemistry of Ni^{2+} and Fe^{2+} , Ni would probably be incorporated in Fe(II) minerals and corrosion products.

5.3.6 Niobium

Nb-94 is a fission product and a component in HLW and spent fuel. There is a general lack of thermodynamic data in the literature for aqueous species of niobium. Which solid phase would limit the solution concentration of niobium is still unclear. In some studies Nb_2O_5 is assumed, e. g. /WER 14/ but it is more likely that hydrous $Nb_2O_5 \cdot xH_2O$ would form which has a much higher solubility /DEB 15/. In the presence of Na and Ca, less soluble simple or mixed sodium and calcium niobates could may form /ATE 10/, but so far, to little is known about their stability.

Therefore, it was excluded from the calculations. The data used in SAM are compiled in Tab. 5.4.

Tab. 5.4 Solubility data for Nb at different geochemical conditions

Study	Solubility limit [Mol/l]			Remark
	BE	Min	Max	
SAM				
-acid	10^{-2}	10^{-3}	10^{-1}	emplacement sites with vitrified glass and SNF (not applied)
-neutral	10^{-4}	10^{-7}	10^{-1}	
-alkaline	10^{-4}	10^{-7}	10^{-1}	emplacement sites with cementitious material drifts; mixing of different brine compositions
-unknown	10^{-4}	10^{-7}	10^{-1}	

BE = best estimate

5.3.7 Palladium

Pd-107 is a long-term relevant fission product occurring in HLW and spent fuel. The element Pd was excluded from the calculation as at that time no reliable data applicable for high-saline solutions were available. As to our present knowledge this situation has not changed much. Under strongly reducing conditions elemental Palladium would be the most thermodynamically stable form. However, its formation may be kinetically inhibited /WER 14/. In that case, Pd(II) would be the next stable oxidation state. There is some

discussion on the solubility limiting phase. In the absence of chloride $\text{Pd}(\text{OH})_2$ would be the least soluble solid phase, but if chloride is present a mixed phase with the formula $\text{PdCl}_{0.27}(\text{OH})_{1.73}$ could form /BOI 07/.

/TAI 91/ determined the temperature dependent speciation of Palladium in NaCl-solutions and derived stability constants. In a more recent paper /CRU 07/ described the complexation of palladium with chloride and hydroxide. It is hypothesized that from such data Pitzer coefficients could be derived. Recently, the Japan Atomic Energy Agency published a report with thermodynamic data for tin, protactinium and palladium /KIT 14/.

The data used in SAM are compiled in Tab. 5.5.

Tab. 5.5 Solubility data for Pd at different geochemical conditions

Study	Solubility limit [Mol/l]			Remark
	BE	Min	Max	
SAM				
-acid	10^{-2}	10^{-3}	10^{-1}	emplacement sites with vitrified glass and SNF (not applied)
-neutral	10^{-4}	10^{-7}	10^{-1}	
-alkaline	10^{-5}	10^{-7}	10^{-3}	emplacement sites with cementitious material drifts; mixing of different brine compositions
-unknown	10^{-4}	10^{-7}	10^{-1}	

BE = best estimate

5.3.8 Samarium

Sm-147 and Sm-151 are fission products occurring in spent fuel and HLW and are considered in long-term safety assessment. Thermodynamic data for Samarium species are discussed in /ALT 11/. These results did not lead to a set of Pitzer coefficients consistent with the HMW-database. Therefore, Samarium could not be considered in our calculations. In future calculations it should be aimed at a general model for three valent lanthanides. For a number of species and solid phases information is available only for one lanthanide. Due to the chemical similarity of lanthanides it is hypothesized that thermodynamic data and solid phase compositions could be estimated in an analogue approach. The data used in SAM are compiled in Tab. 5.6.

Tab. 5.6 Solubility data for Sm at different geochemical conditions

Study	Solubility limit [Mol/l]			Remark
	SAM	BE	Min	
-acid	10 ⁻²	10 ⁻³	10 ⁻¹	emplacement sites with vitrified glass and SNF (not applied)
-neutral	10 ⁻⁵	10 ⁻⁷	10 ⁻³	
-alkaline	10 ⁻⁵	10 ⁻⁷	10 ⁻³	emplacement sites with cementitious material drifts; mixing of different brine compositions
-unknown	10 ⁻⁴	10 ⁻⁷	10 ⁻¹	

BE = best estimate

5.3.9 Selenium

Se-79 is a relevant fission product and contained in vitrified HLW and spent fuel. In the latter a significant fraction occurs as selenide located predominantly in the gaps and grain boundaries and forming a volatile compound of composition Cs₂Se /JOH 97/. It will consequently dissolve from the matrix, under anoxic and reducing environments, in the form of Se(-II) species, HSe⁻ at the pH of the reference groundwater. The presence of Fe(II) in the aqueous solution may cause the precipitation of FeSe(s). However, in the present analysis Se(cr) was considered as solubility limiting phase.

Pitzer coefficients for the interaction of aqueous species of Se with the oceanic system were adopted from an earlier research project /HAG 12/, /BIS 15/. Species and phases taken into account were SeO₃²⁻, SeO₄²⁻, HSeO₃⁻, HSeO₄⁻, H₂SeO₃⁰.

Additional solid phases were adopted from /MOM 05b/: Se(cr), SeO₂(cr), and SeO₃(cr). Some Se mineral phases (heavy metal selenides) were excluded from calculations, since extremely low concentrations were calculated. It is recognized, however, that the formation of such solid phases might pose significant retardation potentials. But credit should only be taken if they can be supported by experimental data.

Under the conditions examined here selenium occurs in solution in the reduced state -2 except in the calculation for HLW in solution 3, when iron is absent, see Tab. 5.7. In this case selenium occurs as selenate in oxidation state +6. In the more reducing systems HSe⁻ is the prevailing species at all pH values above 4 (HLW in solution 1) H₂Se is of no relevance. No Pitzer coefficients were available for aqueous Se(-II)-species for the correction of activity coefficients.

If selenium occurs as selenate its solubility is not limited. In all other cases Se(cr) is assumed to be the mineral determining phase. For very high pH values (spent fuel in solution 3 with metallic iron) PbSe is calculated as selenium concentration determining mineral phase. The concentrations at pH-values between 8 and 9 in the systems with spent fuel are in the range of 10^{-7} to 10^{-9} mol/l, approaching 10^{-6} mol/l for even more alkaline pH values. Lowest values are calculated for pH values of 5 to 6 in system HLW with solution 1 in range of 10^{-11} to 10^{-13} mol/l. These concentrations appear to be unrealistically low. Dissolution of amorphous Se would result in higher concentrations. However, data for such a solid phase were missing.

Tab. 5.7 Solubility data for Se at different geochemical conditions

Study	Solubility limit [Mol/l]						
SAM	BE	Min	Max	Remark			
-acid	10^{-4}	10^{-8}	10^0	emplacement sites with vitrified glass and SNF (not applied) emplacement sites with cementitious material drifts; mixing of different brine compositions			
-neutral	10^{-4}	10^{-8}	10^0				
-alkaline	10^{-4}	10^{-8}	10^0				
-unknown	10^{-4}	10^{-8}	10^0				
GRS	Range			Mineral phase (+Fe)	Mineral phase	Relevant species (+Fe)	Relevant species
HLW, sol. 1	$10^{-11} - 10^{-13}$			Se(cr)	Se(cr)	HSe ⁻	HSe ⁻ , H ₂ Se
HLW, sol. 3	$>10^{-1} - 10^{-4}$			Se(cr)	n.l.	HSe ⁻	SeO ₄ ²⁻
SF, sol. 1	$10^{-7} - 10^{-9}$			Se(cr)	Se(cr)	HSe ⁻	HSe ⁻
SF, sol. 3 modelling	$10^{-6} - 10^{-8}$			Se(cr), (PbSe)	Se(cr)	HSe ⁻	HSe ⁻

BE = best estimate,; n.l. = not limited

Apart from surface complexation type interactions with secondary phase surfaces selenite also forms a number of low-soluble compounds. For instance, /RAI 95/ studied the solubility of ferric selenite hexahydrate. He states, that for the modelling no Pitzer coefficients for Se are needed; instead ion pairs between ferric iron and selenite were considered in his model. Recently, a dissertation was finalized about the migration behaviour of selenium for the safety assessment of radioactive waste disposal /IID 12/. This study covers aspects of thermodynamic data, sorption and precipitation. In the presence of iron, selenium may also precipitate in elemental form, leaving extremely low concentrations of dissolved selenium in solution. Under reducing conditions also the pyrite analogue FeSe₂ may form.

With regard to the extremely low solubility of elemental selenium and Se(-II) compounds it should be evaluated if such compounds are really formed under repository conditions. Modelling of selenide species in aqueous solutions is currently limited because dissociation and association constants are incomplete – especially for polyselenides that may be important under reducing alkaline conditions. Ion interaction coefficients are completely lacking so far.

5.3.10 Strontium

Sr-90 is a fission product occurring in HLW and spent fuel and relevant in case of early releases, since its half-life is only 28.64 years. It also occurs as a minor constituent of salt rock, where it is incorporated in anhydrite or polyhalite or appears as SrSO₄ (Celestine) admixture to halite /BRA 62/, /KUE 87/. The Sr content of rock salt is reported to be in the order of 0.00007 to 0.0007 wt.-% /BRA 62/. Naturally occurring brines may have significant Sr concentrations (up to 100 mg/l or more) /KLA 08/.

Pitzer coefficients for strontium were adopted from /ALT 04/. The solubility determining phase assumed is the solid solution (Sr, Ba, Ra)SO₄.

As mobile complexes only SrSO₄(aq) is regarded, which in nearly all systems occur in a similar order of magnitude as the Sr²⁺ cation. Solubility constants for end members as well as for SrCO₃ and the formation constant for SrSO₄(aq) were taken from the PSI/NAGRA-database /HUM 02/. Some additional phases with Se, BaSeO₃, BaSeO₄, SrSeO₃, were adopted from /MOM 05b/.

Calculations for the maximum concentration of Sr in all considered systems show values in the range of 10⁻² to 10⁻⁶ mol/l (Tab. 5.8) with slightly higher values due to a higher Sr/Ba-ratio in the systems with HLW.

Calculations for R7T7 resulted in a maximum concentration for Sr of 10⁻³ M. This is the order of magnitude where SrSO₄ becomes saturated; therefore, an update of the database and a close inspection of SrSO₄-saturation under relevant conditions might be worthwhile. For the update findings from the THEREDA-report /ALT 11/ should be merged with data in /MOO 14/ to get an internally consistent database.

For Sr (as well as for Ba) an interesting development evolves as the precipitation of low-soluble alkaline earth sulphates and -carbonates poses some annoyance for the use of geothermal energy. In the wake of investigations into thermodynamic properties of these minerals in high saline solutions at elevated temperatures and pressures, new data are gained which can be used in calculations or nuclear waste disposal. Monnin and Galinier determined a nearly complete set of Pitzer coefficients for 25 °C /MON 88/ and eleven years later extended their work to elevated temperatures and pressures /MON 99/. Another model is available from /SAF 14/. There are some doubts, whether for these publications the literature had been gone through as thoroughly as had been done for the report by GRS /ALT 11/. At any rate it does not seem necessary to adopt analogous values for the interaction between Mg and Ca, as practised in a report by the former FZKA-INE (today KIT-INE) /ALT 04/. Another problem is that the solubility constants and Pitzer coefficients from Monnin et al. cannot be adopted straightforwardly as they are probably not consistent with the THEREDA database. Recently, a Pitzer database was released from THEREDA.

Tab. 5.8 Solubility data for Sr at different geochemical conditions

Study	Solubility limit [Mol/l]			Remark			
	BE	Min	Max				
-acid	10 ⁻³	10 ⁻⁶	10 ⁰	emplacement sites with vitrified glass and SNF (not applied) emplacement sites with cementitious material drifts; mixing of different brine compositions			
-neutral	10 ⁻³	10 ⁻⁶	10 ⁰				
-alkaline	10 ⁻⁵	10 ⁻⁶	10 ⁴				
-unknown	10 ⁻³	10 ⁻⁶	10 ⁰				
GRS	Range			Mineral phase (+Fe)	Mineral phase	Relevant species (+Fe)	Relevant species
HLW, sol. 1	10 ⁻² – 10 ⁻⁵			(Ba,Sr,Ra)SO ₄ (cr)		Sr ²⁺	Sr ²⁺ , SrSO ₄
HLW, sol. 3	10 ⁻³ – 10 ⁻⁵			(Ba,Sr,Ra)SO ₄ (cr)		Sr ²⁺ , SrSO ₄	Sr ²⁺ , SrSO ₄
SF, sol. 1	10 ⁻⁴ – 10 ⁻⁶			(Ba,Sr,Ra)SO ₄ (cr)		Sr ²⁺ , SrSO ₄	Sr ²⁺ , SrSO ₄
SF, sol. 3	10 ⁻⁴ – 10 ⁻⁶			(Ba,Sr,Ra)SO ₄ (cr)		Sr ²⁺	Sr ²⁺ , SrSO ₄

BE = best estimate

5.3.11 Technetium

Tc-99 is a long-term relevant fission product in HLW and spent fuel. It is a redox sensitive element. The most stable redox states for Tc are IV and VII. This radioelement may be rather immobile under reducing conditions due to the high stability of Tc(IV) phases. Under oxidising conditions, though, it exhibits high solubilities given the large stability of aqueous Tc(VII) complexes, mainly in the form of TcO_4^- .

Thermodynamic data and Pitzer coefficients for Tc(VII) (as for the actinides) were adopted from the INE-database, as documented in /ALT 04/. All Pitzer coefficients for technetium adopted from /ALT 04/ are listed in the annex A 2

Tab. 5.9 Solubility data for Tc at different geochemical conditions

Study	Solubility limit [Mol/l]			Remark		
	B.E.	Min	Max			
-acid	10^{-4}	10^{-8}	10^0	emplacement sites with vitrified glass and SNF (not applied) emplacement sites with cementitious material drifts; mixing of different brine compositions		
-neutral	10^{-4}	10^{-8}	10^0			
-alkaline	10^{-4}	10^{-8}	10^0			
-unknown	10^{-4}	10^{-8}	10^0			
GRS	Range		Mineral phase (+Fe)	Mineral phase	Relevant species (+Fe)	Relevant species
HLW, sol. 1	10^{-8} - 10^{-9} (Tc ^{+IV})		TcO ₂ ·1.6H ₂ O(s)	TcO ₂ ·1.6H ₂ O(s)	TcO(OH) ₂	TcO(OH) ₂
HLW, sol. 3	10^{-1} (Tc ^{+VII})- 10^{-9} (Tc ^{+IV})		TcO ₂ ·1.6H ₂ O(s)	KTcO ₄	TcO(OH) ₂ , TcO(OH) ₃ ⁻	TcO ₄ ⁻
SF, sol. 1	10^{-8} – 10^{-9} (Tc ^{+IV})		TcO ₂ ·1.6H ₂ O(s)	TcO ₂ ·1.6H ₂ O(s)	TcO(OH) ₂	TcO(OH) ₂
SF, sol. 3	10^{-8} – 10^{-9} (Tc ^{+IV})		TcO ₂ ·1.6H ₂ O(s)	TcO ₂ ·1.6H ₂ O(s)	TcO(OH) ₃ ⁻	TcO(OH) ₂
VSG	BE values		Mineral phase		Species	
NaCl, pH 6	Tc ^{+IV} 10^{-6}	Tc ^{+VII} $>10^{-1}$	TcO ₂ ·xH ₂ O (am)	TcO ₂ ·xH ₂ O (am)	Tc(OH) ₄ (col)	TcO ₄ ⁻
NaCl, pH 9	10^{-6}	$>10^{-1}$				
MgCl ₂ , pH 6	10^{-6}	$>10^{-1}$				
MgCl ₂ , pH 9	10^{-6}	$>10^{-1}$				

BE = best estimate

In our calculations Tc occurs in redox state +7 as TcO_4^- in the most oxidising system of HLW in solution 3 under absence of iron and the solubility is in the range of 10^{-1} mol/l, determined by the mineral phase KTcO_4 , (Tab. 5.9). In all other systems the conditions are more reducing and Tc is present in redox state +4. Under these conditions its

solubility is determined by the hydrous oxide $TcO_2 \cdot 1.6H_2O(s)$ yielding concentrations in the range between 10^{-8} to 10^{-9} mol/l. The most relevant complexes in solution are $Tc(O)(OH)_2$ and $Tc(O)(OH)_3^-$. KIT-INE proposes a value of 10^{-6} mol/l for the VSG but assuming an increase by two to three orders of magnitude due to the formation of intrinsic colloids. KIT INE derived from experimental investigations a stability constant for tetra-valent actinide colloids $\log K_{coll} = 2.5 \pm 0.8$ for the reaction $An(OH)_4(aq) = An(OH)(coll)$ /KIE 12/.

5.3.12 Tin

Sn-126 is a long-term safety relevant fission product contained in HLW and spent fuel. Under reducing conditions, it occurred as Sn(II), the presence of oxidizing agents leads to Sn(IV). The elements Sn was excluded from the calculation as at that time no reliable data applicable for high-saline solutions were available. As to our present knowledge this situation has not changed.

The data used in SAM are compiled in Tab. 5.10.

Tab. 5.10 Solubility data for Sn at different geochemical conditions

Study	Solubility limit [Mol/l]			Remark
	BE	Min	Max	
-acid	10^{-2}	10^{-3}	10^{-1}	emplacement sites with vitrified glass and SNF (not applied)
-neutral	10^{-4}	10^{-7}	10^{-1}	
-alkaline	10^{-5}	10^{-7}	10^{-3}	emplacement sites with cementitious material drifts; mixing of different brine compositions
-unknown	10^{-4}	10^{-7}	10^{-1}	

BE = best estimate

5.3.13 Zirconium

The isotope Zr-93 is a fission product occurring in HLW and spent fuel and considered as relevant for long-term safety. Zirconium is a transition metal that belongs to group 4 in the periodic table of the elements. It occurs predominantly in the tetravalent valence state.

In our calculations Zr was assumed to occur as Zr^{4+} , $Zr(OH)_3^+$, $Zr(OH)_2^{2+}$, and $Zr(OH)_4(aq)$. $ZrOH_4(am)(fresh)$ was assumed to be the only solid phase for Zr. Standard thermodynamic data were adopted from /MOM 05/.

As expected, there is no pH-dependence of the solubility of $ZrOH_4(am)$ in the pH range studied, given that the aqueous speciation is fully dominated by $Zr(OH)_4(aq)$, as shown in Tab. 5.11. In all considered systems the maximum concentration in the range between 10^{-5} to 10^{-6} mol/l is calculated. These values are in good agreement with the maximum concentrations given by KIT-INE of 10^{-6} mol/l, where again the assumption of intrinsic colloids results in an increase of two orders of magnitude /KIE 12/.

Tab. 5.11 Solubility data for Zr at different geochemical conditions

Study	Solubility limit [Mol/l]			Remark			
	BE	Min	Max				
SAM							
-acid	10^{-6}	10^{-8}	10^{-4}	emplacement sites with vitrified glass and SNF (not applied) emplacement sites with cementitious material drifts; mixing of different brine compositions			
-neutral	10^{-6}	10^{-8}	10^{-4}				
-alkaline	10^{-8}	10^{-10}	10^{-6}				
-unknown	10^{-7}	10^{-10}	10^{-4}				
GRS	Range			Mineral phase (+Fe)	Mineral phase	Relevant species (+Fe)	Relevant species
HLW, sol. 1	$10^{-5} - 10^{-6}$			$ZrOH_4(am)$	$ZrOH_4(am)$	$Zr(OH)_4$	$Zr(OH)_4$
HLW, sol. 3	$10^{-5} - 10^{-6}$			$ZrOH_4(am)$	$ZrOH_4(am)$	$Zr(OH)_4$	$Zr(OH)_4$
SF, sol. 1	$10^{-5} - 10^{-6}$			$ZrOH_4(am)$	$ZrOH_4(am)$	$Zr(OH)_4$	$Zr(OH)_4$
SF, sol. 3	$10^{-5} - 10^{-6}$			$ZrOH_4(am)$	$ZrOH_4(am)$	$Zr(OH)_4$	$Zr(OH)_4$
VSG	BE			Mineral phase		Species	
NaCl, pH 6	10^{-6}			$Zr(OH)_4(am)$		$Zr(OH)_4(col)$	
NaCl, pH 9	10^{-6}						
MgCl ₂ , pH 6	10^{-6}						
MgCl ₂ , pH 9	10^{-6}						

BE = best estimate

Zirconium may form solid solutions with tetravalent actinides, thus offering the potential for an additional retention mechanism, see /HEI 88/.

5.4 Actinides and decay products

The second important group of radionuclides is represented by the four decay chains. These are isotopes of the actinides and radium. Most of the actinides are built by nuclear

reactions like neutron capture in the reactor and subsequent decay processes. A comprehensive thermodynamic database for actinides in high saline solutions was published in /ALT 04/. Data and parameters for the elements U, Np, Pu, Am, Th, Cm and Tc used in the calculations from GRS were adopted from this database.

Currently updated thermodynamic values are compiled in the German database for high saline conditions, THEREDA. In general, these data have not been used in the calculations from GRS (a few exceptions exist, which are denoted in the respective sections), since they have not been available at that time. But it is expected that the data for actinides in THEREDA are mostly identical to those from /ALT 04/. All Pitzer coefficients for actinides adopted from /ALT 04/ are listed in the annex A 2

5.4.1 Americium and curium

Americium and curium exist only in the trivalent state under the conditions expected in the disposal area. For the acquisition of thermodynamic data Cm(III) is considered as analogue for Am(III). Therefore, in the following results are discussed for Am(III) only.

For the range investigated the solubility of Americium is strongly dependent on the pH value. Its solubility in high saline solutions is well investigated and thermodynamic data for NaCl and Mg-/CaCl₂ systems are available /NEC 09/. Its solubility is mainly determined by the mineral phase Am(OH)₃.

Our calculations indicate that at lower pH values (5-6) in solution 1 with HLW, which acts as a source for phosphate, the mineral phase AmPO₄(am,hyd) seems to dominate the solubility with a maximum concentration in the range 10⁻⁶ to 10⁻⁸ mol/l, see Tab. 5.12. This is the main difference to data proposed by KIT-INE for solutions at pH 6 with a high solubility > 10⁻¹ mol/l. Nowadays it is recommended to apply data for the amorphous phase /KIE 12/, which was done here. Assuming amorphous Am(OH)₃ /ALT 11/ as determining mineral phase, maximum concentrations at pH values around 9 to 10 are between 10⁻⁶ and 10⁻⁷ mol/l for the HLW system and in the range of 10⁻² to 10⁻⁵ mol/l for the SF system at pH-values around 8. The values proposed for VSG at a pH 9 are at the upper range of the values calculated here. In the calculations Am-hydroxo and Am-silicate-hydroxo complexes appeared as relevant complexes in solution.

Tab. 5.12 Solubility data for Am at different geochemical conditions derived from previous studies

Study	Solubility limit [Mol/l]				
SAM	BE	Min	Max	Remark	
-acid	10 ⁻⁴	10 ⁻⁷	10 ⁻¹	emplacement sites with vitrified glass and SNF (not applied) emplacement sites with cementitious material drifts; mixing of different brine compositions	
-neutral	10 ⁻⁵	10 ⁻⁷	10 ⁻³		
-alkaline	10 ⁻⁷	10 ⁻⁹	10 ⁻⁵		
-unknown	10 ⁻⁵	10 ⁻⁹	10 ⁻¹		
GRS	Range		Mineral phase	Relevant species (+Fe)	Relevant species
-HLW, sol.1	10 ⁻⁶ – 10 ⁻⁸		AmPO ₄ (am,hyd)	Am(SiO)(OH) ₃ ²⁺	Am(SiO)(OH) ₃ ²⁺ , Am(SO ₄) ⁺
-HLW, sol. 3	10 ⁻⁶ – 10 ⁻⁷		Am(OH) ₃ (am)	Am(OH) ₂ ⁺ , Am(SiO)(OH) ₃ ²⁺	Am(SiO)(OH) ₃ ²⁺ , Am(OH) ₂ ⁺
-SF, sol.1	10 ⁻² – 10 ⁻⁵		Am(OH) ₃ (am)	Am(OH) ₂ ⁺	Am(OH) ₂ ⁺
-SF, sol. 3	10 ⁻³ – 10 ⁻⁴		Am(OH) (am)	Am(OH) ₂ ⁺ , Am(OH) ²⁺	Am(OH) ₂ ⁺
VSG	BE		Mineral phase	Species	
NaCl, pH 6	>10 ⁻¹		Am(OH) ₃ (am)	Am ³⁺ Am(OH) ₂ ⁺ Am(OH) ²⁺	
NaCl, pH 9	10 ⁻⁵				
MgCl ₂ , pH 6	>10 ⁻¹				
MgCl ₂ , pH 9	10 ^{-4.5}				

BE = best estimate

Compared to the data used in the SAM study, higher solubilities are proposed for the alkaline conditions to date. For acidic conditions the values proposed for VSG are also much higher than for SAM, except the conditions, under which AmPO₄ is formed. This leads to a lower value as assumed in the SAM study. The solubility constant for AmPO₄(am,hyd) was selected in /ALT 04/ and derives from the Thermochemical Database (TDB) Project of OECD-NEA("NEA-TDB") It is based on a single publication by Rai et al. /RAI 92/. Due to the unknown stoichiometric composition this value must be regarded as questionable.

Given the fact that in some of our calculations AmPO₄(am,hyd) appeared as solubility limiting solid phase and the questionable quality of the applied solubility constant it seems justified for the future to have a closer look on the solubility of Am(III) in phosphate bearing solutions. Information from chemical analogous Cm can be used here as for example given in /MOL 11/.

5.4.2 Neptunium

Neptunium is another actinide with long-term relevant radioactive isotopes. Given its electronic configuration, this radioelement may be found at different oxidation states: +3, +4, +5 and +6 depending on the redox environment. However, the tetravalent and pentavalent redox states are of relevance for the conditions expected in a repository. Under more oxidizing conditions Np(V) is the preferred redox state, for reducing conditions Np(IV) is the dominating state.

In our calculations only one system (HLW in solution 3) is dominated by Np(V) species (Tab. 5.13). In this case the Np-solubility is controlled by $\text{Np}_2\text{O}_5(\text{s, hyd})$ in accordance with recommendations in /ALT 04/. This leads to maximum concentrations of 10^{-6} mol/l at pH 9 in the system HLW in solution 3. The maximum concentration proposed for the VSG for the pentavalent Np at pH 9 is about two to three orders of magnitude higher /KIE 12/.

Under the conditions of all other systems calculated by GRS the predominant redox state is Np(IV). The solubility of Np is then controlled by the mineral phase $\text{Np}(\text{OH})_4(\text{am})$. The relevant complexes in solution are $\text{Np}(\text{OH})_4$ and at lower pH values $\text{Np}(\text{OH})_3^+$. The concentration over the pH range of interest is calculated to about 10^{-9} mol/l. However, for the tetravalent Np intrinsic colloids might increase its concentration. In /KIE 12/ it is treated analogous to Th and concentrations are assumed to increase to 10^{-6} mol/l by formation of intrinsic colloids.

Under more oxidizing conditions, which did not occur in our calculations, Np(V) oxide (Np_2O_5) is expected to become the dominating mineral phase. Under such conditions the solubility of Np can increase by orders of magnitude, resulting in maximum concentrations in the range of 10^{-3} to 10^{-1} mol/l as shown by the results from KIT-INE for the VSG-study /KIE 12/.

Tab. 5.13 Solubility data for Np at different geochemical conditions derived from previous studies

Study	Solubility limit [Mol/l]					
SAM	BE	Min	Max	Remark		
-acid	10 ⁻⁵	10 ⁻⁶	10 ⁻⁴	emplacement sites with vitrified glass and SNF (not applied) emplacement sites with cementitious material drifts; mixing of different brine compositions		
-neutral	10 ⁻⁵	10 ⁻⁶	10 ⁻⁴			
-alkaline	10 ⁻⁷	10 ⁻⁸	10 ⁻⁶			
-unknown	10 ⁻⁶	10 ⁻⁸	10 ⁻⁴			
GRS	Range		Mineral phase (+Fe)	Mineral phase	Relevant species (+Fe)	Relevant species
-HLW, sol.1	10 ⁻⁸ – 10 ⁻⁹ (Np ^{+IV})		Np(OH) ₄ (am)	Np(OH) ₄ (am)	Np(OH) ₃ ⁺ , Np(OH) ₄ ⁺	Np(OH) ₃ ⁺ , Np(OH) ₄ ⁺
-HLW, sol.3	10 ⁻⁶ (Np ^{+V})– 10 ⁻⁹ (Np ^{+IV})		Np(OH) ₄ (am)	Np ₂ O ₅ (s, hyd)	NpOH ₄	NpO ₂ ⁺ , NpO ₂ (PO ₄) ₂ ²⁻ , NpO ₂ (OH)
-SF, sol.1	10 ⁻⁹ (Np ^{+IV})		Np(OH) ₄ (am)	Np(OH) ₄ (am)	NpOH ₄	NpOH ₄
-SF, sol. 3	10 ⁻⁹ (Np ^{+IV})		Np(OH) ₄ (am)	Np(OH) ₄ (am)	NpOH ₄	NpOH ₄
VSG	BE		Mineral phase		Species	
NaCl, pH 6	Np ^{+V} >10 ⁻¹	Np ^{+IV} 10 ^{-6.5}	Analog Th NpO ₂ ·xH ₂ O	Initially NpO ₂ OH(am) altered to Np ₂ OH(aged)	Np(OH) ₄ Np(OH) ₄ (coll)	
NaCl, pH 9	10 ^{-3.5}	10 ^{-6.5}				
MgCl ₂ , pH 6	>10 ⁻¹	10 ^{-6.5}				
MgCl ₂ , pH 9	10 ⁻³	10 ^{-6.5}				

BE = best estimate

5.4.3 Protactinium

Protactinium can occur in the +IV and +V oxidation state. Under repository conditions the aqueous speciation is dominated by PaO₂OH(aq) without dependence on either pH or pe of the system studied. The solid phase that may exert a solubility control is Pa₂O₅(s) and its solubility is also constant with pH and pe within the studied range of variability of these parameters.

The most important uncertainty concerning this element is that thermodynamic data for protactinium available in the literature is rather scarce. Therefore, Pa could not be considered in the calculations.

Data used in the SAM study are listed in Tab. 5.14.

Tab. 5.14 Solubility data for Pa at different geochemical conditions derived from previous studies

Study	Solubility limit [Mol/l]			Remark
	BE	Min	Max	
SAM				
-acid	10 ⁻⁶	10 ⁻⁸	10 ⁻⁴	emplacement sites with vitrified glass and SNF (not applied)
-neutral	10 ⁻⁶	10 ⁻⁸	10 ⁻⁴	
-alkaline	10 ⁻⁸	10 ⁻¹⁰	10 ⁻⁶	emplacement sites with cementitious material drifts; mixing of different brine compositions
-unknown	10 ⁻⁷	10 ⁻¹⁰	10 ⁻⁴	

BE = best estimate

5.4.4 Plutonium

Plutonium is another redox-sensitive actinide, which can occur in the redox states +3, +4, and +5 depending on the environmental redox conditions. Under very reducing conditions Pu(III) will be the most stable form in solution, which can lead to relatively high Pu concentrations, for neutral to slightly acid pH-values.

In agreement with the results of the VSG study concentrations for Pu(III) dominated systems at pH 6 are estimated to >10⁻⁴ mol/l and > 10^{-2.5} mol/l for NaCl and MgCl₂ systems, respectively based on experimental evidence /KIE 12/. For pH values around 8 to 9 the Pu concentration decreases to 10⁻⁸ to 10⁻⁹ mol/l (Tab. 5.15).

The maximum concentration for tetravalent Pu is calculated by GRS to 10⁻⁶ mol/l in the HLW system at pH around 6 where Pu(PO₄)(s,hyd) is considered as the solubility determining phase /ALT 04/. This value is two to three orders of magnitude higher as in a case where Pu(OH)₃(cr) is assumed as solubility determining phase.

In all systems determined by Pu(OH)₄(am) the maximum concentrations are in the range of 10⁻¹⁰ to 10⁻¹¹ mol/l (thermodynamic data used from /ALT 04/). The dominating PU(IV) complex in solution is Pu(OH)₄(aq). However, under the conditions calculated for the systems with spent fuel trivalent Pu species, sulphate and hydroxo complexes, become also relevant in solution. Maximum concentrations for Pu(IV) dominated systems proposed by KIT-INE assuming a similar solubility determining phase denoted as PuO₂(am) for the VSG study are higher with values of 10⁻⁸ mol/l. In the VSG-study, additionally intrinsic Pu(IV) colloids are considered leading to two to three orders of magnitude increased concentrations /KIE 12/, which are then in good agreement with the calculated values.

Tab. 5.15 Solubility data for Pu at different geochemical conditions

Study	Solubility limit [Mol/l]					
SAM	BE	Min	Max	Remark		
-acid	10 ⁻⁶	10 ⁻⁸	10 ⁻⁴	emplacement sites with vitrified glass and SNF (not applied) emplacement sites with cementitious material drifts; mixing of different brine compositions		
-neutral	10 ⁻⁶	10 ⁻⁸	10 ⁻⁴			
-alkaline	10 ⁻⁸	10 ⁻¹⁰	10 ⁻⁶			
-unknown	10 ⁻⁷	10 ⁻¹⁰	10 ⁻⁴			
GRS	Range		Mineral phase (+Fe)	Mineral phase	Relevant species (+Fe)	Relevant species
HLW, sol. 1	10 ⁻⁶ - 10 ⁻¹⁰ (Pu ^{+III} , Pu ^{+IV})		PuPO ₄ (am)	PuPO ₄ (am)	Pu(OH) ²⁺ Pu ³⁺	PuSO ₄ ⁺ , Pu(SO ₄) ₂ ⁻
HLW, sol. 3	10 ⁻¹⁰ - 10 ⁻¹¹ (Pu ^{+IV})		Pu(OH) ₄ (am)	Pu(OH) ₄ (am)	Pu(OH) ₄	Pu(OH) ₄
SF, sol. 1	10 ⁻¹⁰ - 10 ⁻¹¹ (Pu ^{+IV})		Pu(OH) ₄ (am)	Pu(OH) ₄ (am)	Pu(SO ₄) ⁺	Pu(SO ₄) ⁺ Pu(SO ₄) ₂ ⁻ Pu(OH) ²⁺
SF, sol. 3	10 ⁻¹⁰ - 10 ⁻¹¹ (Pu ^{+IV})		Pu(OH) ₄ (am)	Pu(OH) ₄ (am)	Pu(OH) ₄	Pu(OH) ₄
VSG	BE		Mineral phase		Species	
	Pu ^{+III}	Pu ^{+IV}				
NaCl, pH 6	>10 ⁻⁴	10 ⁻⁸	Pu(OH) ₃ (am), PuO ₂ (am)	PuO ₂ (am), PuO _{2+x} (s,hyd)	Pu(OH) ₄ (coll)	
NaCl, pH 9	10 ⁻⁸	10 ⁻⁸				
MgCl ₂ , pH 6	>10 ^{-2.5}	10 ⁻⁸				
MgCl ₂ , pH 9	10 ⁻⁸	10 ⁻⁸				

BE = best estimate

The high range for computed Pu-concentrations in solution 1 in HLW deserves an additional note: with metallic iron present, the calculation was terminated for numerical reason after a reaction progress of 0.001 kg/kg, while without metallic iron more vitrified waste reacted with solution (see section 4.5). The dissolution of the glass matrix releases sulphate ions to the solution which in turn form a complex with Pu³⁺. Formation of this complex leads to a higher solubility of Pu(III). In the light of this finding the lower solubility of 10⁻¹⁰ mol/kg caused by a too low SO₄ concentration can be considered as too low. A further uncertainty in these results is introduced by the fact that for the Pu(III)-sulphato complex no Pitzer coefficients are available.

Our calculations suggest investing further efforts into the interaction between trivalent plutonium and sulphate and the solubility of trivalent plutonium in phosphate bearing solutions. As discussed for Am, in a first step information from chemical analogous lanthanides(III) might be used, see e. g. /MOL 11/.

5.4.5 Radium

Isotopes of Ra are members of the decay chains and particularly Ra-226 was identified as dose relevant in previous safety assessments. Standard formation data for Ra^{2+} , RaCl^+ , $\text{RaCO}_3(\text{aq})$, RaOH^+ , and $\text{RaSO}_4(\text{aq})$ and for $\text{RaSO}_4(\text{cr})$ were adopted from /HUM 02/. Pitzer coefficients for the interaction of Ra^{2+} with HSO_4^- and SO_4^{2-} were adopted from /PAI 98/.

For calculations with HLW $\text{RaSO}_4(\text{cr})$ was added to the system to get the maximum likely Ra-concentration in solution. The mass was estimated according to the HLW inventory given in the VSG-study (assumption: 10.000 years after production). This was necessary because Ra was not considered in the inventory of HLW used in this study.

Tab. 5.16 Solubility data for Ra at different geochemical conditions

Study	Solubility limit [Mol/l]						
SAM	BE	Min	Max	Remark			
-acid	10^{-5}	10^{-8}	10^{-2}	emplacement sites with vitrified glass and SNF (not applied) emplacement sites with cementitious material drifts; mixing of different brine compositions			
-neutral	10^{-6}	10^{-8}	10^{-4}				
-alkaline	10^{-6}	10^{-8}	10^{-4}				
-unknown	10^{-5}	10^{-8}	10^{-2}				
GRS	Range			Mineral phase (+Fe)	Mineral phase	Relevant species (+Fe)	Relevant species
HLW, sol. 1	$10^{-8} - 10^{-11}$			(Ba,Sr,Ra) $\text{SO}_4(\text{cr})$		Ra^{2+} , RaCl^+	Ra^{2+} , RaCl^+
HLW, sol. 3	$10^{-10} - 10^{-11}$			(Ba,Sr,Ra) $\text{SO}_4(\text{cr})$		Ra^{2+}	Ra^{2+}
SF, sol. 1	$10^{-12} - 10^{-14}$			(Ba,Sr,Ra) $\text{SO}_4(\text{cr})$		Ra^{2+} , RaCl^+	Ra^{2+} , RaCl^+
SF, sol. 3	$10^{-12} - 10^{-14}$			(Ba,Sr,Ra) $\text{SO}_4(\text{cr})$		Ra^{2+} , RaCl^+	Ra^{2+} , RaCl^+

BE = best estimate

The GRS calculations indicate that Ra chemistry is dominated by Ra^{2+} and RaCl^+ complexes (Tab. 5.16). Maximum Ra-concentrations in the range of 10^{-4} to 10^{-5} mol/l are calculated, if as concentration determining mineral phase RaSO_4 is applied. However, it is more likely that the Ra concentration is determined by solid solutions of Ra-, Ba-, SrSO_4 . Under that assumption the solubility depends on the ratio of Sr, Ba and Ra in solution. With the Sr and Ba content of the vitrified glass and spent fuel mobile Ra concentrations of 10^{-8} mol/l to 10^{-11} mol/l for HLW and 10^{-12} to 10^{-14} mol/l for spent fuel are calculated. These concentrations are much lower than those applied in the SAM study.

Recently, a comprehensive study of all available data concerning thermodynamic properties of the Na, Ra – Cl, SO₄ – H₂O system has been published /ROS 11a/, /ROS 11b/, /ROS 12/. The study covers Pitzer coefficients as well as kinetic aspects and the formation of solid solutions. Ra may be dissolved in trace amounts in a number of divalent metal carbonates and –sulphates. The thermodynamic exact modelling of such solid solutions would require the calculation of activity of RaSO₄ (or RaCO₃) in the respective phase, which is dependent on its composition. However, as Ra is likely to be present in trace amounts only, the activity coefficient of the “solvent” (the bulk phase constituent) can be set to unity, just as in a diluted aqueous solution, while the activity coefficient of the Ra-component can be set constant. This together with the observed distribution coefficient for the Ra-component between aqueous phase and solid solution allows for a simplified, Henry-like modelling of the solid solution. Distribution coefficients and activity coefficients for Ra-compounds in a number of carbonates and sulphates are given in /LAN 85/ (noted in the work by /ROS 12/, but not for all phases numerically given). These studies add Pitzer coefficients for the interaction between Ra and chloride which are not present in the database used for this study.

In our calculation Ra was present in spent fuel only, and the calculated concentration did not exceed 10⁻¹³. Yet it seems necessary to keep this element in observation: in our calculations the ongoing radioactive decay, which might have increased the amount of radium in the system, was not modelled (see discussion above).

It is suggested to create a thermodynamic database for earth alkaline metal carbonates and sulphates (Sr, Ba, Ra) in THEREDA. In large parts this could be adopted from /MOO 14/.

5.4.6 Thorium

This radionuclide is exclusively found in the redox state +4 and can be considered a non redox sensitive radioelement. The concentration of thorium in groundwater seems to be limited by the solubility of amorphous thorium oxide ThO₂(am).

The systems with pH values around 8 to 9 show maximum concentrations of Th dominated by the mobile Th(OH)₄ and to some extent by the Th(OH)₃⁺ complex, see Tab. 5.17. For the system solution 1 with HLW at a pH value of 5 to 6 higher maximum concentrations up to 10⁻⁴ to 10⁻¹ mol/l were calculated. In these calculations the

concentrations of aqueous species are dominated by sulphate and phosphate complexes /ALT 04/.

For all other systems maximum concentrations are in the range of 10^{-8} to 10^{-9} M in agreement with results from KIT-INE for the VSG, where in systems without colloids data are in this range. Intrinsic colloids, however, can increase the concentration to 10^{-6} M over the considered range between pH 6 and 9 /KIE 12/.

Tab. 5.17 Solubility data for Th at different geochemical conditions derived from previous studies

Study	Solubility limit [Mol/l]			Remark		
	BE	Min	Max			
-acid	10^{-6}	10^{-8}	10^{-4}	emplacement sites with vitrified glass and SNF (not applied) emplacement sites with cementitious material drifts; mixing of different brine compositions		
-neutral	10^{-6}	10^{-8}	10^{-4}			
-alkaline	10^{-8}	10^{-10}	10^{-6}			
-unknown	10^{-7}	10^{-10}	10^{-4}			
GRS	Range		Mineral phase (+Fe)	Mineral phase	Relevant species (+Fe)	Relevant species
HLW, sol. 1	$10^{-3} - 10^{-5}$		Th(OH) ₄ (am)	Th(OH) ₄ (am)	Th(HPO ₄) ²⁺	Th(SO ₄) ₃ ²⁻ , ThSO ₄ ²⁺ , ThHPO ₄ ²⁺
HLW, sol. 3	$10^{-8} - 10^{-9}$		Th(OH) ₄ (am)	Th(OH) ₄ (am)	Th(OH) ₄	Th(OH) ₄
SF, sol. 1	$10^{-8} - 10^{-9}$		Th(OH) ₄ (am)	Th(OH) ₄ (am)	Th(OH) ₄ , Th(OH) ₃ ⁺	Th(OH) ₄
SF, sol. 3	$10^{-8} - 10^{-9}$		Th(OH) ₄ (am)	Th(OH) ₄ (am)	Th(OH) ₄	Th(OH) ₄
VSG	BE values		Mineral phase		Species	
NaCl, pH 6	10^{-6}		ThO ₂ ·xH ₂ O(am)		Th(OH) ₄ (coll)	
NaCl, pH 9	10^{-6}					
MgCl ₂ , pH 6	10^{-6}					
MgCl ₂ , pH 9	10^{-6}					

BE = best estimate

The calculations suggest investing further efforts into the interaction between thorium and sulphate and the solubility of thorium in phosphate bearing solutions.

5.4.7 Uranium

Uranium belongs to the actinide group. Uranium aqueous speciation is very dependent on pe and pH. Under reducing conditions, uranium is predominantly in the tetravalent state; at oxidizing conditions the hexavalent uranyl ion is the dominant component.

At pH values of 5 – 6 uranium concentrations can become rather high as summarized in Tab. 5.18. /KIE 12/ proposes for more oxidising conditions in NaCl-systems $10^{-4.5}$ mol/l as maximum uranium concentration and for $MgCl_2$ systems 10^{-2} at pH values of 6 assuming metaschoepite as the determining phase. In the GRS calculations for the conditions in system HLW in solution 1 with pH between 5 and 6 uranium in the aqueous phase is dominated by hexavalent uranyl chloro complexes with maximum concentrations in the range of 10^{-3} – 10^{-6} mol/l. The determining mineral phase is $U(OH)_4(am)$.

For HLW in brine 3 calculated maximum concentrations are in the range between 10^{-9} and 10^{-11} mol/l. In the more reducing system with iron the mineral determining phase is $U(OH)_4(am)$ with relevant tetravalent uranium complexes ($U(OH)_4$) and hexavalent hydroxo complexes. The system without iron is determined by the mineral $Na_2(UO_2)_2(SiO_5)_3 \cdot 4H_2O$ with hexavalent uranyl hydroxo complexes prevailing in solution.

In the spent fuel systems, the aqueous chemistry of uranium is mainly dominated by $U(OH)_4(aq)$ and to some extent $U(OH)_3^+$. In the systems without iron additionally uranyl hydroxo complexes play a role. The solubility will be controlled in solution 1 by $Ca(UO_2)_2(SiO_3OH)_2 \cdot 5H_2O$ and $Na_2(UO_2)_2(SiO_5)_3 \cdot 4H_2O$, respectively. In solution 3 again $U(OH)_4(am)$ /ALT 04/ is the determining mineral phase. The maximum uranium concentrations are calculated in the range of 10^{-8} to 10^{-9} M. If, analogous to the tetravalent Th, intrinsic U(IV) colloids are considered, the maximum concentrations increase to about 10^{-6} mol/l, i.e two and a half orders of magnitude higher, which is then in good agreement with the values given for U(IV) for the VSG by /KIE 12/.

Under more oxidising conditions concentrations for U(VI) might be controlled by either $Na_2U_2O_7$ in NaCl solutions and by metaschoepite in $MgCl_2$ systems as assumed in /KIE 12/. In the GRS calculations no ternary Mg/Ca-Uranyl-carbonate complexes have been considered at that time.

Tab. 5.18 Solubility data for U at different geochemical conditions derived from previous studies

Study	Solubility limit [Mol/l]					
SAM	B.E.	Min	Max	Remark		
-acid	10 ⁻⁴	10 ⁻⁶	10 ⁻²	emplacement sites with vitrified glass and SNF (not applied) emplacement sites with cementitious material drifts; mixing of different brine compositions		
-neutral	10 ⁻⁴	10 ⁻⁶	10 ⁻²			
-alkaline	10 ⁻⁴	10 ⁻⁶	10 ⁻²			
-unknown	10 ⁻⁴	10 ⁻⁶	10 ⁻²			
GRS	Range		Mineral phase (+Fe)	Mineral phase	Relevant species (+Fe)	Relevant species
HLW, sol. 1	10 ⁻³ – 10 ⁻⁶		U(OH) ₄ (am)	U(OH) ₄ (am)	UO ₂ ⁺ , UO ₂ Cl ⁺ , UO ₂ Cl ₂	UO ₂ Cl ⁺ , UO ₂ Cl ₂ , UO ₂ ⁺
HLW, sol. 3	10 ⁻⁹ – 10 ⁻¹¹		U(OH) ₄ (am)	Na ₂ (UO ₂) ₂ - (SiO ₅) ₃ x4H ₂ O	U(OH) ₄ UO ₂ (OH) ₃ ⁻ , UO ₂ (OH) ₄ ²⁻	UO ₂ (OH) ₃ ⁻ , UO ₂ (OH) ₄ ²⁻
SF, sol. 1	10 ⁻⁸ – 10 ⁻⁹		Ca(UO ₂) ₂ (SiO ₃ OH) ₂ x5H ₂ O	Na ₂ (UO ₂) ₂ - (SiO ₅) ₃ x4H ₂ O	U(OH) ₄ U(OH) ₃ ⁺	UO ₂ ⁺ , U(OH) ₄ UO ₂ (OH) ₂
SF, sol. 3	10 ⁻⁸ – 10 ⁻⁹		U(OH) ₄ (am)	U(OH) ₄ (am)	U(OH) ₄ U(OH) ₃ ⁺	U(OH) ₄ UO ₂ (OH) ₂ , UO ₂ (OH) ₃ ⁻
VSG	BE		Mineral phase		Species	
	U(IV)	U(VI)	UO ₂ ·xH ₂ O	UO ₃ ·2H ₂ O	U(OH) ₄ (coll)	
NaCl, pH 6	10 ⁻⁶	10 ^{-4.5}				
NaCl, pH 9	10 ⁻⁶	10 ^{-6.5}				
MgCl ₂ , pH 6	10 ⁻⁶	>10 ⁻²				
MgCl ₂ , pH 9	10 ⁻⁶	10 ^{-5.5}				

BE = best estimate

Future activities for an improvement of the thermodynamic database for uranium could be directed at the potential formation of CaU(PO₄)₂·2H₂O(cr) (ningyoite) which is besides coffinite and uraninite an important ore mineral /LAN 78/. Uranium may also form ternary complexes with carbonate for which thermodynamic data are available /ALT 11/. For the application to Mg-rich brines Pitzer coefficients with Mg are missing.

6 Summary and conclusions

The objective of this work was to assess the maximum likely solubilities to be used in long-term safety assessment for a high saline environment. For this purpose, existing thermodynamic data from different sources were combined into a single database. Efforts were made to ensure internal data consistency. However, due to the very comprehensive range of elements covered in the calculations, the complexity of the calculated systems, and the often rather limited experimental evidence for some of the data, calculated solubilities presented in this report must be regarded as estimates. Further studies are underway in order to acquire experimental data for the pH dependent solubility of relevant radionuclides in salt solutions (project LÖVE¹¹).

Thermodynamic equilibrium calculations were performed not regarding kinetic effects and retention processes for two representative emplacement areas of a repository in rock salt, namely a borehole for disposal of vitrified waste and a drift for disposal of spent fuel elements. Although the safety concept for a repository in salt is based on a safe containment of the waste, scenarios have to be considered for which an impairment of the barrier integrity and therefore the development of a pathway for brines to the waste cannot be excluded a priori. In order to account for the uncertainties of the inflowing solution two different solutions, namely a magnesium rich and a sodium chloride solution containing small amounts of CaSO_4 have been considered. Interactions of the inflowing solution with cementitious materials, which is intended to be used in drift or shaft sealings, were not considered here. To analyse these interactions additional geochemical calculations are necessary. Results from R&D projects LAVA and LAVA2 /JAN 18/ have to be considered. This kind of calculations is not straightforward and requires further R&D efforts.

Based on the evolution of the geochemical conditions in each regarded system, maximum solubilities have been calculated for the elements with long-term safety relevant radioisotopes. The results of these calculations have been compared with data derived in the past for the SAM study and data previously proposed for the VSG. Based on the evaluation of these calculations Tab. 6.1 has been compiled.

¹¹ FKZ 02E11365

Tab. 6.1 Proposed solubility determining solid phase, calculated solubility limit, relevance for long term Safety (LTS), uncertainty and R&D needs for elements with relevant radionuclides (see text for explanation)

Element	Proposed solid phase for reducing conditions (Calc. solubility limit)	Relevance for LTS	Uncertainty	R&D needs	THEREDA
Am, Cm	Am(OH) ₃ (am), AmPO ₄ (am,hyd), (10 ⁻³ -10 ⁻⁸)	±	±	±	yes
C	Unknown	++	++	++	yes
Cl	n.l.	+	±	+	yes
Cs	n.l.	++	--	-	yes
I	n.l.	++	±	+	no
Mo	CaMoO ₄ (10 ⁻³ -10 ⁻⁶)	-	+	±	no
Nb	Unknown	±	++	+	no
Ni	α-NiS	±	++	+	no
Np	Np(OH) ₄ (am) (10 ⁻⁸ – 10 ⁻⁹)	+	-	-	yes
Pa	Unknown	-	++	-	no
Pd	Unknown	-	++	±	no
Pu	Pu(OH) ₄ (am) *, PuPO ₄ (am) (10 ⁻⁶ – 10 ⁻¹¹)	+	±	±	yes
Ra	(Ba,Sr,Ra)SO ₄ (cr) (10 ⁻⁸ – 10 ⁻¹⁴)	++	±	+	no
Rb	n.l.	--	--	--	no
Se	Se(cr), Heavy metal selenides (10 ⁻⁴ -10 ⁻¹³)	++	++	++	no
Sm	Unknown	--	+	-	no
Sn	Unknown	+	++	+	no
Sr	(Ba,Sr,Ra)SO ₄ (cr) (10 ⁻² -10 ⁻⁶)	--	±	-	yes
Tc	TcO ₂ ·1.6H ₂ O(s) (10 ⁻⁸ -10 ⁻⁹)*	±	-	-	yes
Th	Th(OH) ₄ (am)* (10 ⁻³ -10 ⁻⁹)	±	+	+	yes
U	U(OH) ₄ (am)* Ca(UO ₂) ₂ (SiO ₃ OH) ₂ ·5H ₂ O (10 ⁻³ -10 ⁻¹¹)	++	±	+	yes
Zr	ZrOH ₄ (am) (10 ⁻⁵ -10 ⁻⁶)*	-	±	-	no

n.l. = not limited, ++ = high, + = high/medium, 0 = medium, - = medium/low, -- = low, * = solubility could be increased by colloid formation by 2.5 orders of magnitude /KIE 12/

This table contains for each element

- i. information about the solubility determining phase and the calculated value range, if possible,
- ii. the relevance for long-term safety assessment, which is based on the results from previous safety analyses,

- iii. the uncertainty with respect to the knowledge and available information for geo-chemical calculation of each element, and
- iv. the R&D needs, and
- v. whether thermodynamic data for the respective element exist in THEREDA.

For the columns ii, iii and iv a classification system is used as denoted in the footnote to Tab. 6.1.

The evaluation of the R&D needs is based on both, the relevance for long-term safety and the measure of the uncertainty. The measure of uncertainty is not restricted to solubility but also to retention processes, e. g. isotopic exchange in case of chlorine or co-precipitation of iodine in secondary mineral phases. In the following paragraphs only those elements are considered, which were marked with + or ++ under R&D needs in Tab. 6.1.

Carbon: The speciation of carbon when released from spent fuel elements is largely unknown. This was subject of the R&D project CAST (Final report under preparation). Organic acids may contribute to the complexation of radionuclides which would call for the development of a respective Pitzer model.

Selenium: With regard to the extremely low solubility of elemental selenium and Se(-II) compounds it should be further evaluated if such compounds are really formed under repository conditions. The solubility of one important compound (FeSe) is foreseen to be investigated in the R&D project VESPA-II.

Another approach could be to apply potentiometric methods to determine solubility constants and – if necessary – Pitzer coefficients. Such an approach seems to be promising especially with regard to the extremely low solubilities of selenides.

Chlorine: Future efforts for chloride should focus on other retention mechanisms like surface complexation on secondary phase surfaces or co-precipitation. For Cl-36 incorporation into solid halides by isotopic exchange should be considered.

Iodine: Future efforts for iodine should focus on other retention mechanisms like surface complexation on secondary phase surfaces or co-precipitation, which is foreseen to be investigated in the R&D project VESPA-II. For iodine it should be established whether

elemental iodine $I_2(cr)$ is formed on the surface of corrosion phases, e. g. by oxidation of iodide under conditions where $I_2(cr)$ is thermodynamically stable.

Niobium: There is a general lack of thermodynamic data in high saline solutions for aqueous species of niobium.

Nickel: For a further development of the database it is recommended to have a specific look onto the solubility of Ni in the form of hydroxocarbonates if carbonate is considered to be part of the system. Nickelhydroxide as precipitation product in saline solutions without carbonate should be positively identified in dedicated solubility experiments, as it is not found in nature /GRA 97/. With carbonate the formation of solid solutions with Mg and Fe(II) should be investigated. For the implementation of sulphides an appropriate Pitzer model for HS^- would have to be implemented first.

Radium: It is suggested to create a thermodynamic database for earth alkaline metal carbonates and sulphates (Sr, Ba, Ra) in THEREDA. In large parts this could be adopted from /MOO 14/.

Tin: There is a general lack of thermodynamic data in high saline solutions for aqueous species of tin.

Thorium: The calculations suggest investing further efforts into the interaction between thorium and sulphate and the solubility of thorium in phosphate bearing solutions.

Uranium: Future activities for an improvement of the thermodynamic database for uranium should be directed at the potential formation of $CaU(PO_4)_2 \cdot 2H_2O(cr)$ (ningyosite) which is besides coffinite and uraninite an important ore mineral. Uranium may also form ternary complexes with carbonate for which thermodynamic data are missing. For the application to Mg-rich brines Pitzer coefficients with Mg are missing.

It is evident that for a number of fission products experimental solubility data as well as thermodynamic data are lacking. At the moment it is not possible to derive solubility limits for them. A two-track approach is proposed to close the gaps on both sides.

1. On the one hand it is necessary to acquire experimental solubility data for those radionuclides that so far were not so much in the focus of research activities – especially fission products that are not actinides or technetium. Such efforts are

currently undertaken in the project LÖVE. These solubility data are conditional in that they apply to the conditions under which they were determined only.

2. To allow the calculation of solubilities under varying conditions more efforts are necessary to develop a thermodynamic database. Such a database would include solubility constants for solid phases and stability constants for complex species in aqueous solution. For application to high-saline solutions the determination of interaction coefficients (e. g. "Pitzer coefficients") would be necessary. For many aqueous species some data are already available. Gaps should be identified and become subject of a dedicated research effort. These would probably include speciation of Se(-II), Tc(IV), Nb(V), Pd(II), Mo(III) and Sn(II) in alkaline, chloride and sulphate containing solutions. Some of the outlined missing data (e. g. Se(-II) and Tc(IV)) are addressed in part in the recently started project VESPA-II¹². It should be noted, however, that it is not within the scope of the project VESPA-II, to develop a ready-to-use thermodynamic database to be integrated in THEREDA. The remaining radionuclides and oxidation states would have to be addressed in future projects.

In general, application of speciation and solubility data to brines requires that sufficient ion interaction coefficients are available for the relevant aqueous species. Only for a minor fraction of radionuclide species such information is available. Alternative strategies are necessary to get at least rough but nevertheless reasonable estimates for such ion interaction coefficients. Several methods exist and will be documented and tested within the project LÖVE. Further work will be mandatory to adjust existing methods to complex formed by radionuclides.

Beside the radionuclides research needs are also identified for matrix elements contained in the geotechnical materials used in the repository:

Aluminium and silicon: Existing experimental data need to be integrated into a single internally consistent database, qualified for high saline solutions and including relevant solid phases in cementitious systems (THEREDA).

Barium: A polythermal Pitzer database for Sr, Ba, and Ra was presented in /MOO 14/ used in conjunction with the calculation of earth alkaline sulphate solubilities in high-

¹² FKZ 02E11607A

saline hydrothermal systems. This database should be integrated in THEREDA for future model calculations. However, data gaps persist for some high saline systems, e. g. concentrated MgCl_2 -solutions.

Boron: A reliable model for the speciation of boron in high saline solutions should be created. Prior to such efforts it is essential to determine the maximum possible concentration of boron after leaching experiments in highly mineralized solutions and with the particular glass in question for nuclear waste disposal.

Iron: For future advancements it should be considered to employ a stepwise approach for the creation of a thermodynamic database for iron. In a first step it could be acknowledged that in the near field of a repository only a limited range of conditions (e. g. pH) is of interest, and that a simplified speciation model could be sufficient for the modelling of the most important solid iron phases. In a second step the speciation model could be refined aiming at an improved understanding of redox reactions. It should be noted that the integration of experimental data from previous and running projects with reference to iron aiming at the development of an internally consistent database is not within the scope of any of these projects.

Sulfide: A Pitzer model for HS^- in high saline solutions is needed. Furthermore, solubility constants for relevant metal sulphides need to be critically evaluated. Some metal cations may form complexes with sulphide, which need to be considered in a comprehensive thermodynamic model for sulphide in high saline solutions.

Lithium: It is recommended to implement Pitzer coefficients for the most important interactions with the main components of high saline solutions in THEREDA. Existing experimental data could be used.

Phosphorus: Phosphate has a potential for complex formation and precipitation with actinides. Determination of new experimental data with regard to phosphate complexes and phosphate containing solid phases with radionuclides would be helpful. A revised database could change solubilities calculated here significantly.

7 References

- /ADV 01/ Advokat, T.; Jollivet, P.; Crovisier, J. L.; del Nero, M. (2001): Long-term alteration mechanisms in water for SON68 radioactive borosilicate glass. *Journal of Nuclear Materials*, Volume 298, 55-62.
- /ALT 04/ Altmaier, M.; Brendler, V.; Bosbach, D.; Kienzler, B.; Marquardt, Chr.; Neck, V.; Richter A. (2004): Sichtung, Zusammenstellung und Bewertung von Daten zur geochemischen Modellierung, Abschlussbericht Institut für Nukleare Entsorgung, Forschungszentrum Karlsruhe, FZK-INE 002/04.
- /ALT 11/ Altmaier, M.; Brendler, V.; Bube, C.; Neck, V., Marquardt, C.; Moog, H.C.; Richter, A.; Scharge, T.; Voigt, W.; Wilhelm, S.; Wilms, T.; Wollmann, G. (2011): THEREDA - Thermodynamische Referenzdatenbasis. Report GRS 265 (German), ISBN 978-3-939355-41-0, 876 pages. A short version is available in English from the authors upon request.
- /ATE 10/ Atencio, D.; Andrade, M. B.; Christy, A. G.; Giere, R.; Kartashov, P. M. (2010): The pyrochlore supergroup of minerals: nomenclature. In: *Can. Min.* 48, 673–698. DOI: 10.3749/canmin.48.3.673.
- /BAR 85/ Bard, A. J.; Parsons, R.; Jordan, J. (1985): *Standard Potentials in Aqueous Solution*. IUPAC, Marcel Dekker Inc., New York, Basel.
- /BEC 03/ Becker, D.A.; Buhmann, D.; Storck, R.; Alonso, J.; Cormenzana, J.L.; Hugli, M.; Van Gemert, F.; O'Sullivan, P.; Laciok, A.; Marivoet, J.; Sillen, X.; Norman, H.; Vieno, T.; Niemeyer, M. (2003): Testing of safety and performance indicators (SPIN). EUR 19965 EN, Brussels.
- /BER 14a/ Berner, U. (2014a): Solubility of radionuclides in a bentonite environment for provisional safety analyses for sgt-e2, Nagra, Tech. Rep. (14-06).
- /BER 14b/ Berner, U. (2014b): Solubility of radionuclides in a concrete environment for provisional safety analyses for SGT-E2. Nagra Tech. Rep. (14-07).
- /BET 08/ Bethke, C.M. (2008): *Geochemical and Biogeochemical Reaction Modeling*. Cambridge University Press.

- /BET 14a/ Bethke, C.M.; Yeakel, S. (2014): The Geochemist's Workbench Release 10.0: GWB Essentials Guide. University of Illinois, Urbana-Champaign, Illinois.
- /BET 14b/ Bethke, C.M.; Yeakel, S. (2014): The Geochemist's Workbench Release 10.0: Reference Manual. University of Illinois, Urbana-Champaign, Illinois.
- /BEU 12/ Beuth, T.; Bracke, G.; Buhmann, D.; Dresbach, C.; Keller, S.; Krone, J.; Lommerzheim, A.; Mönig, J.; Mrugalla, S.; Rübél, A.; Wolf, J. (2012): Szenarientwicklung: Methodik und Anwendung. Bericht zum Arbeitspaket 8, Vorläufige Sicherheitsanalyse für den Standort Gorleben. GRS-284, Gesellschaft für Anlagen- und Reaktorsicherheit (GRS) mbH, Köln.
- /BMU 10/ Bundesministerium für Umwelt, Naturschutz und Reaktorsicherheit (BMU): Sicherheitsanforderungen an die Endlagerung wärmeentwickelnder radioaktiver Abfälle. Bonn, Stand: 30. September 2010.
- /BIS 16/ Bischofer, B., Hagemann, S., Altmaier, M., Banik, N., Bosbach, D., Bracke, G., Brendler, V., Curtius, H., Finck, N., Franzen, C., Gaona, X., Geckeis, H., Hebrling, F., Herm, M., Kindlein, J., et al. (2016): Behaviour of long-lived fission and activation products in the nearfield of a nuclear waste repository and the possibilities of their retention. GRS-Bericht, No. 374, Gesellschaft für Anlagen- und Reaktorsicherheit (GRS) mbH, Braunschweig.
- /BOI 07/ Boily, J.-F., Seward, T. M., Charnock, J. M.: The hydrolysis and precipitation of Pd(II) in 0.6 mol kg⁻¹ NaCl: A potentiometric, spectrophotometric, and EXAFS study. *Geochim. Cosmochim. Acta*, Vol. 71, pp. 4834–4845, 2007.
- /BOR 10/ Borkowski, M.; Richmann, M.; Reed, D.; Xiong, Y. (2010): Complexation of Nd(III) with tetraborate ion and its effect on actinide(III) solubility in WIPP brine. *Radiochimica Acta*: Vol. 98, Migration 2009, 577-582.
- /BRA 62/ Braitsch, O. (1962): Entstehung und Stoffbestand der Salzlagerstätten: Springer-Verlag, Berlin.
Online verfügbar unter <http://entw-server.grs.de/12126/>.

- /BRA 71/ Braitsch, O. (1971): Salt Deposits. Their Origin and Composition. Springer-Verlag, Berlin, Heidelberg, New York.
- /BRE 99/ Bremer, M.; Christov, C. (1999): Erstellung einer Datenbasis zur Modellierung der Wechselwirkung von chrom-, kupfer- und nickelhaltigem Deponiegut mit Lösungen des Salzgesteins einer UTD. Abschlußbericht 02 C 0405, Bericht, 93 S.
- /BRU 92a/ Bruno, J.; Stumm, W.; Wersin, P.; Brandberg, F. (1992): On the influence of carbonate in mineral dissolution: I. The thermodynamics and kinetics of hematite dissolution in bicarbonate solutions at T = 25 °C. *Geochimica et Cosmochimica Acta* Vol. 56, 1139-1147.
- /BRU 92b/ Bruno, J.; Wersin, P.; Stumm, W. (1992): On the influence of carbonate in mineral dissolution: II. The solubility of FeCO₃ (s) at 25 °C and 1 atm total pressure. *Geochim. Cosmochim. Acta* Vol. 56, 1149-1155.
- /BRU 00/ Bruno J.; Duro, L. (2000): Reply to W. Hummel's comment on and correction to "On the influence of carbonate in mineral dissolution: 1. The thermodynamics and kinetics of hematite dissolution in bicarbonate solutions at T = 25 °C" by J. Bruno, W. Stumm, P. Wersin, and F. Brandberg. *Geochimica et Cosmochimica Acta*, Vol. 64, 2173–2176.
- /BUH 91/ Buhmann, D.; Nies, A.; Storck, R. (1991): Analyse der Langzeitsicherheit von Endlagerkonzepten für wärmeerzeugende radioaktive Abfälle. GSF-Bericht 27/91. GSF – Forschungszentrum für Umwelt und Gesundheit GmbH, Braunschweig.
- /BUH 99/ Buhmann, D. (1999): Das Programmpaket EMOS. Ein Instrumentarium zur Analyse der Langzeitsicherheit von Endlagern. Gesellschaft für Anlagen- und Reaktorsicherheit (GRS) mbH, GRS-159, Braunschweig.

- /BUH 08/ Buhmann, D.; Mönig, J.; Wolf, J.; Heusermann, S.; Keller, S.; Weber, J.R.; Bollingerfehr, W.; Filbert, W.; Kreienmeyer, M.; Krone, J.; Tholen, M. (2008): Überprüfung und Bewertung des Instrumentariums für eine sicherheitliche Bewertung von Endlagern für HAW (Projekt ISIBEL). Gemeinsamer Bericht von DBE TECHNOLOGY GmbH, Bundesanstalt für Geowissenschaften und Rohstoffe (BGR) und Gesellschaft für Anlagen- und Reaktorsicherheit (GRS) mbH, DBE TECHNOLOGY GmbH, Peine.
- /CRA 11/ Crapse, K. P.; Kyser, E. A. (2011): Literature Review of Boric Acid Solubility Data. Savannah River Nuclear Solutions, LLC. Prepared for the U.S. Department of Energy under contract number DE-AC09-08SR22470. SRNL-STI-2011-00578.
- /CRU 07/ Cruywagen, J. J.; Kriek R. J. (2007): Complexation of palladium(II) with chloride and hydroxide. *Journal of Coordination Chemistry* 60, 439-447.
- /EUG 80/ Eugster, H.P.; Harvie, C.E.; Weare, J.H. (1980): Mineral equilibria in a six-component seawater system, Na-K-Mg-Ca-SO₄-Cl-H₂O, at 25 °C. ISSN 0016-7037, *Geochimica et Cosmochimica Acta*, 44, 1335-1347.
- /FEL 92/ Felmy, A.R.; Marvin, D.R.; Mason J. (1992): The Solubility of CaMoO₄(c) and an Aqueous Thermodynamic Model for Ca²⁺- MoO₄²⁻ Ion -Interactions. *Journal of Solution Chemistry*, Vol. 21, 525-532.
- /GIF 14/ Giffaut, E.; Grivé, M.; Blanc, Ph.; Vieillard, Ph.; Colàs, E.; Gailhanou, H.; Gaboreau, S.; Marty, N.; Madé, B.; Duro L. (2014): Andra thermodynamic database for performance assessment: ThermoChimie, *Applied Geochemistry*, Volume 49, 225-236.
- /GIN 94/ S. Godon, G.N.; Mestre, J.P.; Vernaz E.Y. (1994): Experimental investigation of aqueous corrosion of R7T7 nuclear glass at 90 °C in the presence of organic species. *Applied Geochemistry* 9, 255-269.
- /GRA 92/ Grambow, B.; Müller, R.; Rother, A. (1992): Determination of molybdate mean ionic activity coefficients for the assessment of radionuclide mobility, *Radiochim. Acta* (58-59), 71-77.

- /GRA 96/ Grambow, B.; Lutze, W.; Kahl, L.; Geckeis, H.; Bohnert, E.; Loida, A.; Dressler, P. (1996): Long-Term Safety of Radioactive Waste Disposal. Retention of Pu, Am, Np and Tc in the Corrosion of COGEMA Glass R7T7 in Salt Solutions. Final Report. Forschungszentrum Karlsruhe: FZKA 5767.
- /GRA 99/ Grambow, B.; Bernotat, W.; Kelm, M. (1999): Erstellung eines integrierten Nahfeldmodells von Gebinden hochaktiver Abfälle im Salzstock Gorleben: geochemisch fundierter Quellterm für HAW-Glas, abgebrannte Brennelemente und Zement. HAW-Glas Auslaugverhalten und Freisetzung von Radionukliden. Forschungszentrum Karlsruhe - Institut für Nukleare Entsorgungstechnik, FZK-INE 07/99.
- /GRA 97/ Grambow, B.: Solubility limitations: an „old timer’s view“. In: I. Grenthe, I. Puigdomenech (1997): Modelling in aquatic chemistry. Nuclear Energy Agency (OECD).
- /HAG 12/ Hagemann, S.; Moog, H. C.; Herbert, H.-J.; Erich, A. (2012): Rückhaltung und thermodynamische Modellierung von Iod und Selen in hochsalinaren Lösungen, GRS-245, (BMWA: FKZ 02 E 9440 6, ISBN 978-3-939355-20-5.
- /HAG 15/ Hagemann, S.; Scharge, T.; Willms, T. (2015): Entwicklung einer thermodynamischen Datenbasis für ausgewählte Schwermetalle. GRS-244. ISBN 978-3-939355-18-2.
- /HAR 80/ Harvie, C.E.; Weare, J.H. (1980): The prediction of mineral solubilities in natural waters: the Na-K-Mg-Ca-Cl-SO₄-H₂O system from zero to high concentration at 25 °C. ISSN 0016-7037, *Geochimica et Cosmochimica Acta* 44, 981-997.
- /HAR 84/ Harvie, C.E.; Moller, N.; Weare, J.H. (1984): The prediction of mineral solubilities in natural waters, The Na-K-Mg-Ca-H-Cl-SO₄-OH-HCO₃-CO₃-CO₂-H₂O system to high ionic strengths at 25 °C. *Geochim. Cosmochim. Acta* 48, 723-751.
- /HEI 88/ Heimann, R.B.; Vandergraaf, T.T. (1988): Cubic zirconia as a candidate waste form for actinides: Dissolution studies. *Journal of Materials Science Letters* 7,6, 583-586. <http://dx.doi.org/10.1007/BF01730301>.

- /HER 00/ Herbert, H.-J. (2000): Zur Geochemie und geochemischen Modellierung hochsalinärer Lösungen mineralischer Rohstoffe. Geol. Jb., Reihe D, Heft SD1, Hannover.
- /HER 07/ Herbert, H.-J.; Schwand, A. (2000): Salzlösungszuflüsse im Salzbergbau Mitteldeutschlands. GRS-226, Gesellschaft für Anlagen- und Reaktorsicherheit (GRS) mbH, Köln.
- /HOE 41/ Höltje, R.; Geyer, R. (1941): Das Verhalten von Molybdänlösungen gegen Reduktionsmittel. In: Z. Anorg. Allg. Chem. 246, 243–257. DOI: 10.1002/zaac.19412460302.
- /HOS 85/ Hossain, S.; Podschaske, T.; Rimkus, D.; Stelte, N.; Storck, R.; Weber, P. (1985): Einzeluntersuchungen zur Radionuklidfreisetzung aus einem Modellsalzstock. Projekt Sicherheitsstudien Entsorgung (PSE). Fachband 15. Berlin.
- /HUM 00/ Hummel, W. (2000): Comment on “On the influence of carbonate in mineral dissolution: 1. The thermodynamics and kinetics of hematite dissolution in bicarbonate solutions at T = 25 °C” by J. Bruno, W. Stumm, P. Wersin, and F. Brandberg. Geochimica et Cosmochimica Acta, Vol. 64, 2167–2171.
- /HUM 02/ Hummel, W.; Berner, U.; Curti, E. (2002): NAGRA / PSI Chemical Thermodynamic Data Base 01/01. Nagra, Technical Report, 02 (16).
- /IID 12/ Iida, Y. (2012): Study on Migration Behaviour of Selenium for Safety Assessment of Radioactive Waste Disposal. Dissertation, Kyoto University.
- /INA 06/ Inagaki, Y.; Shinkai, A.; Idemitsu, K.; Arima, T.; Yoshikawa, H.; Yui, M. (2006): Aqueous alteration of Japanese simulated waste glass P0798 - Effects of alteration-phase formation on alteration rate and caesium retention. Journal of Nuclear Materials 354, 171–184.

- /JAN 18/ Jantschik, K.; Czaikowski, O.; Hertes, U.; Meyer, T.; Moog, H.C.; Zehle, B. (2018): Development of chemical-hydraulic models for the prediction of long-term sealing capacity of concrete based sealing materials in rock salt. Project Report for projects LAVA (funding number 02E1132) and LAVA-2 (funding number 02E1122). GRS-493. ISBN 978-3-946607-78-6.
- /JOH 97/ Jonson, L.H.; Tait, (1997): Release of segregated nuclides from spent fuel. SKB Technical Report 97-18.
- /JOR 09/ Lovera, J. A.; Graber, T.A.; Galleguillos, H.R. (2009): Correlation of solubilities for the NaCl C LiCl C H₂O system with the Pitzer model at 15, 25, 50, and 100 °C. CALPHAD: Computer Coupling of Phase Diagrams and Thermochemistry 33, 388–392.
- /KAN 02/ Kaneko, S.; Tanabe, H.; et al. (2002): A Study on the Chemical Forms and Migration Behavior of Carbon-14 Leached from the Simulated Hull Waste in the Underground Condition. Scientific Basis of Nuclear Waste Management, Boston.
- /KIE 00/ Kienzler, B.; Schüßler, W.; Metz, V. (2000): Berechnung der maximalen Radionuklidkonzentration im geochemischen Milieu des Nahfelds der Abfälle. In: Berechnung der maximalen Radionuklidkonzentrationen im geochemischen Milieu des Nahfeldes der Abfälle. FZL-INE 002/00.
- /KIE 01/ Kienzler, B.; Loida, A. (2001): Endlagerrelevante Eigenschaften von hochradioaktiven Abfallprodukten - Charakterisierung und Bewertung - Empfehlungen des Arbeitskreises HAW-Produkte. ISSN 0947-8620, Wissenschaftliche Berichte FZKA, 6651.
- /KIE 12/ Kienzler, B.; Altmeier, M.; Bube, Ch.; Metz, V. (2012): Radionuclide source term for HLW glass, spent nuclear fuel, and compacted hulls and end pieces (CSD-C waste). KIT Scientific Reports 7624.
- /KIM 88a/ Kim, H.-T.; Frederick Jr., W. J. (1988): Evaluation of Pitzer ion interaction parameters of aqueous electrolytes at 25 °C. 1. Single salt parameters, J. Chem. Eng. Data 33,2, 177-184.

- /KIM 88b/ Kim, H.-T.; Frederick Jr., W.J. (1988): Evaluation of Pitzer ion interaction parameters of aqueous mixed electrolyte solutions at 25 °C. 2. Ternary mixing parameters. ISSN 0021-9568, eISSN 1520-5134, Journal of Chemical and Engineering Data, 33, 278-283.
- /KIT 14/ Kitamura, A.; Doi, R.; Yoshida, Y. (2014): Update of JAEA-TDB: Update of Thermodynamic Data for Palladium and Tin, Refinement of Thermodynamic Data for Protactinium, and Preparation of PHREEQC Database for Use of the Brønsted-Guggenheim-Scatchard Model. JAEA-Data/Code 2014-009. Japan Atomic Energy Agency. June 2014./KTA 88/Kerntechnischer Ausschuss: KTA 3401.1. Reaktorsicherheitsbehälter aus Stahl, Teil 1: Werkstoffe und Erzeugnisformen; Fassung September 1988, BAnz Nr. 37a vom 22. Februar 1989.
- /KLA 08/ Klaus, J. (2008): Evaluation of $^{87}\text{Sr}/^{86}\text{Sr}$, $\delta^{18}\text{O}$, $\delta^2\text{H}$, and cation contents as geochemical tracers for provenance and flow paths of saline solutions in German Zechstein deposits. Dissertation. Georg-August-Universität zu Göttingen, Göttingen. Online verfügbar unter <http://ediss.uni-goettingen.de/bitstream/handle/11858/00-1735-0000-0006-B284-E/klaus.pdf?sequence=1>, zuletzt geprüft am 20.02.2018.
- /KUE 87/ Kühn, R.; Müller-Schmitz, S. (1987): Die Verteilung des Strontiums zwischen Anhydrit und Polyhalit im deutschen Zechstein. In: Kali und Steinsalz 9 (12), S. 396–399. Online verfügbar unter <http://entw-server.grs.de/3054/>.
- /LAN 78/ Langmuir, D. (1978): Uranium solution-mineral equilibria at low temperatures with applications to sedimentary ore deposits. Geochimica and Cosmochimica Acta 42, 547-569.
- /LAN 85/ Langmuir, D.; Riese, A.C. (1985): The thermodynamic properties of radium. Geochimica et Cosmochimica Acta 49, 1593-1601.
- /MAR 04/ Mariner, P.E. (2004): In-Drift Precipitates/Salts Model. Bechtel SAIC Company, LLC, 10.2172/840433, Technischer Bericht. DOI: 10.2172/840433.

- /MAT 07/ Matschei, Th.; Lothenbach, B.; Glasser, F.P. (2007): Thermodynamic properties of Portland cement hydrates in the system CaO-Al₂O₃-SiO₂-CaSO₄-CaCO₃-H₂O. *Cement and Concrete Research* 37, 1379–1410.
- /MCI 68/ McIntire, W. L. (1968): Effect of Temperature on the Partition of Rubidium between Sylvite Crystals and Aqueous Solutions. *GSA Special Papers* 88, 505-524. DOI: 10.1130/SPE88-p505.
- /MEN 98/ Ménard, O.; Advokat, T.; Ambrosi, J. P.; Michard, A. (1998): Behaviour of actinides (Th, U, Np and Pu) and rare earths (La, Ce and Nd) during aqueous leaching of a nuclear glass under geological disposal conditions. *Applied Geochemistry* 13, 105-126.
- /MEY 09/ Meyer, T.; Willms T. (2009): Geochemische Modellierung des Langzeitverhaltens von silikatischen und alumosilikatischen Materialien bis 90 °C. GRS-Report GRS-A-3493, Project Number BMBF 02-C-0993.
- /MOE 12/ Mönig, J.; Buhmann, D.; Rübél, A.; Wolf, J.; Baltes, B.; Fischer-Appelt, K. (2012): Sicherheits- und Nachweiskonzept. Bericht zum Arbeitspaket 4, Vorläufige Sicherheitsanalyse für den Standort Gorleben, GRS-277, Gesellschaft für Anlagen- und Reaktorsicherheit (GRS) mbH, Köln.
- /MOL 11/ Moll, H.; Brendler, V.; Bernhard, G. (2011): Aqueous curium(III) phosphate species characterized by time-resolved laser-induced fluorescence spectroscopy. *Radiochimica Acta* 99, 775-782.
- /MOM 05a/ Mompean, F.J.; Perrone, J.; Illemassène, M. (2005): Chemical Thermodynamics of Zirconium. Vol. 8 from Chemical Thermodynamics. OECD-NEA, Elsevier, Amsterdam.
- /MOM 05b/ Mompean, F.J.; Illemassène, M.; Perrone, J. (2005): Chemical Thermodynamics of Selenium. Vol. 7 from Chemical Thermodynamics. OECD-NEA, Elsevier, Amsterdam.
- /MON 88/ Monnin, Ch.; Galinier, C. (1988): The solubility of celestite and barite in electrolyte solutions and natural waters at 25 °C - A thermodynamic study. *Chemical Geology* 71, 283-296.

- /MON 99/ Monnin, C.: A thermodynamic model for the solubility of barite and celestite in electrolyte solutions and seawater to 200\textdegreeC and to 1kbar. *Chemical Geology*, Vol. 153, pp. 187–209, 1999.
- /MOO 04/ Moog, H. C.; Hagemann, S.; Rumyantsev, A. (2004): Isopiestic Investigation of the Systems FeCl₂ - (Na, K, Mg, Ca) - Cl - H₂O at 298.15 K, *Z. Physikal. Chemie* 218, 1063-1087.
- /MOO 14/ Moog, H. C.; Cannepin, R. (2014): Entwicklung einer thermodynamischen Datenbasis für die Geothermie (GeoDat) und Erstellung eines Reservoirmodells für den Standort Groß-Schönebeck. Report GRS - 337, 160p., ISBN 978-3-944161-17-4.
- /MOO 15/ Moog, H.C.; Bok, F.; Marquardt, C.M.; Brendler V. (2015): Disposal of nuclear waste in host rock formations featuring high-saline solutions – Implementation of a thermodynamic reference database (THEREDA). *Applied Geochemistry* 55, 72-84.
- /MOR 10/ Morales, J.W.; Galleguillos, H.R.; Graber, T.A.; Hernández-Luis, F. (2010): Activity coefficients of LiCl in (PEG 4000 + water) at T = (288.15, 298.15, and 308.15) K. *J. Chem. Thermodynamics* 42, 1255–1260.
- /NEC 09/ Neck, V.; Altmaier, M.; Rabung, T.; Lützenkirchen, J.; Fanghänel, T. (2009): Thermodynamics of trivalent actinides and neodymium in NaCl, MgCl₂, and CaCl₂ solutions: Solubility, hydrolysis, and ternary Ca-M(III)-OH complexes. *Pure and Applied Chemistry* 81, 1555-1568.
- /NEC 98/ Neck, V.; Könnecke, T.; Fanghänel, T. (1998): Activity coefficients and Pitzer parameters for the fission product ions Cs⁺ and TcO₄⁻ in the system Cs⁺/Na⁺/K⁺/Mg²⁺/Cl⁻/SO₄²⁻/TcO₄⁻/ H₂O at 25 °C. *Radiochimica Acta* 83, 75-80.
- /NEM 11/ Nemer, M.B.; Xiong, Y.; Ismail, A.E.; Jang, J. (2011): Solubility of Fe₂(OH)₃Cl (pure-iron end-member of hibbingite) in NaCl and Na₂SO₄ brines. *Chemical Geology* 280, 26–32.

- /PAB 87/ Pabalan, R.T.; Pitzer, K.S. (1987): Thermodynamics of concentrated electrolyte mixtures and the prediction of mineral solubilities to high temperatures for mixtures in the system Na-K-Mg-Cl-SO₄-OH-H₂O. *Geochimica et Cosmochimica Acta* 51, 2429-2443.
- /PAI 98/ Paige, C. R.; Kornicker, W. A.; Hileman, Jr., O. E.; Snodgrass, W. J. (1998): Solution equilibria for uranium ore processing: The BaSO₄-H₂SO₄-H₂O system and the RaSO₄-H₂SO₄-H₂O system, *Geochim. Cosmochim. Acta* 62, 15-23.
- /PAL 11 Palmer, D. A.; Bénézech, P.; Xiao, C. (2011): Solubility measurements of crystalline NiO in aqueous solution as a function of temperature and pH. In: *J. Solution Chem.* 40, 680–702.
- /PAR 13/ Parkhurst, D.L.; Appelo, C.A.J. (2013): Description of input and examples for PHREEQC version 3—A computer program for speciation, batch-reaction, one-dimensional transport, and inverse geochemical calculations: U.S. Geological Survey Techniques and Methods, book 6, chap. A43, 497 p., available only at <http://pubs.usgs.gov/tm/06/a43/>.
- /PET 07/ Petersen, K. (2007): The Thermochemistry Library ChemApp and its applications. *Int. J. Mat. Res. (formerly Z. Metallkd.)* 98 (2007) 10: 935-945. Carl Hanser Verlag GmbH & Co. Kg.
- /PIE 10/ Pierce, E.M.; Windisch, C.F.; Burton, S.D.; Bacon, D.H.; Cantrell, K.J.; Serne, R.J.; Kerisit, S.N.; Valenta, M.M.; Mattigod, S.V. (2010): Integrated Disposal Facility FY2010 Glass Testing Summary Report. Pacific Northwest National Laboratory, Prepared for the U.S. Department of Energy under Contract DE-AC05-76RL01830.
- /PIT 73a/ Pitzer, K.S. (1973): Thermodynamics of electrolytes: I. Theoretical basis and general equations. *J. Phys. Chem.* 77, 268-277.
- /PIT 73b/ Pitzer, K.S.; Mayorga, G. (1973): Thermodynamics of electrolytes: II. Activity and osmotic coefficients for strong electrolytes with one or both ions univalent. *J. Phys. Chem.* 77, 2300-2308.

- /PIT 74a/ Pitzer, K.S.; Mayorga, G. (1974): Thermodynamics of electrolytes: III. Activity and osmotic coefficients for 2-2 electrolytes. *J. Solution Chem.*, 3, 539-546.
- /PIT 74b/ Pitzer, K.S. (1974): Thermodynamics of electrolytes: IV. Activity and osmotic coefficients for mixed electrolytes. *J. Am. Chem. Soc.* 96, 5701-5707.
- /PIT 75/ Pitzer, K.S. (1975): Thermodynamics of electrolytes: V. Effects of higher-order electrostatic terms. *J. Solution Chem.* 4, 249-265.
- /PIT 91/ Pitzer, K.S. (1991): Activity coefficients in electrolyte solutions, 2nd edn, CRC, Boca Raton, Florida.
- /RAI 92/ Rai, D.; Felmy, A. R.; Fulton, R.W. (1992): Solubility and ion activity product of $\text{AmPO}_4 \cdot x\text{H}_2\text{O}(\text{am})$. *Radiochim. Acta* 56, 7-14.
- /RAI 95/ Rai, D.; Felmy, A.R.; Moore D.A. (1995): The Solubility Product of Crystalline Ferric Selenite Hexahydrate and the Complexation Constant of FeSeO_3^+ . *Journal of Solution Chemistry* 24, 735-752.
- /RAR 07/ Rard, J.A.; Clegg, S.L.; Palmer, D.A. (2007): Isopiestic Determination of the Osmotic and Activity Coefficients of $\text{Li}_2\text{SO}_4(\text{aq})$ at $T = 298.15$ and 323.15 K, and Representation with an Extended Ion-interaction (Pitzer) model. UCRL-JRNL-227057, *Journal of Solution Chemistry*.
- /REA 90/ Reardon, E.J. (1990): An ion interaction model for the determination of chemical equilibria in cement/water systems. ISSN 0008-8846, *Cement and Concrete Research* 20, 175-192.
- /ROS 11a/ Rosenberg, Y.O.; Metz, V.; Ganor, J. (2011): Co-precipitation of radium in high ionic strength systems - 1. Thermodynamic properties of the Na–Ra–Cl–SO₄–H₂O system – Estimating Pitzer parameters for RaCl_2 . *Geochimica et Cosmochimica Acta* 75, 5389–5402.
- /ROS 11b/ Rosenberg, Y.O.; Metz, V.; Oren, Y.; Volkman, Y.; Ganor J. (2011): Co-precipitation of radium in high ionic strength systems - 2. Kinetic and ionic strength effects. *Geochimica et Cosmochimica Acta* 75, 5403–5422.

- /ROS 12/ Rosenberg, Y.O.; Metz, V.; Ganor, J. (2012): Radium Removal in a Large Scale Evaporitic System, *Geochimica et Cosmochimica Acta* 103, 121-137.
- /RAR 97/ Rard, J.A. und Clegg, S.L. (1997): Critical evaluation of the thermodynamic properties of aqueous calcium chloride. 1. Osmotic and activity coefficients of 0-10,77 mol.kg⁻¹ aqueous calcium chloride solutions at 298.15 K and correlation with extended Pitzer ion-interaction models. ISSN 0021-9568, eISSN 1520-5134, *Journal of Chemical and Engineering Data*, 42, 819-849.
- /RUM 04/ Rumyantsev, A.; Hagemann, S.; Moog, H. C. (2004): Isopiestic Investigation of the Systems Fe₂(SO₄)₃ - H₂SO₄ - H₂O, FeCl₃ - H₂O, and Fe(III) - (Na, K, Mg, Ca)Cl_n - H₂O at 298.15 K, *Z. Physikal. Chemie* 218, 1089-1127.
- /SAF 14/ Safari, H., Shokrollahi, A., Moslemizadeh, A., Jamialahmadi, M., Ghazanfari, M. H.: Predicting the solubility of SrSO₄ in Na–Ca–Mg–Sr–Cl–SO₄–H₂O system at elevated temperatures and pressures. *Fluid Phase Equilibria*, Vol. 374, pp. 86–101, DOI 10.1016/j.fluid.2014.04.023, 2014.
- /SAV 12/ Savary, V.; Berger, G.; Dubois, M. (2012): The solubility of CO₂ + H₂S mixtures in water and 2M NaCl at 120 °C and pressures up to 35 Mpa. *International Journal of Greenhouse Gas Control* 10, 123-133.
- /SCH 12/ Scharge, T.; Munoz, A.G.; Moog, H.C. (2012): Activity Coefficients of Fission Products in Highly Salinary Solutions of Na⁺, K⁺, Mg²⁺, Ca²⁺, Cl⁻, and SO₄²⁻: Cs⁺. *J. Chem. Eng. Data* 57, 1637–1647.
- /SCH 13/ Scharge, T.; Munoz, A.G.; Moog, H.C. (2013): Thermodynamic modelling of high salinary phosphate solutions. I. Binary systems. *J. Chem. Thermodynamics* 64, 249–256.
- /SCH 13a/ Scharge, T.; Munoz, A.G.; Moog, H.C. (2013): Addition to “Activity Coefficients of Fission Products in Highly Salinary Solutions of Na⁺, K⁺, Mg²⁺, Ca²⁺, Cl⁻, and SO₄²⁻: Cs⁺”. *J. Chem. Eng. Data* 58, 187–188.
- /SCH 15/ Scharge, T.; Munoz, A.G.; Moog, H.C. (2015): Thermodynamic modeling of high salinary phosphate solutions II. Ternary and higher systems. *J. Chem. Thermodynamics* 80, 172-183.

- /SCH 11/ Schlesinger, M.E.; Brow R.K. (2011): Thermodynamic Development of Corrosion Rate Modeling in Iron Phosphate Glasses. Final report, NEUP Project CFP-09-800.
- /SCH 05/ Schmidt, C.; Thomas, R.; Heinrich W. (2005): Boron speciation in aqueous fluids at 22 to 600 °C and 0.1 MPa to 2 GPa. *Geochimica et Cosmochimica Acta*, Vol. 69, 275–281.
- /SCH 71/ Schock, H.H.; Puchelt, H. (1971): Rubidium and cesium distribution in salt minerals — I. Experimental investigations. *Geochimica et Cosmochimica Acta* 35,3, 307-317. [http://dx.doi.org/10.1016/0016-7037\(71\)90039-1](http://dx.doi.org/10.1016/0016-7037(71)90039-1).
- /SCO 14/ Scourse, E.; Williams, S. (2014): CArbon-14 Source Term CAST. Project Presentation (Deliverable D7.2). <http://www.projectcast.eu/publications>.
- /SON 84/ Sonnenfeld, P. (1984): *Brines and Evaporites*. – Verlag Academic Press, Inc., Orlando, San Diego, New York.
- /STU 81/ Stumm, W.; Morgan, J.J. (1981): *Aquatic Chemistry, Chemical Equilibria and Rates in Natural Waters*. John Wiley & Sons, Inc., New York.
- /TAI 91/ Tait, C.D.; Janecky, D.R.; Rogers, P.S. (1991): "Speciation of aqueous palladium (II) chloride solutions using optical spectroscopies." *Geochimica et Cosmochimica Acta* 55.5, 1253-1264.
- /TAN 07/ Tanabe, H. (2007): Characterization of hull waste in underground condition. International Workshop on Mobile Fission and Activation Products in Nuclear Waste Disposal (MoFAP), L'Hermitage, La Baule (France), 16-19.
- /VER 92/ Vernaz, E.Y.; Dussossoy J.L. (1992): Current state of knowledge of nuclear waste glass corrosion mechanisms: the case of R7T7 glass. *Applied Geochemistry*, Suppl. Issue No. 1, 13-22.
- /VER 01/ Vernaz, E.; Gin, S.; Jégou, C.; Ribet I. (2001): Present understanding of R7T7 glass alteration kinetics and their impact on long-term behavior modeling. *Journal of Nuclear Materials* 298, 27–36.

- /WAG 82/ Wagman, D.D.; Evans, W.H.; Parker, V.B.; Schumm, R.H.; Halow, I.; Bailey, S.M.; Churney, K.L.; Nuttall, R.L. (1982), The NBS Tables of Chemical Thermodynamic Properties: Selected Values for Inorganic and C1 and C2 Organic Substances in SI Units: American Chemical Society and the American Institute of Physics for the National Bureau of Standards (J. Phys. Chem. Ref. Data, V. 11, supp. 2, 392 p.). TIC: 248311.
- /WAN 10/ Wang, P.; Wilson, L.L.; Wesolowski, D.J.; Rosenqvist, J.; Anderko, A. (2010): Solution chemistry of Mo(III) and Mo(IV). Thermodynamic foundation for modeling localized corrosion. In: Corr. Sci. 52, 1625–1634.
- /WER 04/ Werme, L.; Johnson, L H; Oversby V M; King, F.; Spahiu, K.; Grambow, B.; Shoesmith, D.W. (2004): Spent fuel performance under repository conditions: A model for use in SR-Can. SKB Technical Report TR-04-19.
- /WER 14/ Wersin, P., Kiczka, M., Rosch, D. (2014): Safety case for the disposal of spent nuclear fuel at Olkiluoto. Radionuclide solubility limits and migration parameters for the canister and buffer. Posiva Rep, 2012-39.
- /WOL 02/ Wolery, T.J. (2002): EQ3/6 - Software for Geochemical Modeling, Version 8.0, UCRL-CODE-2003-009, Lawrence Livermore National Laboratory, Livermore, California.
- /WOL 92/ Wolery, T.J. (1992): EQ3/6, A software package for geochemical modeling of aqueous systems, UCRL-MA-110662 Part I, Lawrence Livermore National Laboratory, Livermore, California.
- /XIA 00/ Xia, J.; Pérez-Salado, A.; Kamps, R.; Rumpf, B.; Maurer, G. (2000): Solubility of hydrogen sulfide in aqueous solutions of single strong electrolytes sodium nitrate, ammonium nitrate, and sodium hydroxide at temperatures from 313 to 393 K and total pressures up to 10 MPa. Fluid Phase Equilibria 167, 263–284.
- /XUE 99/ Xuewu L.; Millero F. J. (1999): The solubility of iron hydroxide in sodium chloride solutions. Geochimica et Cosmochimica Acta 63, 3487–3497.

A Appendices

Contents of appendices

A 1	Calculation of the composition of model solutions	93
A 1.1	Speciation of model solutions without radio nuclides	94
A 1.1.1	Gipshut-solution – CO ₂	94
A 1.1.2	Q-brine – CO ₂	96
A 1.2	Preface to the calculations with actinides.....	98
A 1.3	Solubility of Americium.....	99
A 1.3.1	Gipshut solution	99
A 1.3.2	Q-Brine solution	103
A 1.4	Solubility of Neptunium(+V)	105
A 1.4.1	Gipshut solution	105
A 1.5	Solubility of Neptunium(+IV)	112
A 1.5.1	Gipshut solution	112
A 1.6	Solubility of Plutonium(+IV).....	115
A 1.6.1	Gipshut solution	115
A 1.7	Solubility of Uranium(+VI)	118
A 1.7.1	Gipshut solution	118
A 1.7.2	Q-Brine solution	123
A 2	Pitzer coefficients for actinides and Tc.....	126

A 1 Calculation of the composition of model solutions

Data and parameters for the elements U, Np, Pu, Am, Th, Cm were adopted from the INE-database, as documented in /ALT 04/. As a consequence, all calculations presented in our report, were performed with a database that was published four years after the completion of the INE-report, to which our report refers. Though we do not expect considerable differences between data used at INE in the years 2000 and 2004 in general, it cannot be excluded, that a few data were modified in the time between. It can therefore not be excluded altogether, that the database for calculations presented here is not entirely consistent with those data used for /KIE 00/.

In table 4 of their report /ALT 04/ INE tabulates three solutions, which were used for model calculations. Solution I is a so-called “Q-brine”. It is in thermodynamic equilibrium with halite (NaCl), sylvite (KCl), carnallite ($\text{KMgCl}_3 \cdot 6\text{H}_2\text{O}$), and kainite ($\text{KMgClSO}_4 \cdot 3\text{H}_2\text{O}$). Solution II (“CaCl₂-solution”) has a composition mutually agreed upon in the commission “HAW-Produkte”. Solution III (“Gipshut-Loesung”) contains NaCl and CaSO₄ only and is in thermodynamic equilibrium with halite and anhydrite (CaSO₄).

To check the ChemApp parameter file prepared for our calculations, all three solutions were calculated applying the following boundary conditions:

- Solution 1 (Q-brine): H₂O = 1000 mol, activities of halite, sylvite, carnallite, and kainite set to unity.
- Solution 2 (CaCl₂-solution): H₂O = 1000 mol, halite = 1,49 mol, sylvite = 0,4 mol, Mg²⁺ = 97,21 mol, Ca²⁺ = 5,68 mol, Cl⁻ = 205,78 mol, activity of anhydrite set to unity.
- Solution 3 (Gipshut-Loesung): H₂O = 1000 mol, activities of halite and anhydrite set to unity.

Tab. 7.1 compares the composition of all three solutions as given in the INE-report with our results. As reference for an additional checking of the parameter file it also contains a calculation of IP21-solution, being defined to be in equilibrium with halite, sylvite, carnallite, kainite, and polyhalite at 25 °C (activities set to unity). IP21-solution is not further considered in this report.

Tab. A1.1 Comparison of three model solutions as given from INE /KIE 00/, and calculated for this report with CHEMAPP (CA) and EQ3/6, with CA: pH and density calculated – Concentration unit: mol (1000 mol H₂O)⁻¹

Solution	Na	K	Mg	Ca	Cl	SO ₄	Remark
1(Q) INE	6.8	17.4	80.5	0	178.8	3.2	T=55 °C
CA	8.7	10.2	75.7	0	159.1	5.6	T=25 °C
EQ3/6	8.3	10.0	76.6	0	160.2	5.6	T=25°C
2 INE	1.49	0.4	97.21	5.69	207.67	0.01	T=25 °C
CA	1.49	0.4	97.21	5.68	207.67	0.004	T=25 °C
EQ3/6							
3 INE	112.2	0.33	0.33	0.66	112.2	1.234	T=55 °C
CA	109.4			0.779	109.4	0.779	T=25°C
EQ3/6	110.0			0.788	110.0	0.788	T=25°C
IP21 CA	8.67	10.23	75.74	0.01	159.12	5.65	T=25 °C
EQ3/6	8.34	10.02	76.56	0.01	160.20	5.65	T=25°C

A 1.1 Speciation of model solutions without radio nuclides

A 1.1.1 Gipshut-solution – CO₂

Synopsis:

Tab. A1.2 Gipshut-solution with CO₂

Step	Description
1.	Calculate 1 kg H ₂ O in equilibrium with halite and anhydrite and
a)	p(CO ₂) = 0.1 bar
b)	p(CO ₂) = 0.01 bar
2.	Set constant molar masses of halite, anhydrite, and CO ₂ from first step and check resulting solid phase activities and CO ₂ -fugacity.
3.	Titrate with 1 mol NaOH
The resulting stream for step 2 is:	
a)	55.5084391 mol H ₂ O 6.0716 mol NaCl 4.3254·10 ⁻² mol Anhydrite 1.0340·10 ⁻³ mol CO ₂ leading to p(CO ₂) = 0.1 bar with n(NaOH) = 0
b)	55.5084391 mol H ₂ O 6.0718 mol NaCl 4.3259·10 ⁻² mol Anhydrite 1.1054·10 ⁻⁴ mol CO ₂ leading to p(CO ₂) = 0.01 bar with n(NaOH) = 0

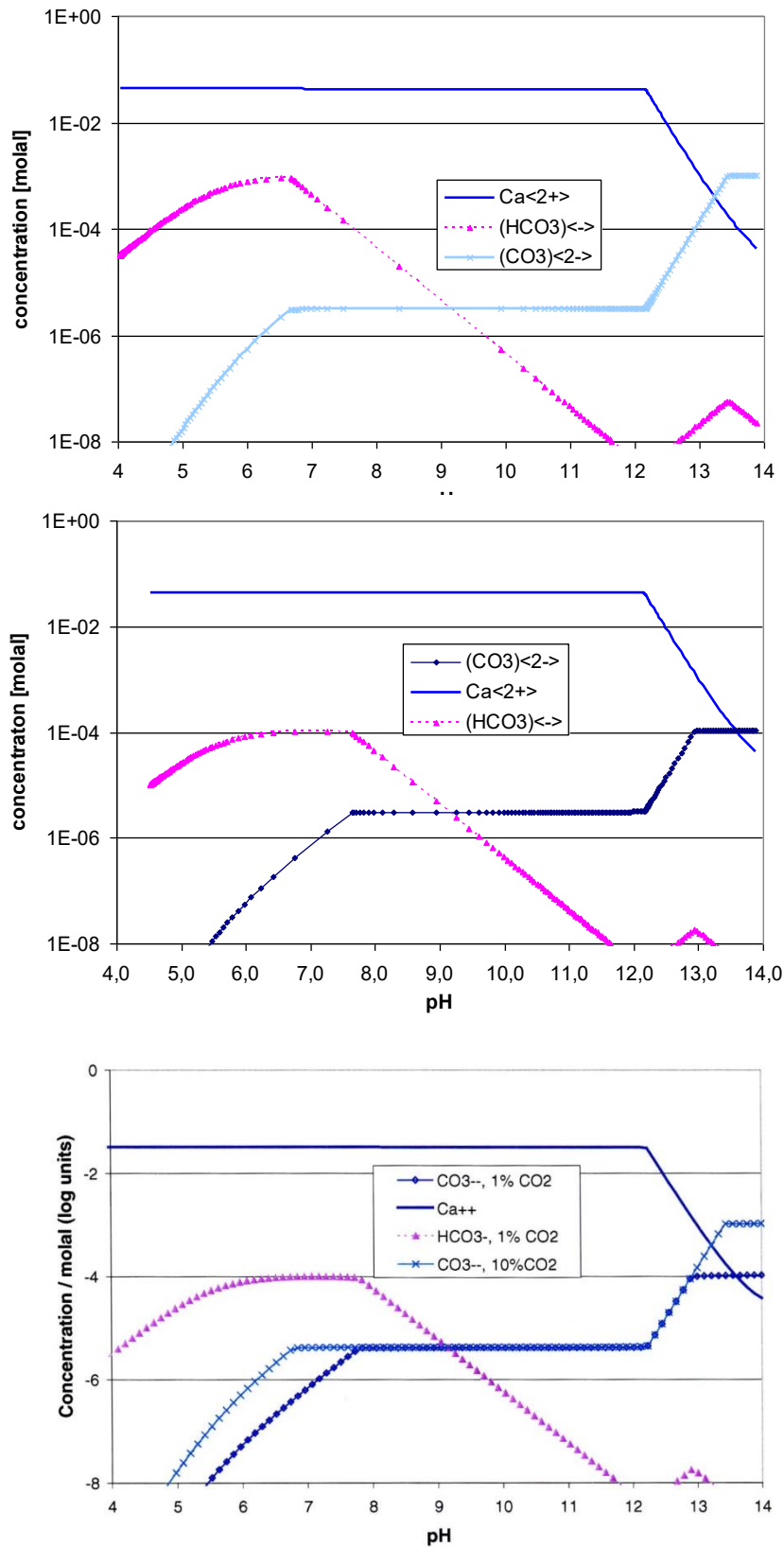


Fig. A1.1 C-speciation in Gipschut-solution: top = p(CO₂) = 0.1 bar (GRS), centre = p(CO₂) = 0.01 bar (GRS) and bottom = /KIE 00/

As can be taken from Fig. 7.1 calculations from GRS and INE are in excellent agreement. It should be noted, However, that all calculated equilibria do not correspond to an equilibrium partial pressure of CO₂ of 0.01 or 0.1 bar; the assumed total molar mass of CO₂ (n(CO₂)) corresponds to these partial pressures at n(NaOH) = 0 only. Along the titration path with NaOH and with a fixed total molar mass of CO₂ the partial pressure of CO₂ in equilibrium decreases. With p(CO₂) set constant the total mass of dissolved carbon would increase with pH, eventually leading to the precipitation of calcite and therefore leading to a complete different result.

Calculations with Gipshut-solution or Q-brine (next chapter) alone were performed in /KIE 00/ tacitly at constant n(CO₂). All solubility calculations with radionuclides, however, were performed at constant p(CO₂)!

A 1.1.2 Q-brine – CO₂

Tab. A1.3 Q-brine with CO₂

Step	Description
1.	Calculate 1 kg H ₂ O in equilibrium with halite, sylvite, carnallite, kainite and
a)	p(CO ₂) = 0.1 bar
b)	p(CO ₂) = 0.01 bar
2.	Set constant molar masses of halite, sylvite, carnallite, kainite and CO ₂ from first step and check resulting solid phase activities and CO ₂ -fugacity.
3.	Titrate with 1.69·10 ⁺¹ mol NaOH
The resulting stream for step 2 is:	
a)	55.5084391 mol H ₂ O 8.5619·10 ⁻¹ mol NaCl -6.4655 mol Sylvite 6.9181 mol Car- nallite 5.5705·10 ⁻¹ mol Kainite 1.2780·10 ⁻⁴ mol CO ₂ leading to p(CO ₂) = 0.01 bar with n(NaOH) = 0
b)	55.5084391 mol H ₂ O 8.5613·10 ⁻¹ mol NaCl -6.4655 mol Sylvite 6.9182 mol Car- nallite 5.5696·10 ⁻¹ mol Kainite 1.1554·10 ⁻³ mol CO ₂ leading to p(CO ₂) = 0.1 bar with n(NaOH) = 0

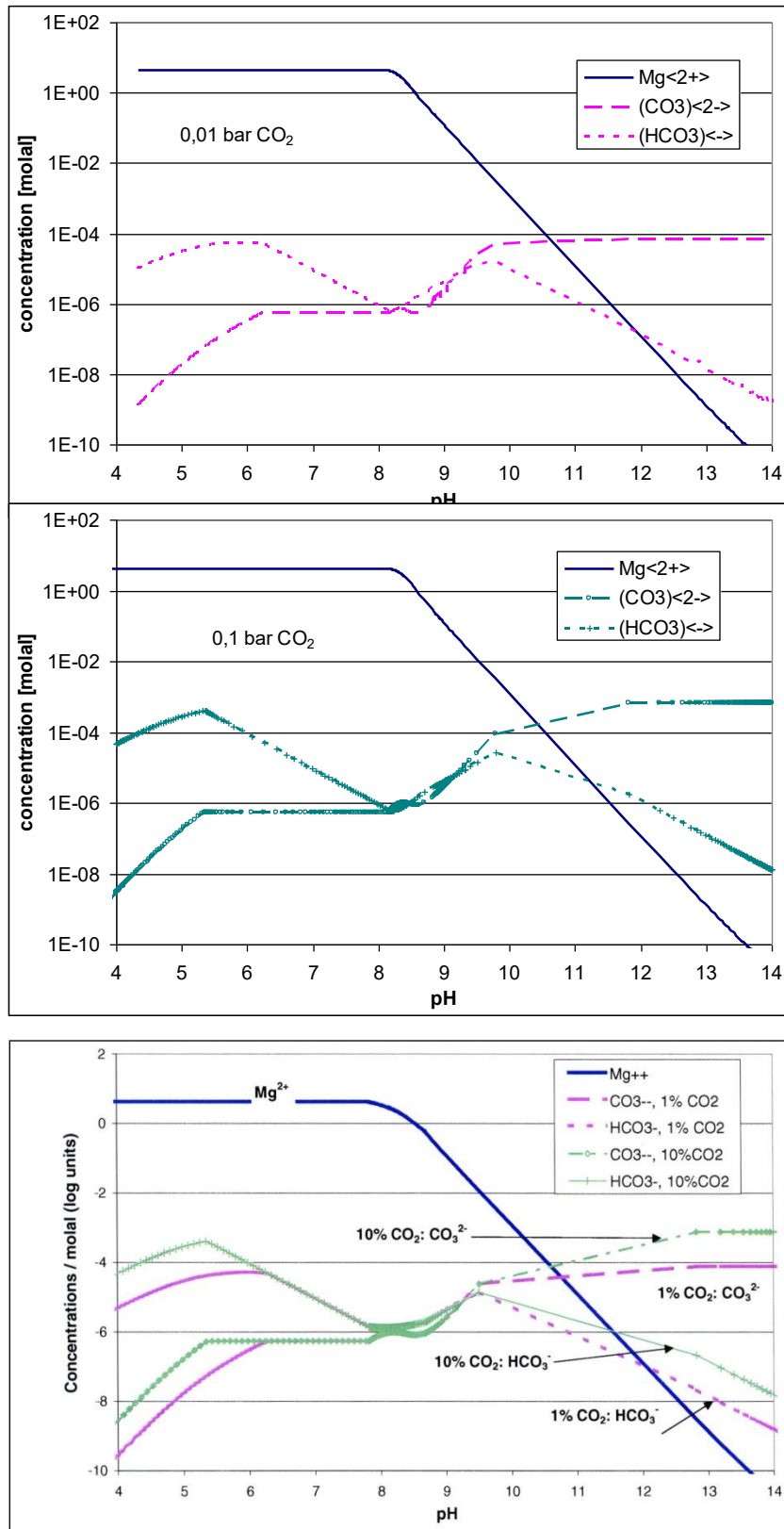


Fig. A1.2 C-speciation in Q-Brine: top = $p(\text{CO}_2) = 0.01$ bar (GRS), centre = $p(\text{CO}_2) = 0.1$ bar (GRS) and bottom = /KIE 00/

Fig. 7.2 reveals excellent agreement in general; minor differences occur for the concentration of HCO_3^- at the minimum around $\text{pH}\sim 8$. At this pH brucite begins to precipitate leading to a decreasing concentration of Mg^{2+} .

A 1.2 Preface to the calculations with actinides

To further test the ChemApp parameter file prepared for our calculations, solubilities for some actinides were calculated in simple systems as described in /KIE 00/. Discrepancies between calculations presented here and those from 2000 may arise because of modifications or deletions of existing parameters/species or the addition of new parameters/species. Tab. 7.4 compares solubility constants of three solid phases. The 2000-values have kindly been given us by INE (personal communication with Volker Metz).

Tab. A1.4 Comparison of solubility constants used in /KIE 00/ and this report

Old value	Present value
$\text{Pu}(\text{OH})_4(\text{am}) + 4\text{H}^+ \rightarrow \text{Pu}^{4+} + 4\text{H}_2\text{O}$: $\log K = -2.5 \rightarrow \Delta_f G^\theta = -144.082 \text{ J/mol}$	$\text{Pu}(\text{OH})_4(\text{am}) \rightarrow \text{Pu}^{4+} + 4\text{OH}^-$: $\log K = -58.33 \rightarrow \Delta_f G^\theta = -143.992 \text{ J/mol}$
$\text{Np}(\text{OH})_4(\text{am}) + 4\text{H}^+ \rightarrow \text{Np}^{4+} + 4\text{H}_2\text{O}$: $\log K = -0.7 \rightarrow \Delta_f G^\theta = -144.433 \text{ J/mol}$	$\text{Np}(\text{OH})_4(\text{am}) \rightarrow \text{Np}^{4+} + 4\text{OH}^-$: $\log K = -56.7 \rightarrow \Delta_f G^\theta = -144.405 \text{ J/mol}$
$\text{UO}_2(\text{OH})_2 \cdot 2\text{H}_2\text{O} (\text{Schoepite}) + 2\text{H}^+$ $\rightarrow \text{UO}_2^{2+} + 3\text{H}_2\text{O}$: $\log K = 5.1 \rightarrow \Delta_f G^\theta = -1.634.860 \text{ J/mol}$	$\text{UO}_3 \cdot 2\text{H}_2\text{O}(\text{c}) (\text{Schoepite})$: $\Delta_f G^\theta = -1.636.510 \text{ J/mol}$ $1\text{UO}_3 \cdot 2\text{H}_2\text{O}(\text{c}) (\text{Metaschoepite})$ $\rightarrow (\text{UO}_2)^{2+} + 2\text{OH}^- + 1\text{H}_2\text{O}$: $\log K = -22.65 \rightarrow \Delta_f G^\theta = -1.633.471 \text{ J/mol}$

It is very likely that these differences are not the only ones. However, more detailed information is not possible because the original database from 1999 which INE used to perform the calculations discussed in their report is lacking.

Obvious causes for differing results might be

- different solubility constant for solid phases,
- solid phases, which were presumably present in the old database, but not in the database from 2004,
- new solid phases in the database from 2004, which were not present in the old database,

- new aq. species which were not present in the database (this may especially cause problems in high saline solutions when no Pitzer coefficients are provided for new species, e. g. $U^{(+VI)}$ -sulphato-complexes), and / or
- mistyping either in the original database supplied by INE (e. g. sign of solubility constant $\log K$ for $(U^{(+VI)}O_2)_3(CO_3)_6^{6-}$ was changed for the preparation of this report from 54 to -54) or by the author of this report.

A 1.3 Solubility of Americium

A 1.3.1 Gipshut solution

Tab. A1.5 Solubility of Americium in Gipshut-solution

Step	Description
1.	Calculate 1 kg H ₂ O in equilibrium with halite and anhydrite
a)	p(CO ₂) = 0 bar
b)	p(CO ₂) = 0.0003 bar
4.	Eliminate all Am-species the oxidation number of which is different from +III. and all reduced S-species whose oxidation number is different from +VI. namely: $Am^{(+II)2+}$, $Am^{(+IV)4+}$, $(Am^{(+V)}O_2)(CO_3)^-$, $(Am^{(+V)}O_2)(CO_3)_2^{3-}$, $(Am^{(+V)}O_2)(CO_3)_3^{5-}$, $(Am^{(+V)}O_2)^+$, $(Am^{(+VI)}O_2)^{2+}$, H ₂ S ⁰ , and HS ⁻ . Leaving reduced S-species in the calculation led to numerical instabilities.
5.	Set constant molar masses of halite. anhydrite from first step and check resulting solid phase activities; CO ₂ -fugacity remains fixed at 30 Pa.
6.	Add $1 \cdot 10^{-2}$ mol $Am^{(+III)}(OH)_3(c)$. adjust to pH~4 by adding $3 \cdot 10^{-2}$ mol HCl
7.	Titrate with 1 mol NaOH
The resulting stream for step 6 is:	
55.5084391	mol H ₂ O
6.0719	mol NaCl
$4.3258 \cdot 10^{-2}$	mol Anhydrite
$1.0 \cdot 10^{-2}$	mol $Am^{(+III)}(OH)_3(c)$
$3.0 \cdot 10^{-2}$	mol H ⁺
$3.0 \cdot 10^{-2}$	mol Cl ⁻
a)	0 mol CO ₂
b)	30 Pa CO ₂ leading to p(CO ₂) = 0.0003 bar in any step

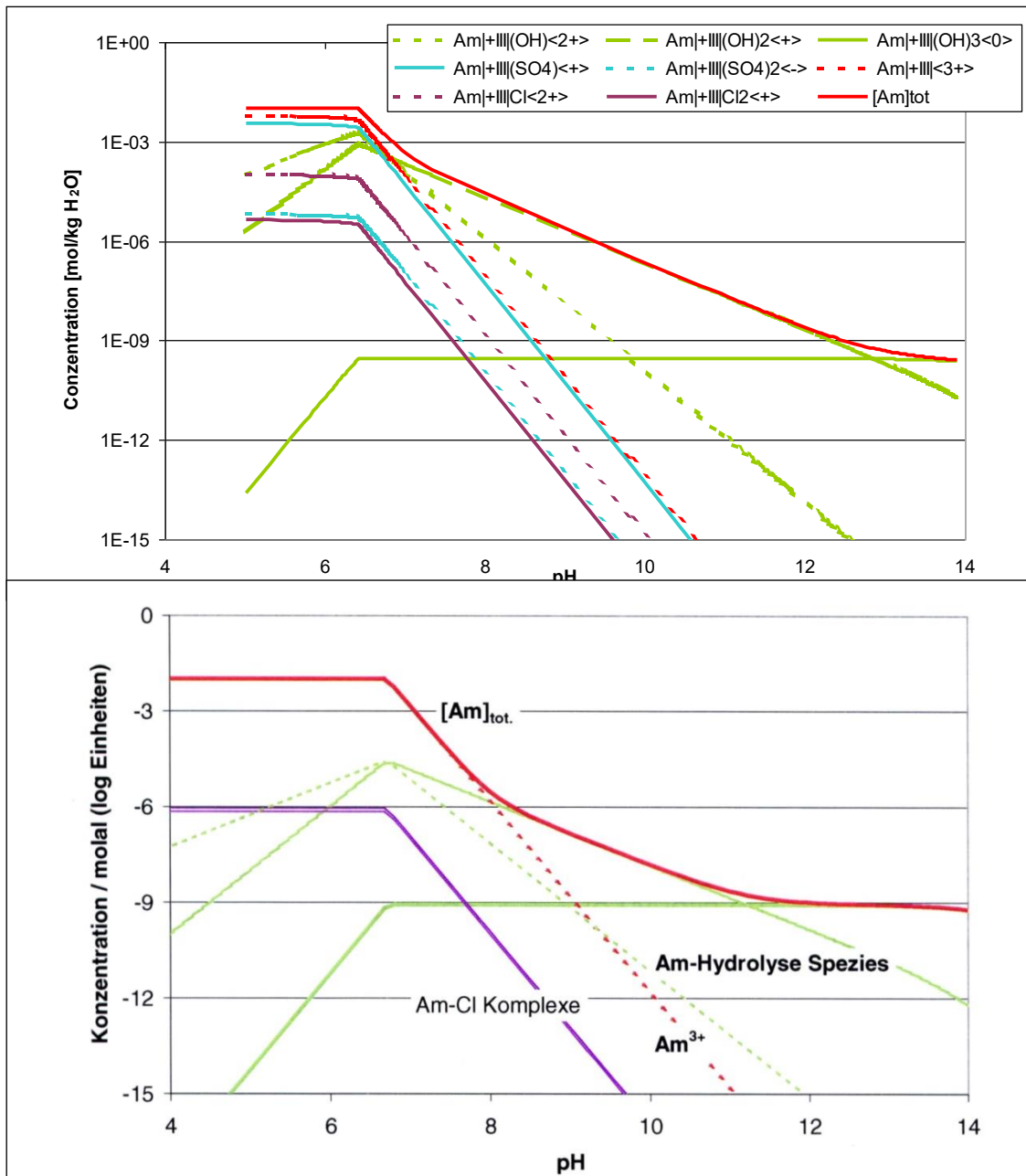


Fig. A1.3 Solubility of $\text{Am}^{(\text{III})}$ in Gipschut-solution with $p(\text{CO}_2) = 0$ bar, top = this report (GRS) and bottom = /KIE 00/

The result for case a (without CO_2) is shown in Fig. 7.3. Below $\text{pH} = 6.42$ the added mass of $\text{Am}^{(\text{III})}(\text{OH})_3(\text{c})$ is completely dissolved. It is only at higher pH -values that $\text{Am}^{(\text{III})}(\text{OH})_3(\text{c})$ is precipitated, which is in accordance with results from /KIE 00/.

However, looking into details reveals differences in the results. In our calculation solubility of $\text{Am}^{(\text{III})}$ drops to $2.53 \cdot 10^{-10}$ at $\text{pH} = 13.9$ whereas in /KIE 00/ it levels out to a bit less

than $1 \cdot 10^{-9}$. INE does not mention sulphato-complexes in their figure. At high pH $\text{Am}^{(\text{III})}$ -sulphato-complexes do not contribute markedly to the composition of the solution. Consequently, even when sulphato-complexes with $\text{Am}^{(\text{III})}$ are eliminated our results remain the same (no figure shown). The solubility at pH~14 coincides with the concentration of the tri-hydroxo-complex of $\text{Am}^{(\text{III})}$ which eventually becomes the predominant Am-species. As to our best knowledge, equilibrium constants for all relevant complex or solid phase formation reactions are those as published in /ALT 04/ whereas we have no access to the database used for calculations in /KIE 00/. Therefore, we can only hypothesize that differences in calculated solubilities are due to differences in this kind of data.

The result for case b ($p(\text{CO}_2) = 0.0003$ bar) is shown in Fig. 7.4. A minimum solubility of $9.59 \cdot 10^{-8}$ is calculated at pH = 8.22, which seems to be in accordance with the results from /KIE 00/ ($2 \cdot 10^{-7}$ at pH slightly above 8). Precipitation of $\text{Am}^{(\text{III})}(\text{CO}_3)(\text{OH}) \cdot 0.5\text{H}_2\text{O}$ commences at pH=5.59 whereas in /KIE 00/ precipitation begins at pH ~ 7 only. Furthermore, /KIE 00/ differs in that Am-phases accounted for were different. INE reported a phase transition from “ $\text{AmOHCO}_3(\text{cr})$ ” to “ $\text{NaAm}(\text{CO}_3)_2 \cdot \text{H}_2\text{O}$ ” at pH~5.7. These phases, however, are not present in the updated version of the INE-database. where $\text{Am}^{(\text{III})}(\text{CO}_3)(\text{OH})(\text{am.hyd})$ and $\text{NaAm}^{(\text{III})}(\text{CO}_3)_2 \cdot 5\text{H}_2\text{O}(\text{c})$ are found. As the utilized databases are obviously not equivalent, computational results for the solubility of $\text{Am}^{(\text{III})}$ are bound to be different. One consequence is that the increase in solubility following the minimum is different. Also, the calculated species concentration are not strictly equal.

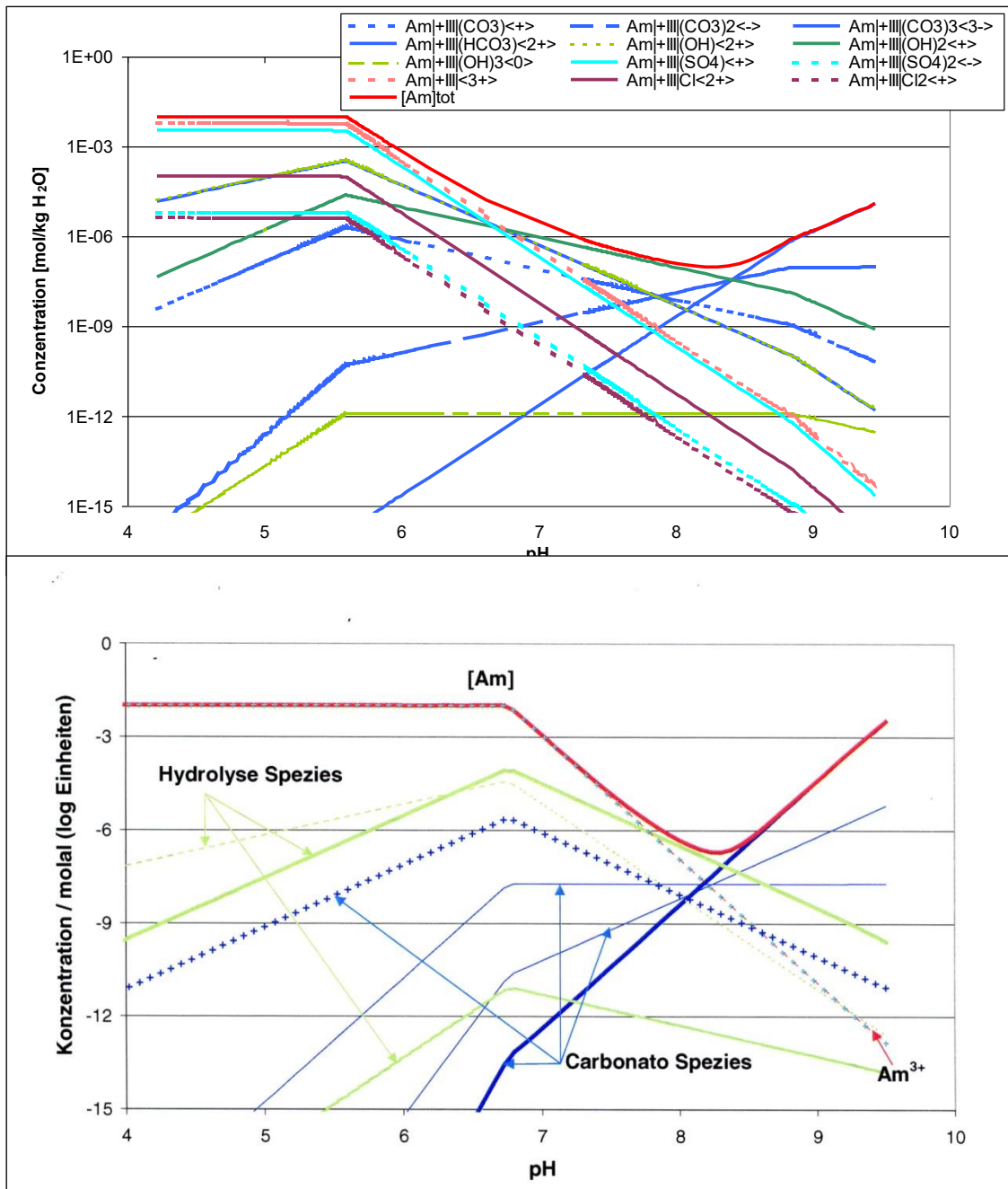


Fig. A1.4 Solubility of Am^(+III) in Giphshut-solution with p(CO₂) = 0.0003 bar, top = this report (GRS) and bottom = /KIE 00/

A 1.3.2 Q-Brine solution

Tab. A1.6 Solubility of Americium in Q-Brine-solution

Step	Description
1.	Calculate 1 kg H ₂ O in equilibrium with halite, sylvite, carnallite, kainite and p(CO ₂) = 0 bar
2.	Set constant molar masses of halite, sylvite, carnallite, and kainite from first step and check resulting solid phase activities.
3.	Eliminate all Am-species the oxidation number of which is different from +III. and all reduced S-species whose oxidation number is different from +VI, namely: Am ^{(+II)2+} , Am ^{(+IV)4+} , (Am ^(+V) O ₂)(CO ₃) ⁻ , (Am ^(+V) O ₂)(CO ₃) ₂ ³⁻ , (Am ^(+V) O ₂)(CO ₃) ₃ ⁵⁻ , (Am ^(+V) O ₂) ⁺ , (Am ^(+VI) O ₂) ²⁺ , H ₂ S ⁰ , and HS ⁻ . Leaving reduced S-species in the calculation led to numerical instabilities.
4.	Add 1.78·10 ⁻² mol Am ^(+III) (OH) ₃ (c) (which is just enough to give 10 ⁻² mol Am ^(+III) (kg H ₂ O) ⁻¹ in the first step; add 5.810 ⁻² mol HCl to adjust to pH~2.
5.	Titrate with 1.0·10 ⁻¹ mol NaOH
The resulting stream for step 4 is:	
55.5084391 mol H ₂ O	
8.5620·10 ⁻¹ mol NaCl	
-6.4655 mol Sylvite	
6.9181 mol Carnallite	
5.5705·10 ⁻¹ mol Kainite	
0 mol CO ₂	
1.78·10 ⁻² mol Am ^(+III) (OH) ₃ (c)	
5.8·10 ⁻² mol H ⁺	
5.8·10 ⁻² mol Cl ⁻	

Modelling of this system only proceeded up to pH~8.17. because at that point brucite precipitation is initiated and the solution pH is hence buffered as long as Mg²⁺ remains present in solution.

Up to pH=7.09 Am^(+III) remains dissolved quantitatively. Above this pH precipitation of Am^(+III)(OH)₃(c) begins.

In the INE-report no quantitative information is given as to the final solubility of Am^(+III). Visual comparison of the diagrams given in Fig. 7.5 indicates that the calculated solubility in this report is slightly higher than that given by INE. Whereas concentrations of hydroxo complexes seem to be equivalent, concentration of free Am^(+III) is lower in this report. Chloro- and sulphato-complexes in both calculations seem to match, though the second sulphato-complex Am^(+III)(SO₄)₂⁻ is not mentioned in the INE-figure at all.

All in all, for this system, the compared results are in good agreement.

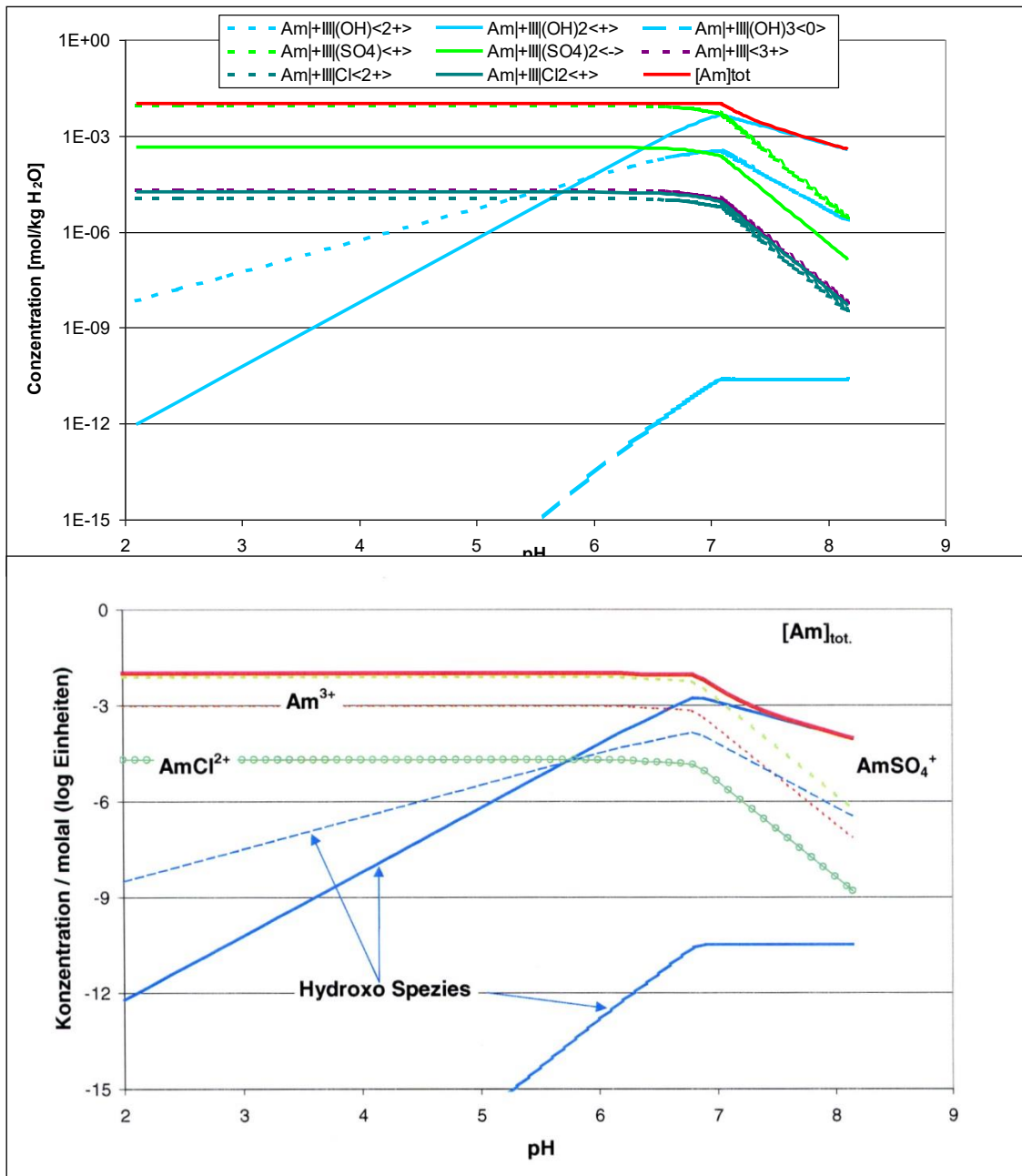


Fig. A1.5 Solubility of Am^(+III) in Q-brine with p(CO₂) = 0 bar, top = this report (GRS) and bottom = /KIE 00. Fig. 18/

A 1.4 Solubility of Neptunium(+V)

A 1.4.1 Gipshut solution

Tab. A1.7 Solubility of Neptunium(+V) in Gipshut-solution

Step	Description
1.	Calculate 1 kg H ₂ O in equilibrium with halite and anhydrite and
2.	p(CO ₂) = 0 bar
3.	p(CO ₂) = 0.0003 bar
4.	Eliminate all Np-species the oxidation number of which is different from +V, and all reduced S-species whose oxidation number is different from +VI, namely: Np ^(+III) (CO ₃) ₃ ³⁻ , Np ^(+III) (OH) ₂ ²⁺ , Np ^(+III) ₃ ³⁺ , Np ^(+IV) (CO ₃) ₄ ⁴⁻ , Np ^(+IV) (CO ₃) ₅ ⁶⁻ , Np ^(+IV) (OH) ₃ ³⁺ , Np ^(+IV) (OH) ₂ (CO ₃) ₂ ²⁻ , Np ^(+IV) (OH) ₂ ²⁺ , Np ^(+IV) (OH) ₃ ³⁺ , Np ^(+IV) (OH) ₄ (CO ₃) ₂ ⁻ , Np ^(+IV) (OH) ₄ (CO ₃) ₂ ⁴⁻ , Np ^(+IV) (OH) ₄ ⁰ , Np ^(+IV) (OH) ₃ ³⁺ , Np ^(+IV) (OH) ₄ (CO ₃) ₂ ⁻ , Np ^(+IV) (OH) ₄ (CO ₃) ₂ ⁴⁻ , Np ^(+IV) (OH) ₄ ⁰ , Np ^(+IV) (SO ₄) ₂ ²⁺ , Np ^(+IV) (SO ₄) ₂ ⁰ , Np ^(+IV) ₄ ⁴⁺ , Np ^(+IV) Cl ₃ ³⁺ , (Np ^(+VI) O ₂)(CO ₃) ₀ , (Np ^(+VI) O ₂)(CO ₃) ₂ ²⁻ , (Np ^(+VI) O ₂)(CO ₃) ₃ ⁴⁻ , (Np ^(+VI) O ₂)(OH) ₁ ⁺ , (Np ^(+VI) O ₂)(SO ₄) ₀ , (Np ^(+VI) O ₂)(SO ₄) ₂ ²⁻ , (Np ^(+VI) O ₂) ₂ ²⁺ , (Np ^(+VI) O ₂) ₂ (CO ₃)(OH) ₃ ⁻ , (Np ^(+VI) O ₂) ₂ (OH) ₂ ²⁺ , (Np ^(+VI) O ₂) ₃ (CO ₃) ₆ ⁶⁻ , (Np ^(+VI) O ₂) ₃ (OH) ₅ ⁺ , (Np ^(+VI) O ₂)Cl ₁ ⁺ , H ₂ S ₀ , and HS ₋ . Leaving reduced S-species in the calculation led to numerical instabilities.
5.	Eliminate the following solid phases: Np ^(+IV) (OH) ₄ (am), (Np ^(+VI) O ₂)(CO ₃)(s), K ₄ (Np ^(+VI) O ₂)(CO ₃) ₃ (s), Np ^(+VI) O ₃ ·H ₂ O(c), Np ^(+V) O _{2.5} (s,hyd). In terms of "allowed" solid Np ^(+V) -phases to form, more scenarios were calculated: Elimination of Np ^(+V) O ₅ (c), leaving (Np ^(+V) O ₂)(OH)(am,aged) as solubility limiting phase, and vice versa.
6.	Set constant molar masses of halite. anhydrite from first step and check resulting solid phase activities; CO ₂ -fugacity remains fixed at a) 0 or b) 30 Pa.
7.	Add 1·10 ⁻⁵ mol (Np ^(+V) O ₂)(OH)(am,aged) or 0.5·10 ⁻⁵ mol Np ^(+V) O ₅ (c). Adjust to pH~5 by adding HCl.
8.	Titrate with a) 1 mol NaOH b) 1·10 ⁻² mol NaOH
The resulting stream for step 8 is:	
	55.5084391 mol H ₂ O
	6.0719 mol NaCl
	4.3258·10 ⁻² mol Anhydrite
a)	1.0·10 ⁻⁵ mol (Np ^(+V) O ₂)(OH)(am.aged)
b)	0.5·10 ⁻⁵ mol Np ^(+V) O ₅ (c)
a)	0 mol CO ₂ 3.0·10 ⁻⁵ mol H ⁺ 3.0·10 ⁻⁵ mol Cl ⁻
b)	30 Pa CO ₂ leading to p(CO ₂) = 0.0003 bar in any step 2.0·10 ⁻⁵ mol H ⁺ 2.0·10 ⁻⁵ mol Cl ⁻

Dependent on whether an amorphous or a crystalline $\text{Np}^{(+V)}$ -phase are provided (the other being eliminated) results for solubility differ. In the INE-report “solid Np_2O_5 ” is mentioned rather vaguely as solubility limiting phase. As to the present database used for the presented calculation this might be $(\text{Np}^{(+V)}\text{O}_2)(\text{OH})(\text{am,aged})$ or $\text{Np}^{(+V)}_2\text{O}_5(\text{c})$. Consequently, each calculation was carried out two-fold, with one of both solid phases being eliminated and the other being left active.

In Fig. 7.6 the result is shown for $(\text{Np}^{(+V)}\text{O}_2)(\text{OH})(\text{am,aged})$ as solubility limiting phase and with $p(\text{CO}_2) = 0$ bar. Given the total mass of $\text{Np}^{(+V)}$, solubility is limited in a small pH-range only: $9.70 < \text{pH} < 12.0$. In the INE-report this range extends to about $9 < \text{pH} < 13$. In our calculation minimum solubility of $3.41 \cdot 10^{-6}$ mol/kg is attained at $\text{pH} = 10.9$. While the pH of minimum solubility is about the same as in the INE report ($\text{pH} = 10.7$), solubility differs by about one order of magnitude (INE: $6 \cdot 10^{-7}$).

If $\text{Np}^{(+V)}_2\text{O}_5(\text{c})$ is assumed as limiting phase, the calculated solubility is lower as might be expected, as is demonstrated in Fig. 7.7.

In this case minimum solubility of $4.16 \cdot 10^{-9}$ is calculated at $\text{pH} = 10.9$, which is about two orders of magnitude lower as given by INE. In other words: $\text{Np}^{(+V)}$ solubility in CO_2 -free Gipsbut solution as given in the INE-report cannot be reproduced, regardless of the “ Np_2O_5 ”-phase used for the calculation.

With $p(\text{CO}_2) = 0.0003$ bar solubility of $\text{Np}^{(+V)}$ is higher due to the formation of carbonato-complexes. However, differences between our calculations and those in the INE-report appear.

Fig. 7.8 displays the result of titrating a solution of $(\text{Np}^{(+V)}\text{O}_2)(\text{OH})(\text{am,aged})$.

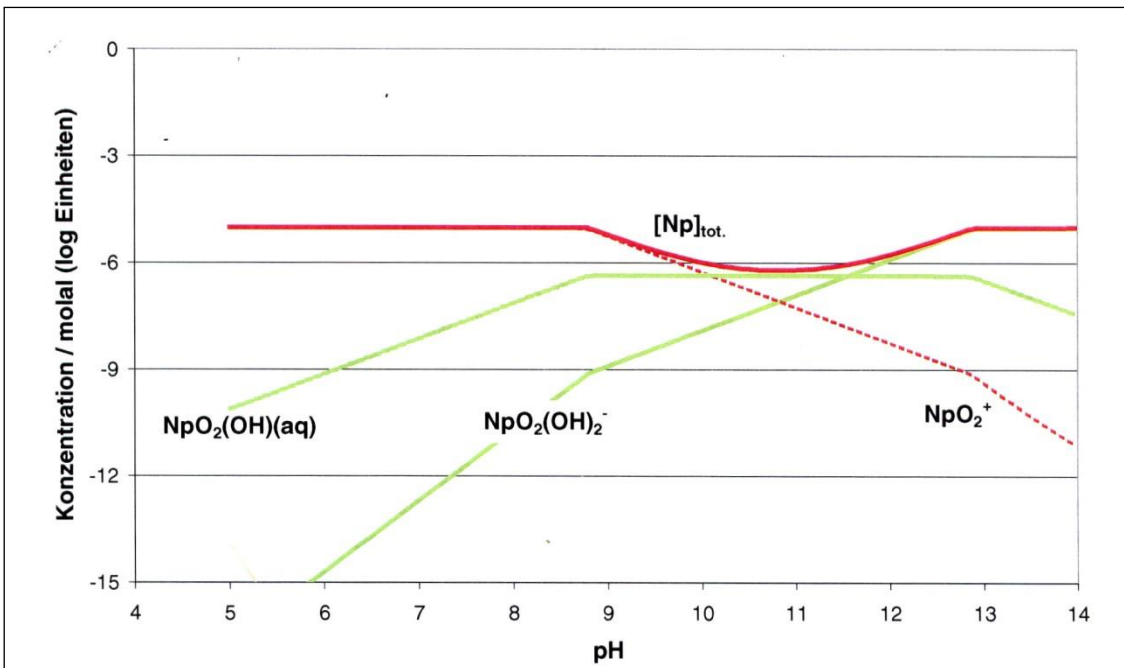
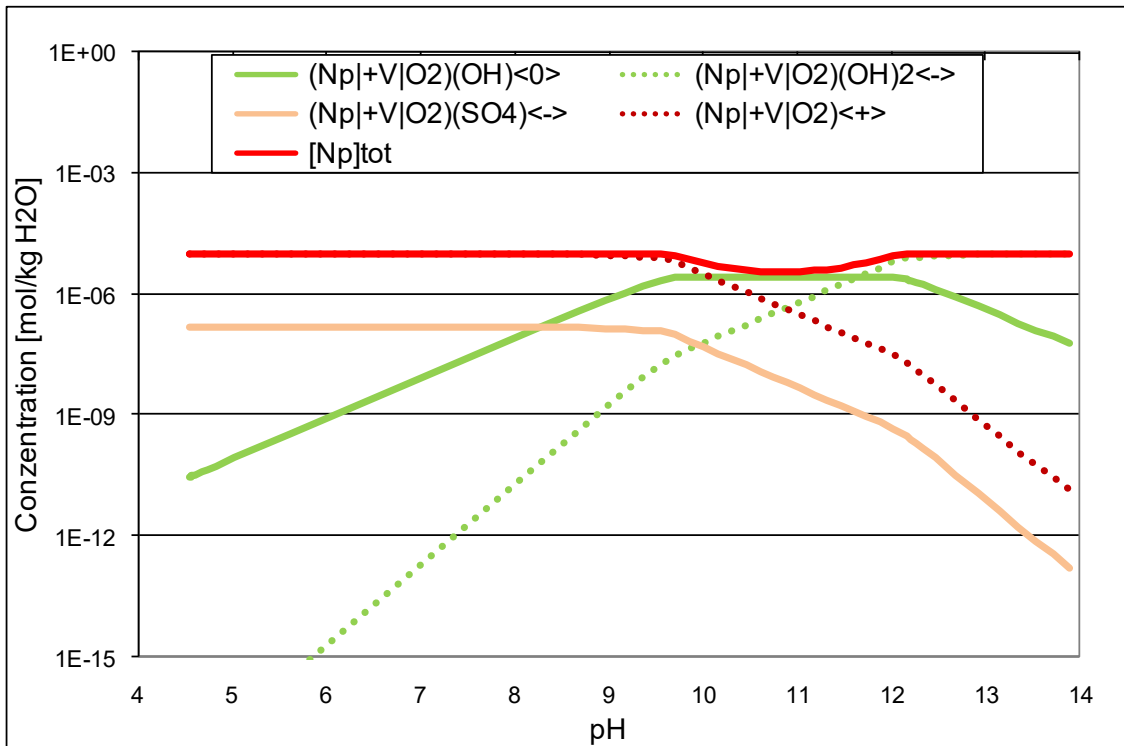


Fig. A1.6 Solubility of Np^(+V) in Gipshut-solution with p(CO₂) = 0 bar and (Np^(+V)O₂)(OH)(am.aged) as solubility limiting phase, top = this report (GRS) and bottom = /KIE 00/

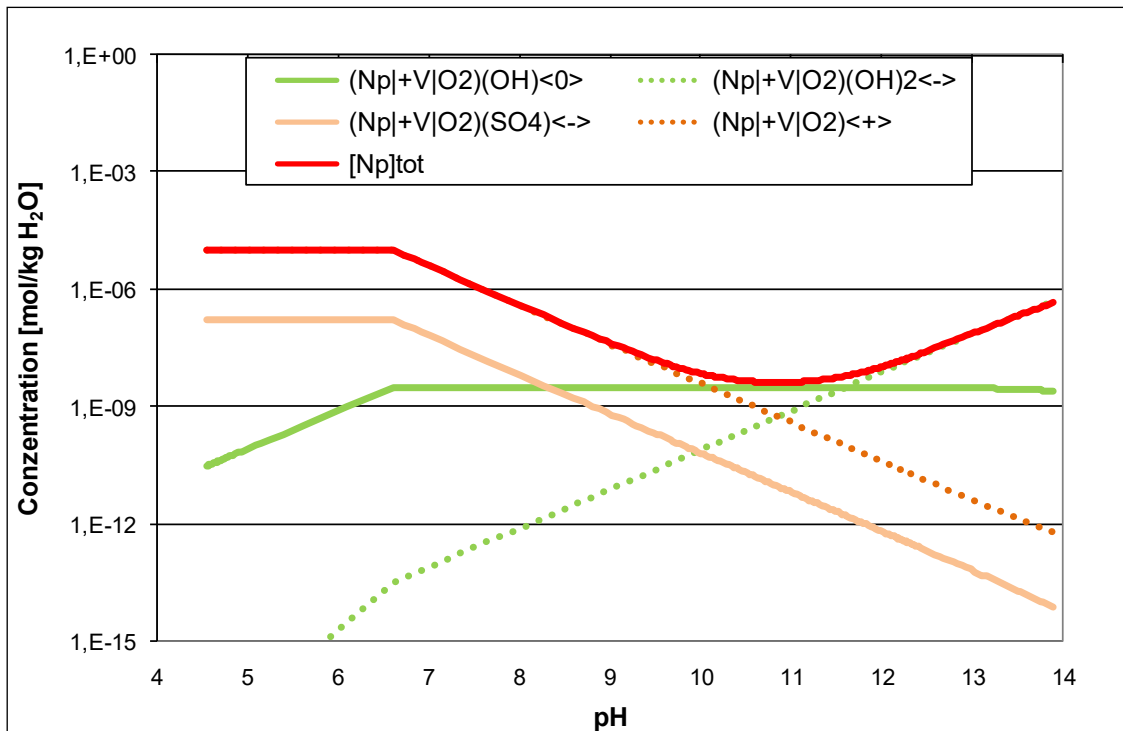


Fig. A1.7 Solubility of $\text{Np}^{(+V)}$ in Gipsht-solution with $p(\text{CO}_2) = 0$ bar and $\text{Np}^{(+V)}_2\text{O}_5(\text{c})$ as solubility limiting phase (compare with result from the INE-report as given in the bottom of Fig. 7.8 /KIE 00/)

In our calculation $(\text{Np}^{(+V)}\text{O}_2)(\text{OH})(\text{am,aged})$ does not precipitate at all. In the INE-calculation two minima appear. The first one at lower pH-values is reported as “ $\text{NaNpO}_2\text{CO}_3 \cdot 0.5\text{H}_2\text{O}$ ”. However, this mineral phase does not appear in the present database, a similar being $\text{Na}(\text{Np}^{(+V)}\text{O}_2)(\text{CO}_3) \cdot 3.5\text{H}_2\text{O}$. The second minimum in the INE-calculation was attributed to $\text{Na}_3\text{Np}(\text{CO}_3)_2(\text{s})$, being equivalent to $\text{Na}_3(\text{Np}^{(+V)}\text{O}_2)(\text{CO}_3)_2(\text{c})$ in the present database. In our calculation this mineral phase does not even approach a state of saturation.

It should be noted that in this system, as it was modelled for Fig. 7.8, $\text{Ca}(\text{CO}_3)$ (Calcite) and $\text{Na}_2\text{Ca}(\text{CO}_3)_2 \cdot 2\text{H}_2\text{O}$ (Pirssonite) (beside some anhydrite) did precipitate, thereby withdrawing some carbonate from aqueous solution. To explore whether this have some impact on the non-formation of $\text{Np}^{(+V)}$ -carbonates, the calculation depicted in Fig. 7.8 was repeated, this time with the following oceanic carbonated eliminated from calculation: $\text{Ca}(\text{CO}_3)$ (Aragonite), $\text{Ca}(\text{CO}_3)$ (Calcite), $\text{Na}(\text{HCO}_3)$ (Nahcolite), $\text{Na}_2\text{Ca}(\text{CO}_3)_2 \cdot 2\text{H}_2\text{O}$ (Pirssonite), $\text{CaNa}_2(\text{CO}_3)_2 \cdot 5\text{H}_2\text{O}$ (Gaylussite), $\text{Na}_2(\text{CO}_3) \cdot 10\text{H}_2\text{O}$ (Natron), $\text{Na}_2(\text{CO}_3) \cdot 7\text{H}_2\text{O}$, $\text{Na}_2(\text{CO}_3) \cdot \text{H}_2\text{O}$ (Thermonatrite), $\text{Na}_3(\text{CO}_3)(\text{HCO}_3) \cdot 2\text{H}_2\text{O}$ (Trona), $\text{Na}_6(\text{CO}_3)(\text{SO}_4)_2$ (Burkeite).

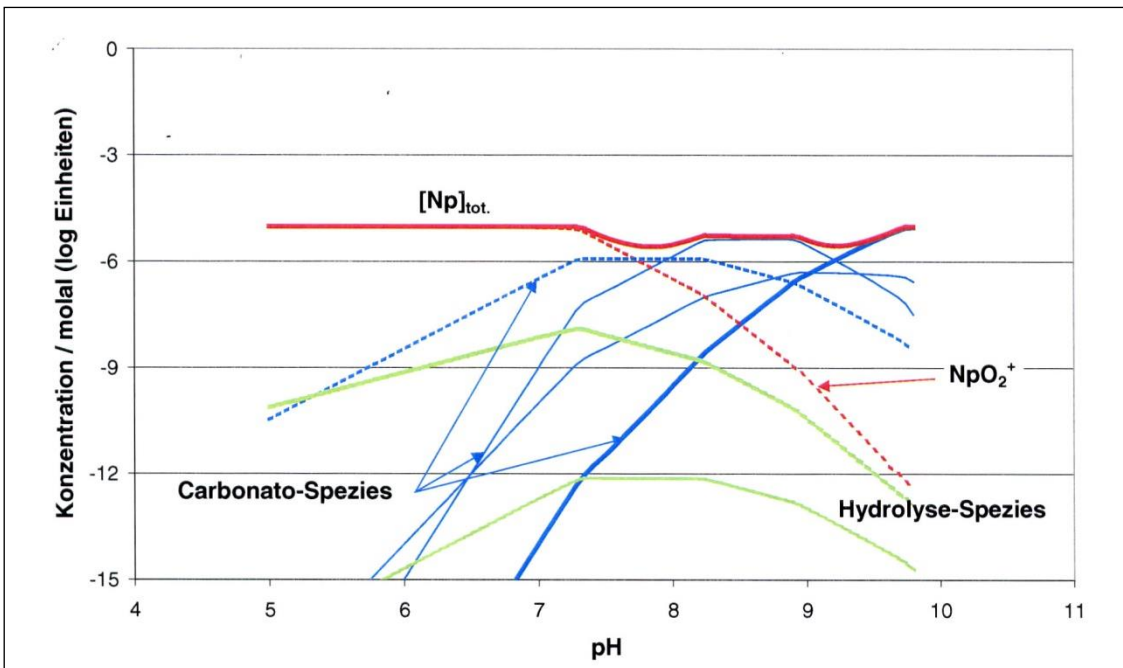
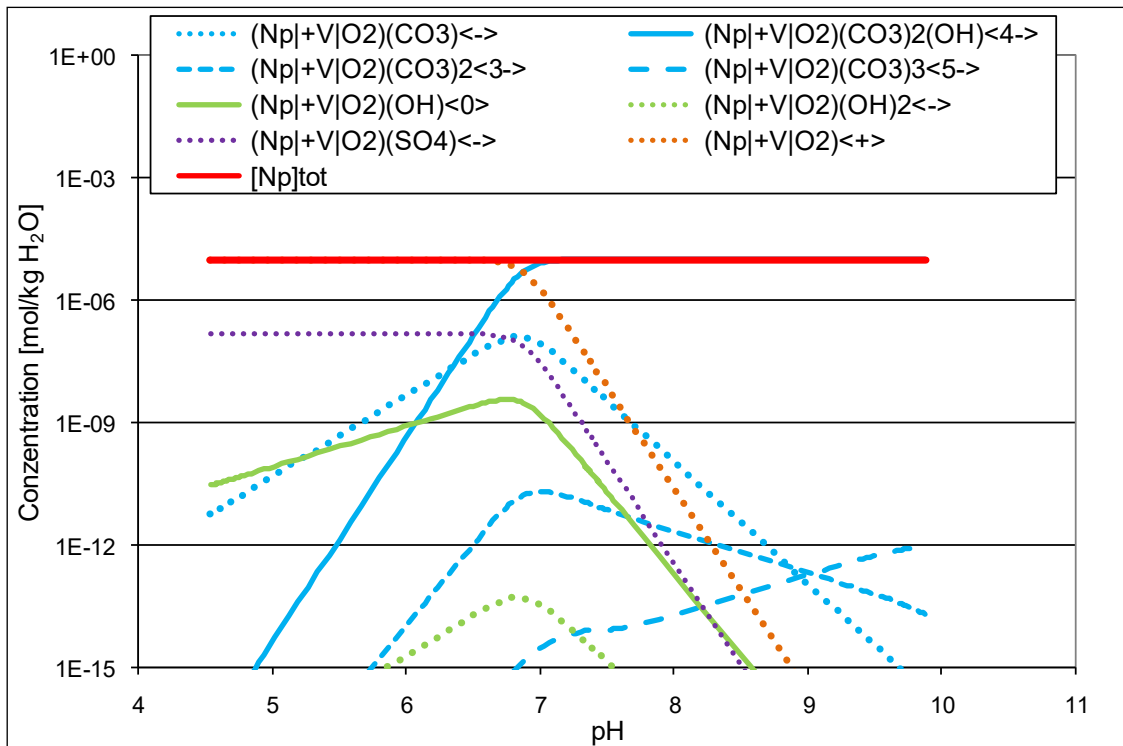


Fig. A1.8 Solubility of $\text{Np}^{(+V)}$ in Gipshut-solution with $p(\text{CO}_2) = 0.0003$ bar and $(\text{Np}^{(+V)}\text{O}_2)(\text{OH})(\text{am,aged})$ as solubility limiting phase, top = this report (GRS) and bottom = /KIE 00/

Fig. 7.9 to Fig. 7.11 show selected solid phase activities. As was expected, activities of $\text{Np}^{(+V)}$ -carbonates were higher when oceanic carbonates were eliminated from calculation. However, still none of them would attain saturation.

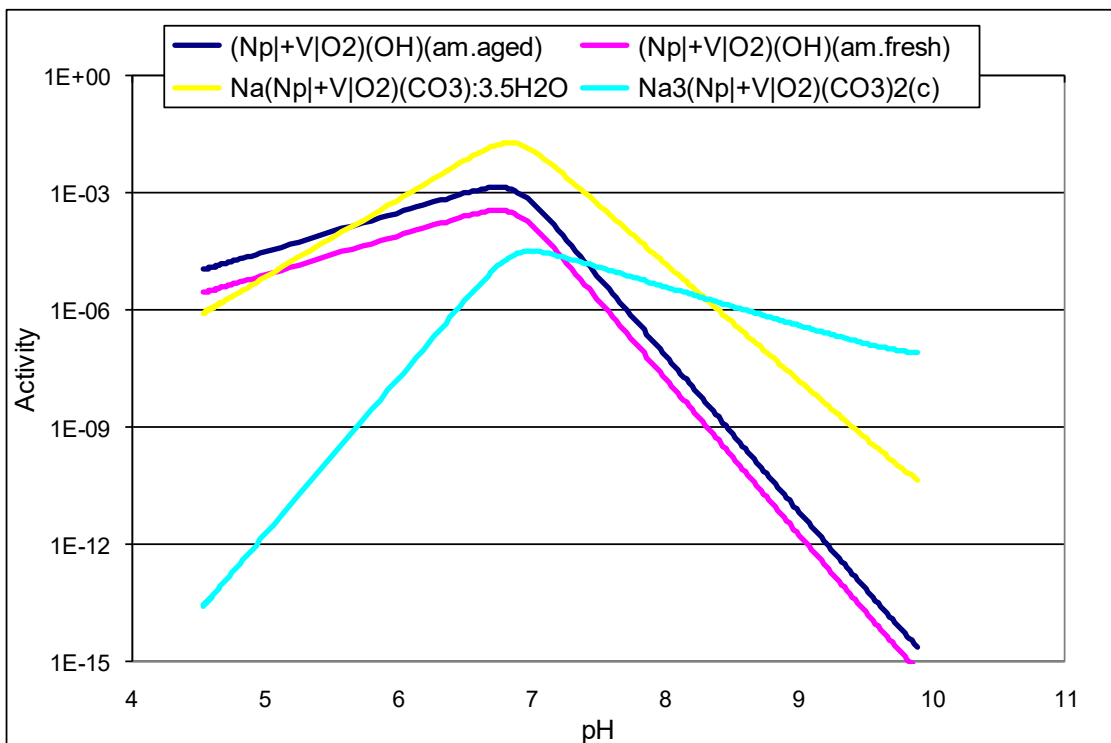
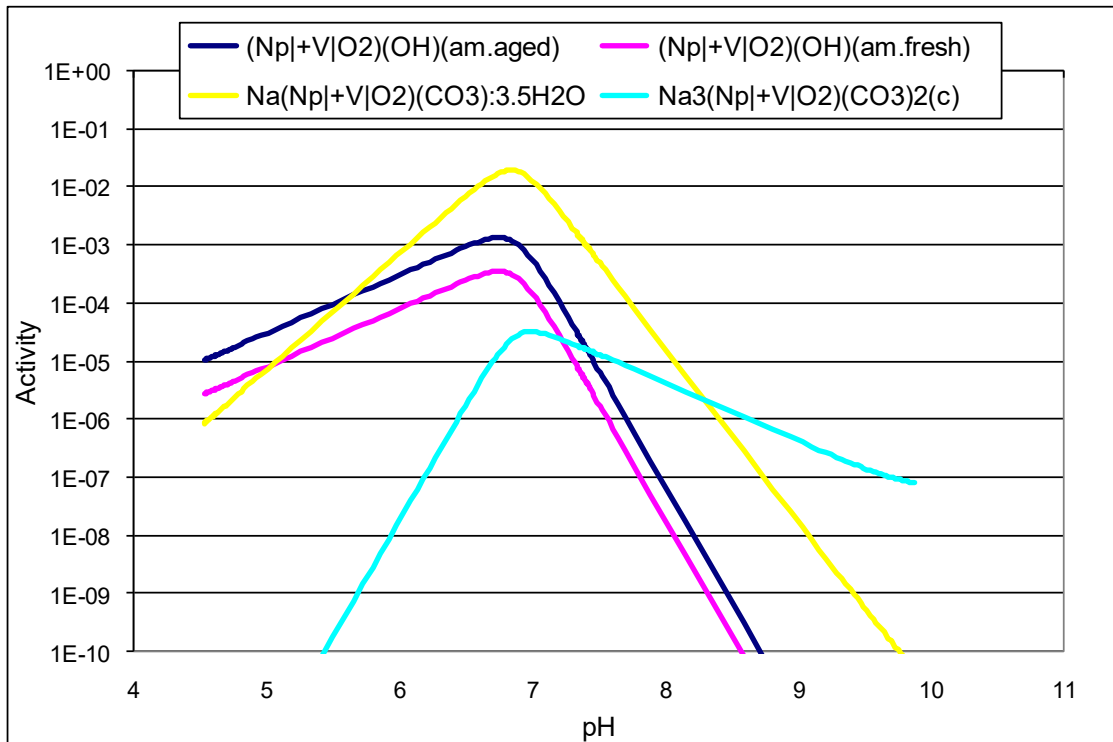


Fig. A1.9 $\text{Np}^{(+V)}$ in Gipshut-solution with $p(\text{CO}_2) = 0.0003$ bar and $(\text{Np}^{(+V)}\text{O}_2)(\text{OH})(\text{am,aged})$ as solubility limiting phase: solid phase activities, top = oceanic carbonates included and bottom = oceanic carbonates eliminated

With $\text{Np}^{(+V)}_2\text{O}_5(\text{c})$ as limiting phase the situation is not entirely different (Fig. 7.10), but there is a small pH-range between 6.62 and 6.87 where very small masses of this phase are precipitated.

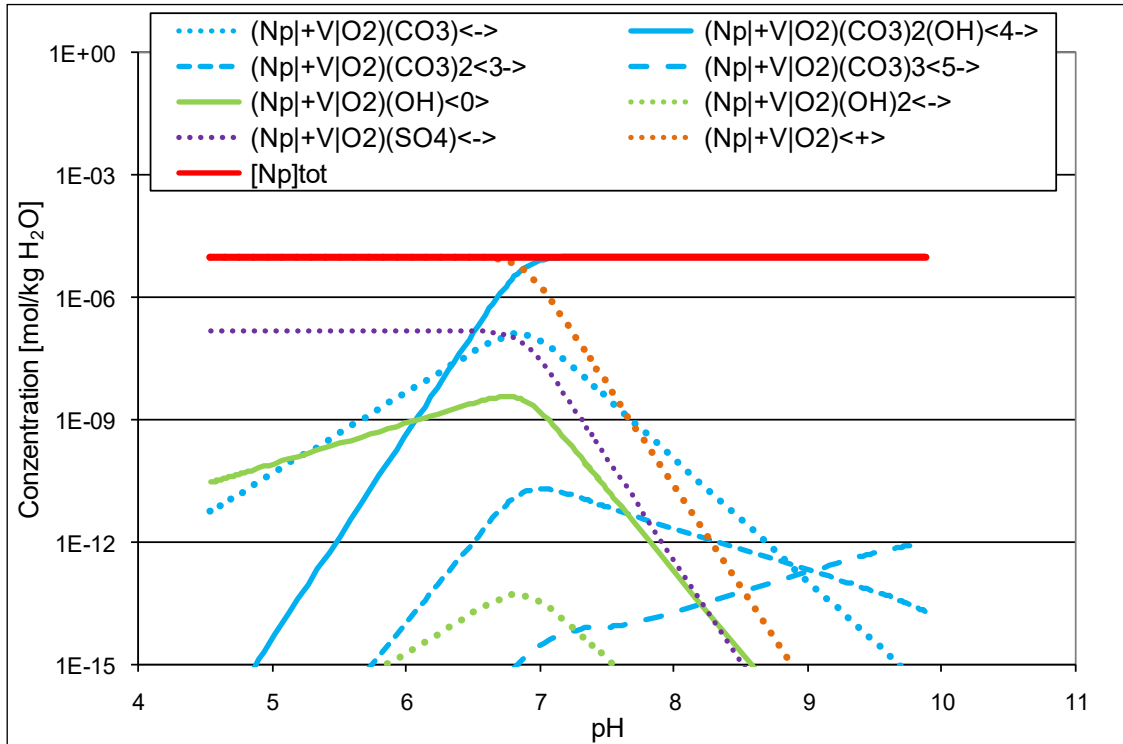


Fig. A1.10 Solubility of $\text{Np}^{(+V)}$ in Gipschut-solution with $p(\text{CO}_2) = 0.0003$ bar and $\text{Np}^{(+V)}_2\text{O}_5(\text{c})$ as solubility limiting phase (compare with result from the INE-report as given in the bottom of Fig. 7.9 /KIE 00/)

Eliminating oceanic carbonates did not change the results significantly. The calculated pH-range of $\text{Np}^{(+V)}_2\text{O}_5(\text{cr})$ precipitation was exactly the same as in the former case. Fig. 7.11 shows the solid phase activities with oceanic carbonates eliminated. It can be seen that $\text{Na}(\text{Np}^{(+V)}\text{O}_2)(\text{CO}_3) \cdot 3.5\text{H}_2\text{O}$ is well below saturation. Activity of $\text{Na}_3\text{Np}^{(+V)}(\text{CO}_3)_2(\text{s})$ remains below $1 \cdot 10^{-4}$.

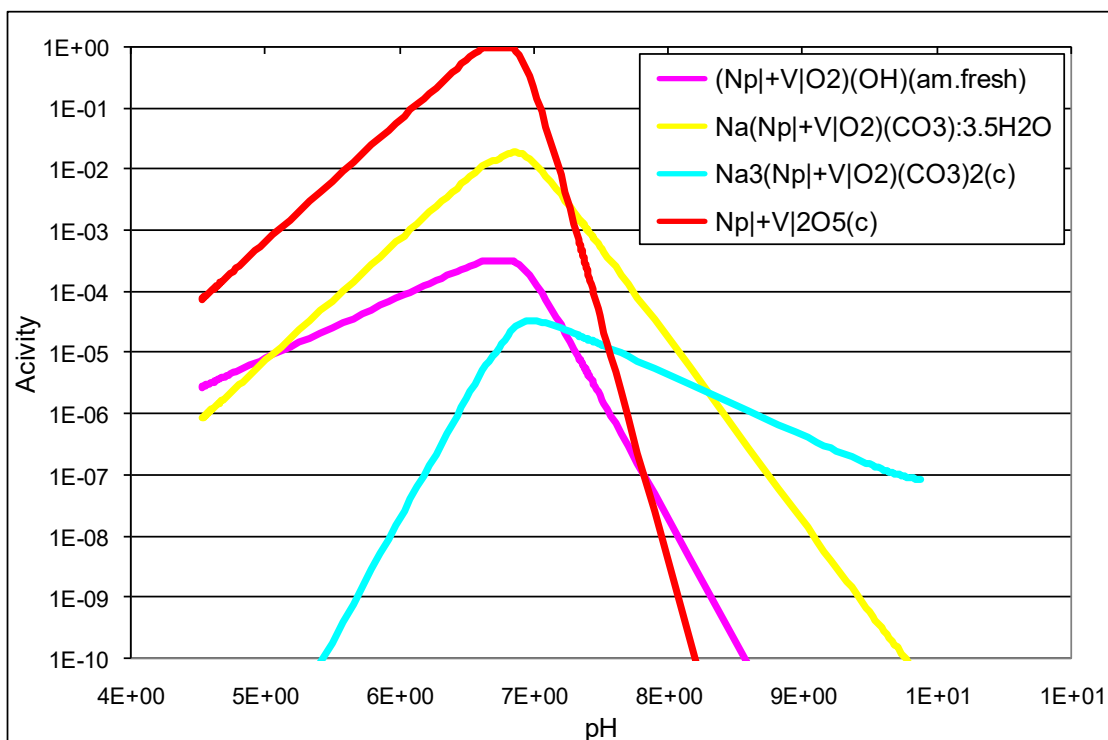


Fig. A1.11 Solid phase activities in the system $\text{Np}^{(+V)}$ in Gipshut-solution with $p(\text{CO}_2) = 0.0003$ bar and $\text{Np}^{(+V)}_2\text{O}_5(\text{c})$ as solubility limiting phase (oceanic carbonates eliminated)

Regardless of whether oceanic carbonates were included or excluded from calculation: the obvious differences between our calculation and those given in the INE-report for this system cannot be explained at this time.

A 1.5 Solubility of Neptunium(+IV)

A 1.5.1 Gipshut solution

Situation in this system is easier in that there is only one solid phase for $\text{Np}^{(+IV)}$ in the database, which is $\text{Np}^{(+IV)}(\text{OH})_4(\text{am})$. INE reports the minimum solubility as $6 \cdot 10^{-9}$ molal whereas we calculate $1.06 \cdot 10^{-9}$ at $\text{pH}=6.72$. However, in our calculations solubility increases due to the formation of the complex species $\text{Np}^{(+IV)}(\text{CO}_3)_5^{6-}$. In the figure given by INE carbonato-complexes with $\text{Np}^{(+IV)}$ are indicated, but no information is given in the report as to their exact nature.

Tab. A1.8 Solubility of Neptunium(+IV) in Gipshut-solution

Step	Description
1.	Calculate 1 kg H ₂ O in equilibrium with halite and anhydrite and p(CO ₂) = 0.0003 bar
2.	Eliminate all Np-species and Np-solids the oxidation number of which is different from +IV, and all reduced S-species whose oxidation number is different from +VI, namely: (Np ^(+V) O ₂)(CO ₃) ⁻ , (Np ^(+V) O ₂)(CO ₃) ₂ (OH) ⁴⁻ , (Np ^(+V) O ₂)(CO ₃) ₂ ³⁻ , (Np ^(+V) O ₂)(CO ₃) ₃ ⁵⁻ , (Np ^(+V) O ₂)(OH) ⁰ , (Np ^(+V) O ₂)(OH) ₂ ⁻ , (Np ^(+V) O ₂)(SO ₄) ⁻ , (Np ^(+V) O ₂) ⁺ , (Np ^(+VI) O ₂)(CO ₃) ⁰ , (Np ^(+VI) O ₂)(CO ₃) ₂ ²⁻ , (Np ^(+VI) O ₂)(CO ₃) ₃ ⁴⁻ , (Np ^(+VI) O ₂)(OH) ⁺ , (Np ^(+VI) O ₂)(SO ₄) ⁰ , (Np ^(+VI) O ₂)(SO ₄) ₂ ²⁻ , (Np ^(+VI) O ₂) ²⁺ , (Np ^(+VI) O ₂) ₂ (CO ₃)(OH) ₃ ⁻ , (Np ^(+VI) O ₂) ₂ (OH) ₂ ²⁺ , (Np ^(+VI) O ₂) ₃ (CO ₃) ₆ ⁶⁻ , (Np ^(+VI) O ₂) ₃ (OH) ₅ ⁺ , (Np ^(+VI) O ₂)Cl ⁺ , (Np ^(+V) O ₂)(OH)(am,aged), (Np ^(+V) O ₂)(OH)(am,fresh), K(Np ^(+V) O ₂)(CO ₃)(s), K ₃ (Np ^(+V) O ₂)(CO ₃) ₂ (s), Na(Np ^(+V) O ₂)(CO ₃)·3,5H ₂ O, Na ₃ (Np ^(+V) O ₂)(CO ₃) ₂ (c), Np ^(+V) O ₂ (c), Np ^(+V) O _{2,5} (s,hyd), (Np ^(+VI) O ₂)(CO ₃)(s), K ₄ (Np ^(+VI) O ₂)(CO ₃) ₃ (s), Np ^(+VI) O ₃ ·H ₂ O(c), H ₂ S ⁰ , and HS ⁻ . Leaving reduced S-species in the calculation led to numerical instabilities.
3.	Set constant molar masses of halite, anhydrite from first step and check resulting solid phase activities; CO ₂ -fugacity remains fixed at 30 Pa.
4.	Add 1·10 ⁻⁵ mol Np ^(+IV) (OH) ₄ (am). Adjust to pH~4 by adding HCl.
5.	Titrate with 1 mol NaOH
The resulting stream for step 4 is:	
55.5084391 mol H ₂ O	
6.0719 mol NaCl	
4.3259·10 ⁻² mol Anhydrite	
3.0·10 ⁻⁵ mol H ⁺	
3.0·10 ⁻⁵ mol Cl ⁻	
30 Pa CO ₂ leading to p(CO ₂) = 0.0003 bar in any step	
1.0·10 ⁻⁵ mol Np ^(+IV) (OH) ₄ (am)	

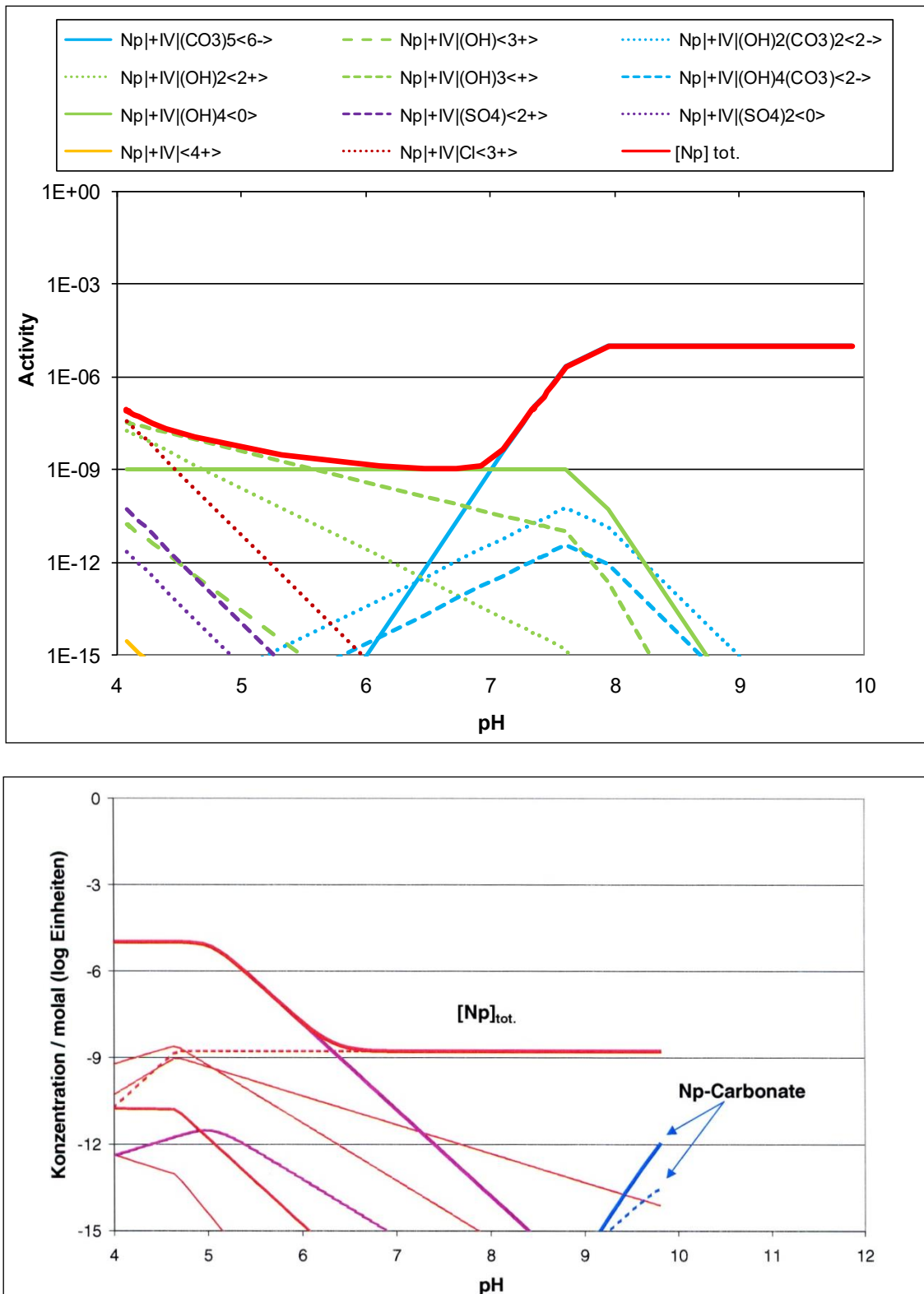


Fig. A1.12 Solubility of Np^{+IV} in Gipshut-solution with $p(\text{CO}_2) = 0.0003$ bar and $\text{Np}^{+IV}(\text{OH})_4(\text{am})$ as solubility limiting phase, top = this report (GRS) and bottom = /KIE 00/

As can be seen in Fig. 7.12 confinement to $\text{Np}^{(+IV)}$ should not be the cause for differences at lower pH because $\text{Np}^{(+III)}$ becomes dominant at $\text{pH} < 4$ only. As the calculated solubility is of about the same order of magnitude, it is hypothesized that differences at $\text{pH} > 7$ (increasing solubility) are due to different formation constants and Pitzer coefficients for $\text{Np}^{(+IV)}$ carbonato complexes.

A 1.6 Solubility of Plutonium(+IV)

A 1.6.1 Gipshut solution

Tab. A1.9 Solubility of Plutonium(+IV) in Gipshut-solution

Step	Description
1.	Eliminate all Pu-species and Pu-solids the oxidation number of which is different from +IV, and oceanic carbonates which otherwise would precipitate under conditions covered by the calculations, namely: $\text{Pu}^{(+III)}(\text{OH})^{2+}$, $\text{Pu}^{(+III)}(\text{SO}_4)^+$, $\text{Pu}^{(+III)}(\text{SO}_4)_2^-$, $\text{Pu}^{(+III)3+}$, $(\text{Pu}^{(+V)}\text{O}_2)(\text{CO}_3)^-$, $(\text{Pu}^{(+V)}\text{O}_2)(\text{CO}_3)_3^{5-}$, $(\text{Pu}^{(+V)}\text{O}_2)(\text{OH})^0$, $(\text{Pu}^{(+V)}\text{O}_2)^+$, $(\text{Pu}^{(+VI)}\text{O}_2)(\text{CO}_3)^0$, $(\text{Pu}^{(+VI)}\text{O}_2)(\text{CO}_3)_2^{2-}$, $(\text{Pu}^{(+VI)}\text{O}_2)(\text{CO}_3)_3^{4-}$, $(\text{Pu}^{(+VI)}\text{O}_2)(\text{OH})^+$, $(\text{Pu}^{(+VI)}\text{O}_2)(\text{OH})_2^0$, $(\text{Pu}^{(+VI)}\text{O}_2)(\text{SO}_4)^0$, $(\text{Pu}^{(+VI)}\text{O}_2)(\text{SO}_4)_2^{2-}$, $(\text{Pu}^{(+VI)}\text{O}_2)^{2+}$, $(\text{Pu}^{(+VI)}\text{O}_2)_2(\text{OH})_2^{2+}$, $(\text{Pu}^{(+VI)}\text{O}_2)_3(\text{OH})_5^+$, $(\text{Pu}^{(+VI)}\text{O}_2)\text{Cl}^+$, $(\text{Pu}^{(+VI)}\text{O}_2)\text{Cl}_2^0$, $\text{Pu}^{(+III)}(\text{OH})_3(\text{c})$, $(\text{Pu}^{(+V)}\text{O}_2)(\text{OH})(\text{am})$, $(\text{Pu}^{(+VI)}\text{O}_2)(\text{CO}_3)(\text{s})$, $(\text{Pu}^{(+VI)}\text{O}_2)(\text{OH})_2 \cdot \text{H}_2\text{O}(\text{c})$, $\text{Na}_2(\text{CO}_3) \cdot 10\text{H}_2\text{O}$ (Natron), $\text{Na}_2(\text{CO}_3) \cdot 7\text{H}_2\text{O}$, $\text{Na}_3(\text{CO}_3)(\text{HCO}_3) \cdot 2\text{H}_2\text{O}$ (Trona), $\text{K}_2\text{Na}(\text{HCO}_3)(\text{CO}_3) \cdot 2\text{H}_2\text{O}$ (Trona-K), $\text{Na}(\text{HCO}_3)$ (Nahcolite), $\text{Na}_2(\text{CO}_3) \cdot \text{H}_2\text{O}$ (Thermonatrite).
2.	Calculate 1 kg H_2O in equilibrium with 0.5 mol halite, 0.01 mol $\text{Pu}(\text{OH})_4(\text{am})$, and a) $p(\text{CO}_2) = 0$ bar b) $p(\text{CO}_2) = 10^{-5}$ bar c) $p(\text{CO}_2) = 10^{-3.5}$ bar d) $p(\text{CO}_2) = 10^{-2}$ bar e) $p(\text{CO}_2) = 1$ bar
3.	Adjust to $\text{pH} \sim 1$ by adding HCl.
4.	Titrate with NaOH
The resulting stream for step 3 is:	
	55.5084391 Mol H_2O
	0.5 Mol NaCl
	$1.0 \cdot 10^{-2}$ Mol $\text{Pu}(\text{OH})_4(\text{am})$
	$1.0 \cdot 10^{-2}$ Mol H^+
	$1.0 \cdot 10^{-2}$ mol Cl^-
a)	0 Pa (no CO_2 at all)
b)	1.0 Pa resulting in 10^{-5} bar CO_2
c)	31.6227766 Pa resulting in $10^{-3.5}$ bar CO_2
d)	1000.0 Pa resulting in 10^{-2} bar CO_2
e)	100000.0 Pa resulting in 1 bar CO_2

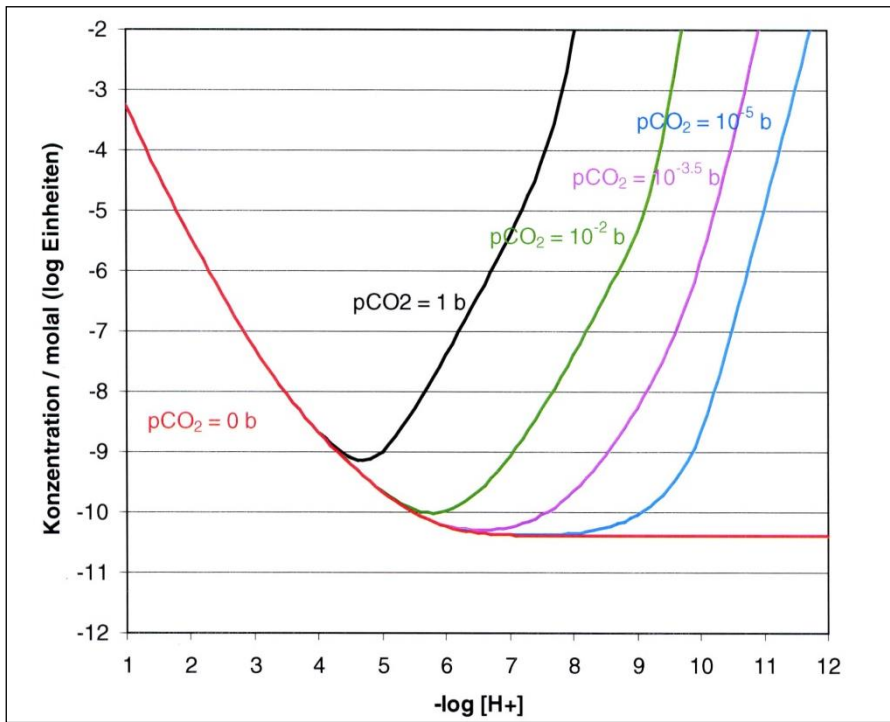
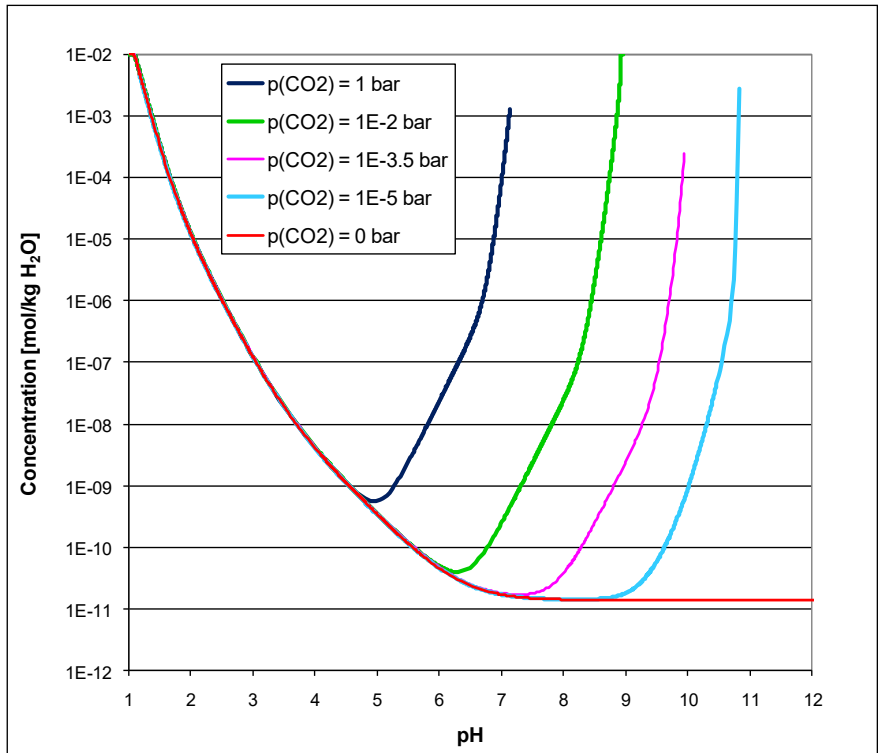


Fig. A1.13 Solubility of $\text{Pu}^{(\text{IV})}$ in 0.5 M NaCl-solution at various CO_2 -partial pressures and $\text{Pu}^{(\text{IV})}(\text{OH})_4(\text{am})$ as solubility limiting phase, top = this report (GRS) and bottom = /KIE 00/

As to the general pattern of calculated solubility, both calculations give consistent results:

1. When no CO₂ is present, solubility is decreasing homogeneously, gradually approaching a minimum solubility at pH~8.
2. When CO₂ is present solubility is going through a minimum; at higher pH-values solubility increases due to the formation of Pu^(+IV)-carbonato-complexes.
3. An increasing CO₂-fugacity leads to a shift of solubility minimum to lower pH-values, the range of solubility minimum becoming increasingly narrow.
4. The minimum solubility increases with increasing CO₂-fugacity.
5. Below pH~5 solubility is unaffected by the presence of CO₂.

However, looking into details reveals differences. At $p(\text{CO}_2) = 1$ bar minimum solubility is about the same, but at all other partial pressures solubility minimum calculated by GRS is lower and at slightly higher pH-values. Though this may not seem significant at the first glance, large differences become obvious when for a given pH and CO₂-partial pressure calculated solubilities are compared. For example, at $p(\text{CO}_2) = 10^{-3.5}$ bar INE calculated a solubility between $1 \cdot 10^{-9}$ and $1 \cdot 10^{-10}$ (estimated from the figure) while we calculate $4.8 \cdot 10^{-11}$. At the best, these values differ by one order of magnitude. At higher pH-values and the same partial pressure these differences become even more profound as the calculated gradient of solubility seems to be larger than is the case in the INE-calculation.

With no CO₂ at all solubility approaches $1.43 \cdot 10^{-11}$ while in /KIE 00/ this limiting value seems to be somewhat higher though no numerical value is given there.

A 1.7 Solubility of Uranium(+VI)

A 1.7.1 Gipshut solution

Tab. A1.10 Solubility of Uranium(+VI) with Gipshut-solution

Step	Description
1.	Calculate 1 kg H ₂ O in equilibrium with halite and anhydrite and p(CO ₂) = 0.0003 bar
2.	Eliminate all U-species and U-solids the oxidation number of which is different from +VI, all reduced S-species whose oxidation number is different from +VI, and all oceanic carbonates which otherwise would eventually precipitate during the calculation, namely: H ₂ S ⁰ , HS ⁻ , U ^{(+III)3+} , U ^{(+IV)(CO₃)₄⁴⁻} , U ^{(+IV)(CO₃)₅⁶⁻} , U ^{(+IV)(OH)₃³⁺} , U ^{(+IV)(OH)₂(CO₃)₂²⁻} , U ^{(+IV)(OH)₂²⁺} , U ^{(+IV)(OH)₃⁺} , U ^{(+IV)(OH)₄⁰} , U ^{(+IV)(SO₄)₂²⁺} , U ^{(+IV)(SO₄)₂⁰} , U ^{(+IV)4+} , U ^{(+IV)Cl₃³⁺} , (U ^{(+V)O₂})(CO ₃) ₃ ⁵⁻ , (U ^{(+V)O₂}) ⁺ , U ^{(+IV)(OH)₂(SO₄)(c)} , U ^{(+IV)l(OH)₄(am)} , U ^{(+IV)(SiO₄)(c)} (Coffinite). Leaving reduced S-species in the calculation led to numerical instabilities.
3.	Set constant molar masses of halite, anhydrite from first step and check resulting solid phase activities; CO ₂ -fugacity remains fixed at 30 Pa.
4.	Add 5·10 ⁻⁴ mol Na ₂ (U ^(+VI) ₂ O ₇)(c). Adjust to pH~3.5 by adding HCl.
5.	Titrate with 1·10 ⁻² mol NaOH
The resulting stream for step 4 is:	
55.5084391	mol H ₂ O
6.0719	mol NaCl
4.3259·10 ⁻²	mol Anhydrite
3.1·10 ⁻³	mol H ⁺
3.1·10 ⁻³	mol Cl ⁻
30	Pa CO ₂ leading to p(CO ₂) = 0.0003 bar in any step
5.0·10 ⁻⁴	mol Na ₂ (U ^(+VI) ₂ O ₇)(c)

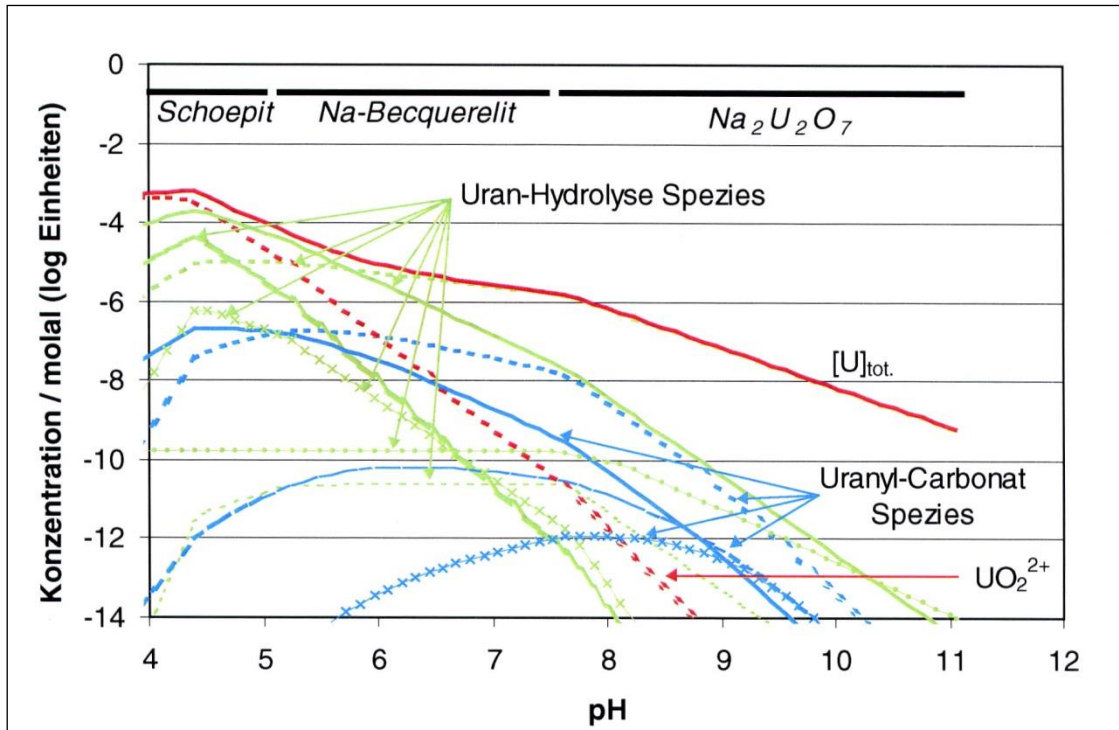
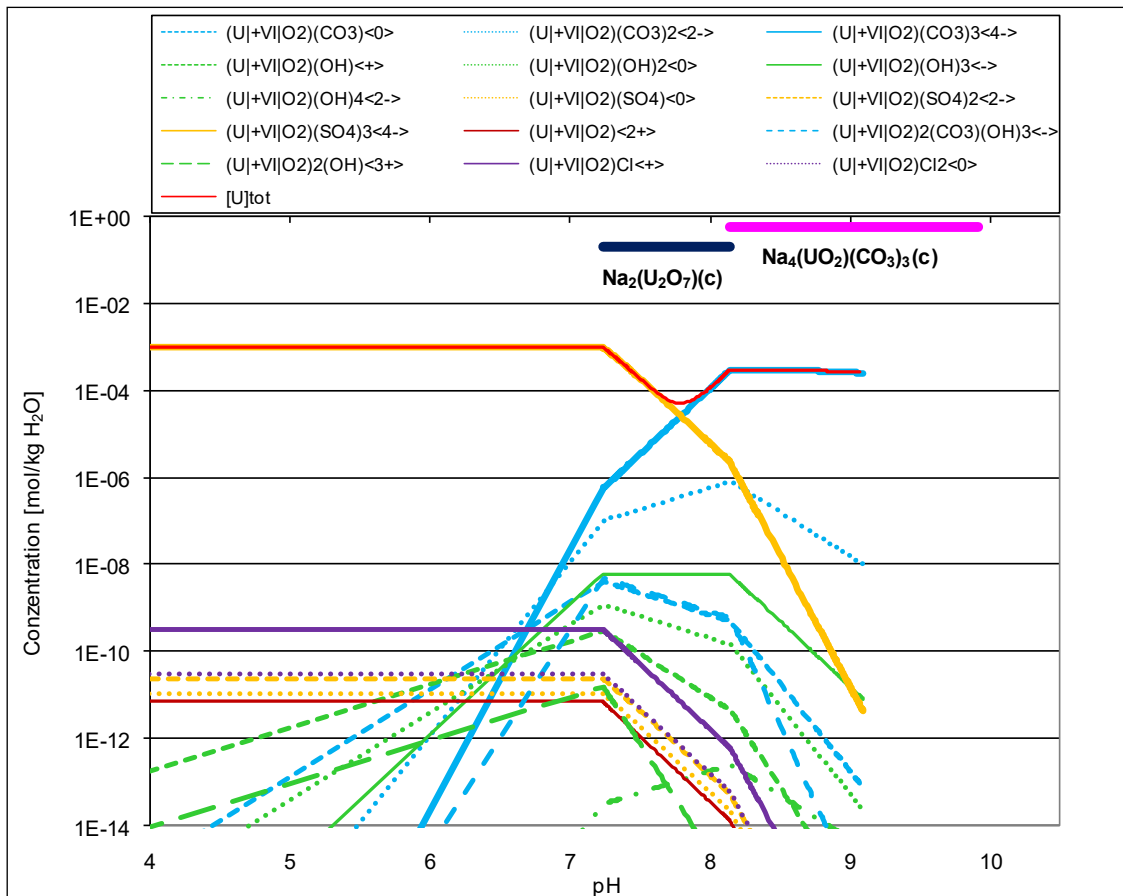


Fig. A1.14 Solubility of $U^{(VI)}$ in Gipshut-solution with $p(\text{CO}_2) = 0.0003$ bar, top = this report (GRS) and bottom = /KIE 00/

According to the INE-report, Schoepite, Na-Becquerelite, and $\text{Na}_2(\text{U}^{(+\text{VI})}_2\text{O}_7)(\text{c})$ were the solubility limiting phases, depending on the pH-value. As in this report, $\text{Na}_2(\text{U}^{(+\text{VI})}_2\text{O}_7)(\text{c})$ began to precipitate at $\text{pH} > 7$ ($\text{pH} = 7.23$). A minimum solubility of $5.34 \cdot 10^{-5}$ is found at $\text{pH} = 7.79$, see Fig. 7.14. At higher pH solubility increases due to the formation of carbonato complexes. Between $\text{pH} = 7.79$ and 8.14 Na-Diuranate dissolves. At $\text{pH} = 8.14$ a second solid phase, $\text{Na}_4(\text{U}^{(+\text{VI})}\text{O}_2)(\text{CO}_3)_3(\text{c})$, is formed. At $\text{pH} = 8.14$ its solubility is $3.87 \cdot 10^{-4}$ which slowly decreases with increasing pH.

$\text{U}^{(+\text{VI})}\text{O}_3 \cdot 2\text{H}_2\text{O}(\text{c})$ (Schoepite) was present in the database but did not form. Na-Becquerelite was not present in the database, but $\text{Ca}(\text{U}^{(+\text{VI})}_6\text{O}_{19}) \cdot 11\text{H}_2\text{O}(\text{c})$ (Becquerelite). Fig. 7.15 shows that none of the two phases attained saturation. Thus up to a $\text{pH} = 7.23$ the added mass of Na-Diuranate remained dissolved quantitatively. On the other hand $\text{Na}_4(\text{U}^{(+\text{VI})}\text{O}_2)(\text{CO}_3)_3(\text{c})$ which did form in our calculation, was not mentioned at all in the INE-report.

As to $\text{Na}_2(\text{U}^{(+\text{VI})}_2\text{O}_7)(\text{c})$ situation is difficult to overview. In /ALT 04/ two values are given: $\log K_{\text{sp}}^0 = -30.7 \pm 0.5$ ($\text{Na}_2\text{U}_2\text{O}_7(\text{cr})$) and $\log K_{\text{sp}}^0 = -29.45 \pm 1.0$ ($\text{Na}_2\text{U}_2\text{O}_7(\text{cr},\text{hydr})$). In Appendix 2, p. 349 of the same document only a Gibbs Free Energy of formation is given, which was used for calculations in this report. In the INE-report, however, solubility constants of -22.6 and 26 are given. Departing from such a situation all agreeing results could not be expected.

Another striking feature of the INE-calculation is that apparently no sulphato-complexes were involved. At least no reference is given for them in the corresponding figure. In our calculation, however, $(\text{U}^{(+\text{VI})}\text{O}_2)(\text{SO}_4)_3^{4-}$ is calculated to be the dominating species at pH-values < 7.23 .

To explore the influence neglecting sulphato-complexes of hexavalent uranium might have, the calculation depicted in Fig. 7.14 was repeated with the following complexes eliminated: $(\text{U}^{(+\text{VI})}\text{O}_2)(\text{SO}_4)^0$, $(\text{U}^{(+\text{VI})}\text{O}_2)(\text{SO}_4)_2^{2-}$, $(\text{U}^{(+\text{VI})}\text{O}_2)(\text{SO}_4)_3^{4-}$.

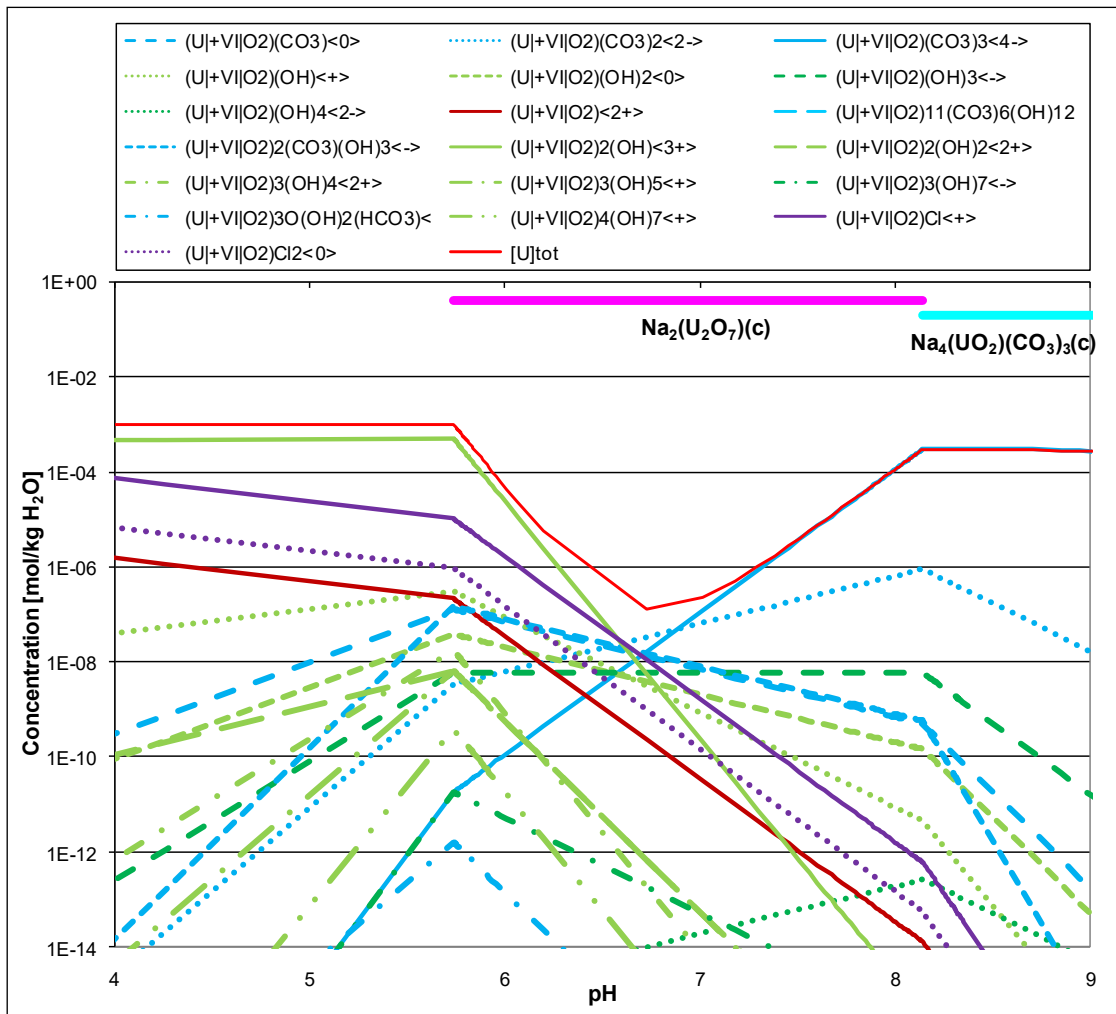


Fig. A1.15 Solubility of $U^{(VI)}$ in Giphshut-solution with $p(CO_2) = 0.0003$ bar; $U|+VI|$ -sulphato-complexes were eliminated

The same solid phases appear as in the former calculation. But, as can be seen, when Fig. 7.14 and Fig. 7.15 are compared, Na-Diuranate begins to precipitate at a lower pH (pH = 5.73), and minimum solubility is lower ($1.30 \cdot 10^{-7}$ at pH = 6.72). On the other hand, $Na_4(U^{(VI)}O_2)(CO_3)_3(c)$ precipitates at the same pH = 8.14 with about the same solubility ($1.60 \cdot 10^{-5}$).

It should further be noted that the sign of the formation constant for $(UO_2)_3(CO_3)_6^{6-}$ as given in /ALT 04/ was probably in error and was reversed for calculations for this report. Otherwise $U^{(VI)}$ would not have been precipitated regardless of carbonate concentration and pH.

It might be questioned whether this calculation resembles any situation occurring naturally. As mentioned in the synopsis to this calculation. oceanic carbonates were excluded

from calculation. Fig. 7.16 exhibits the calculated solid phase activities. It can be seen that for a number of solid phases calculated activities are greater than unity. This means that these phases, had they not been excluded from calculation, would have been formed, leading essentially to another computational result. Furthermore, to have a pH value of ~ 9.9 it was necessary to add 1 mol NaOH. In the report by INE, solubilities were calculated beyond pH ~ 11. To obtain such a pH – in equilibrium with $p(\text{CO}_2) = 30 \text{ Pa}$ – no less than 25 mol of NaOH would be necessary to add. Under these conditions other oceanic carbonates would precipitate

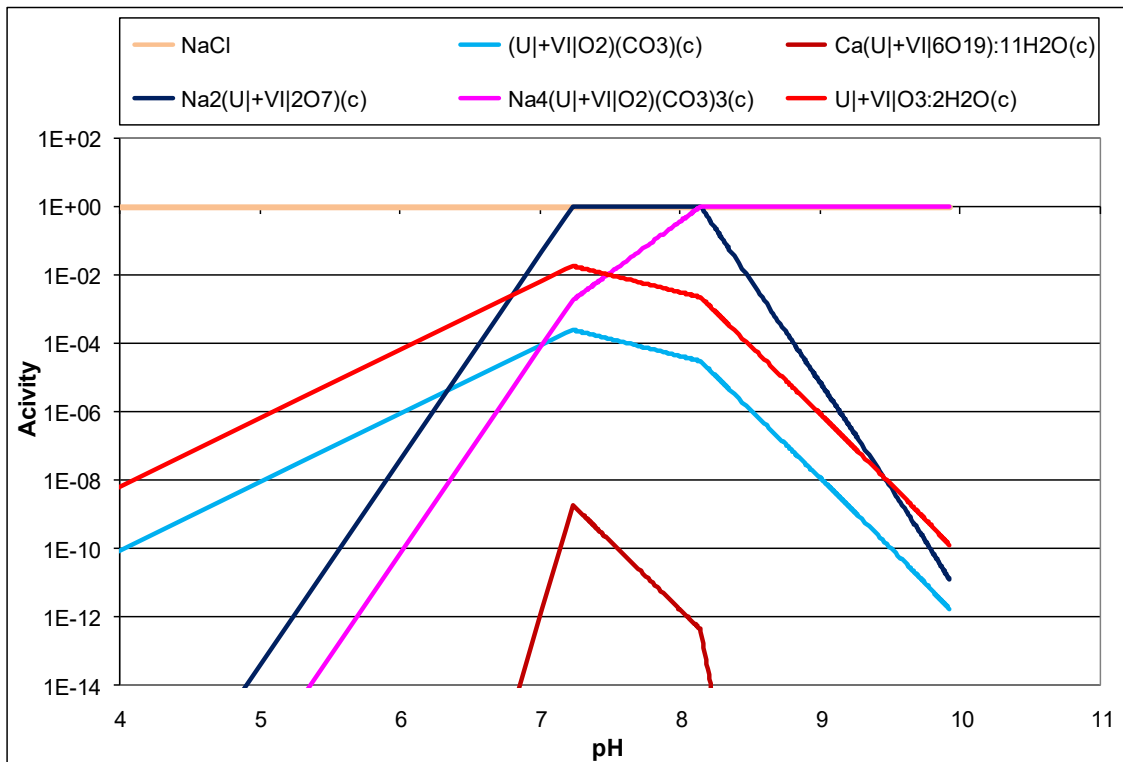


Fig. A1.16 Solid phase activities in the calculation of solubility of $\text{U}^{(+VI)}$ in Gipshut-solution with $p(\text{CO}_2) = 0.0003 \text{ bar}$

Summarized, calculated solubilities for $\text{U}^{(+VI)}$ in this report differ markedly from those given in /KIE 00/.

A 1.7.2 Q-Brine solution

Tab. A1.11 Solubility of Uranium(+VI) in Q-Brine-solution without CO₂

Step	Description
1.	Calculate 1 kg H ₂ O in equilibrium with halite, sylvite, carnallite, kainite and p(CO ₂) = 0 bar
2.	Set constant molar masses of halite, sylvite, carnallite, and kainite from first step and check resulting solid phase activities.
3.	Eliminate all U-species the oxidation number of which is different from +VI, all reduced S-species whose oxidation number is different from +VI, and all U ^(+VI) -sulphato-complexes, namely: H ₂ S(g), H ₂ S ⁰ , HS ⁻ , U ^(+III) 3 ⁺ , U ^(+IV) (CO ₃) ₄ ⁴⁻ , U ^(+IV) (CO ₃) ₅ ⁶⁻ , U ^(+IV) (OH) ³⁺ , U ^(+IV) (OH) ₂ (CO ₃) ₂ ⁺ , U ^(+IV) (OH) ₂ ²⁺ , U ^(+IV) (OH) ₃ ⁺ , U ^(+IV) (OH) ₄ ⁰ , U ^(+IV) (SO ₄) ₂ ²⁺ , U ^(+IV) (SO ₄) ₂ ⁰ , U ^(+IV) 4 ⁺ , U ^(+IV) Cl ³⁺ , (U ^(+V) O ₂)(CO ₃) ₃ ⁵⁻ , (U ^(+V) O ₂) ⁺ , U ^(+IV) (OH) ₂ (SO ₄)(c), U ^(+IV) (OH) ₄ (am), U ^(+IV) (SiO ₄)(c) (Coffinite), (U ^(+VI) O ₂)(SO ₄) ⁰ , (U ^(+VI) O ₂)(SO ₄) ₂ ²⁻ , (U ^(+VI) O ₂)(SO ₄) ₃ ⁴⁻ . Leaving reduced S-species in the calculation led to numerical instabilities.
4.	Add 1.00·10 ⁻³ mol Na ₂ (U ^(+VI)) ₂ O ₇ (c); add 5.99·10 ⁻³ mol HCl to adjust to pH~4.
5.	Titrate with 2.1·10 ⁻² mol NaOH
The resulting stream for step 4 is:	
55.5084391 mol H ₂ O 8.5620·10 ⁻¹ mol NaCl -6.4655 mol Sylvite 6.9181 mol Carnallite 5.5705·10 ⁻¹ mol Kainite 0 mol CO ₂ 1.00·10 ⁻³ mol Na ₂ (U ^(+VI)) ₂ O ₇ (c) 5.99·10 ⁻³ mol H ⁺ 5.99·10 ⁻³ mol Cl ⁻	

According to the INE-report schoepite and Na-Becquerelite are the solubility-limiting solid phases. Our result in comparison to those from INE is shown in Fig. 7.17.

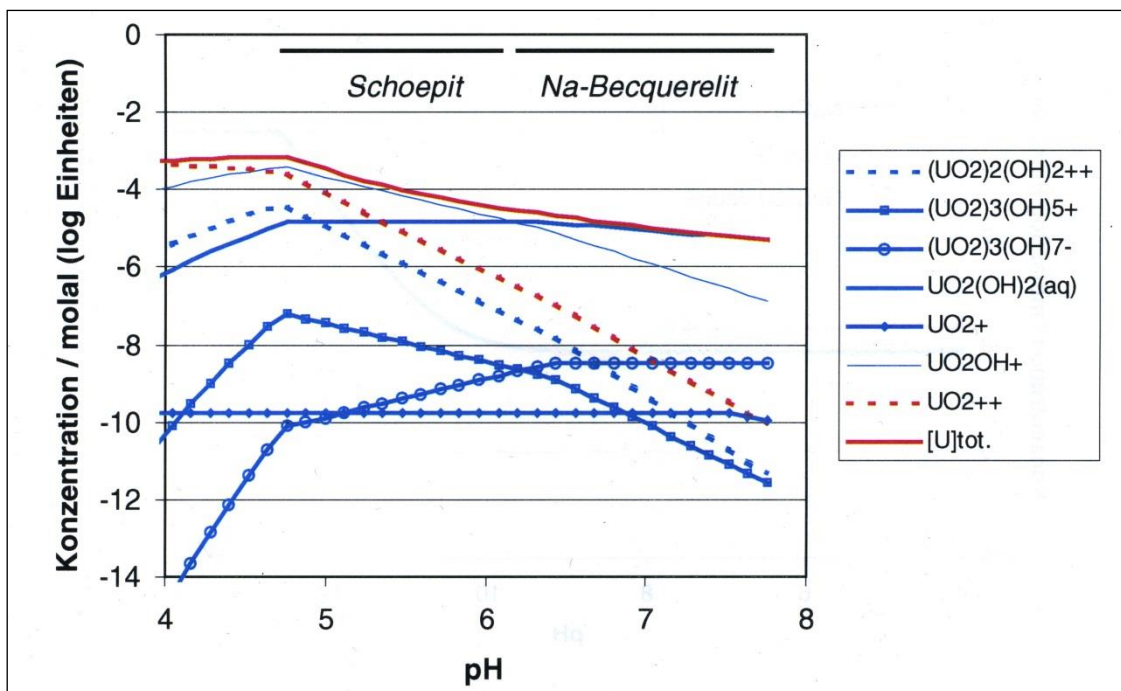
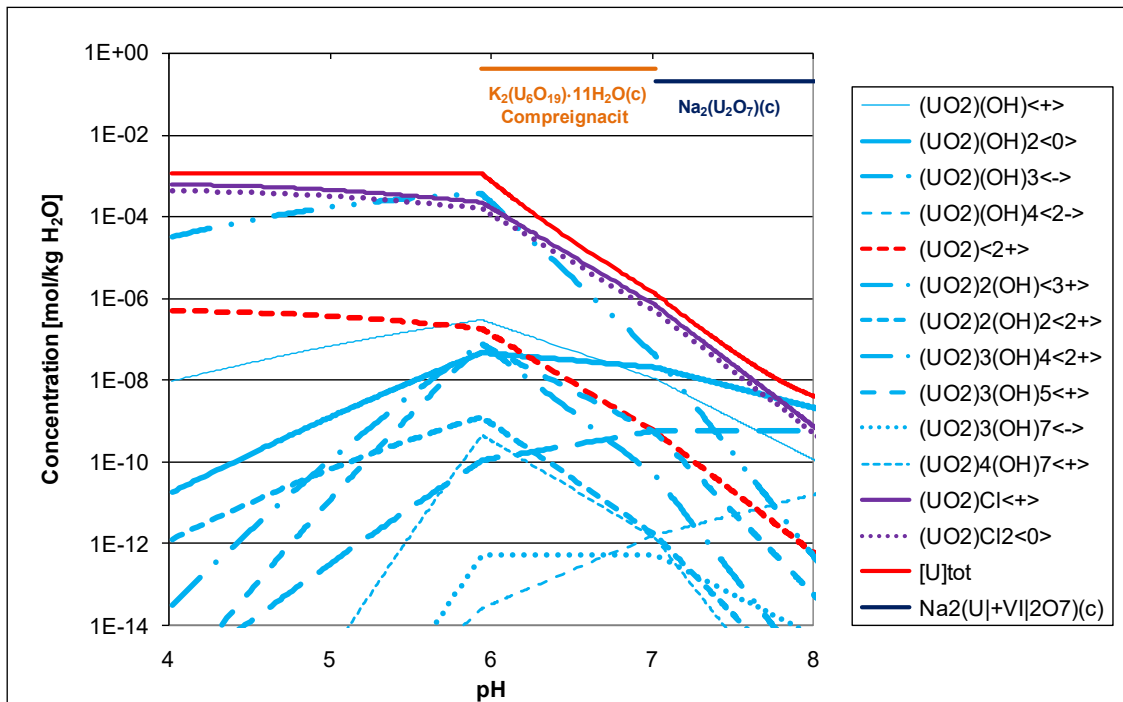


Fig. A1.17 Solubility of $U^{(VI)}$ in Q-Brine (without CO_2), top = this report (GRS) and bottom = /KIE 00/

In our calculation $U^{(VI)}O_3 \cdot 2H_2O(c)$ (Schoepite) was close to saturation as is depicted in Fig. 7.18. Instead $K_2(U^{(VI)}_6O_{19}) \cdot 11H_2O(c)$ (compreignacite) precipitated at $pH = 5.94$. At $pH \sim 7.00$ it began to re-dissolve. At $pH = 7.02$ precipitation of $Na_2(U^{(VI)}_2O_7)(c)$ commenced. At $pH > 8$ the system was pH-buffered by the precipitation of brucite. Calculated

$U^{(VI)}$ -solubility at pH = 8.0 was $4.14 \cdot 10^{-9}$, which after visual inspection of the figure supplied by INE is about three orders of magnitude lower as given in /KIE 00/. Note that our calculation in this system was performed without $U^{(VI)}$ -sulphato-complexes, for which no Pitzer coefficients were given by INE.

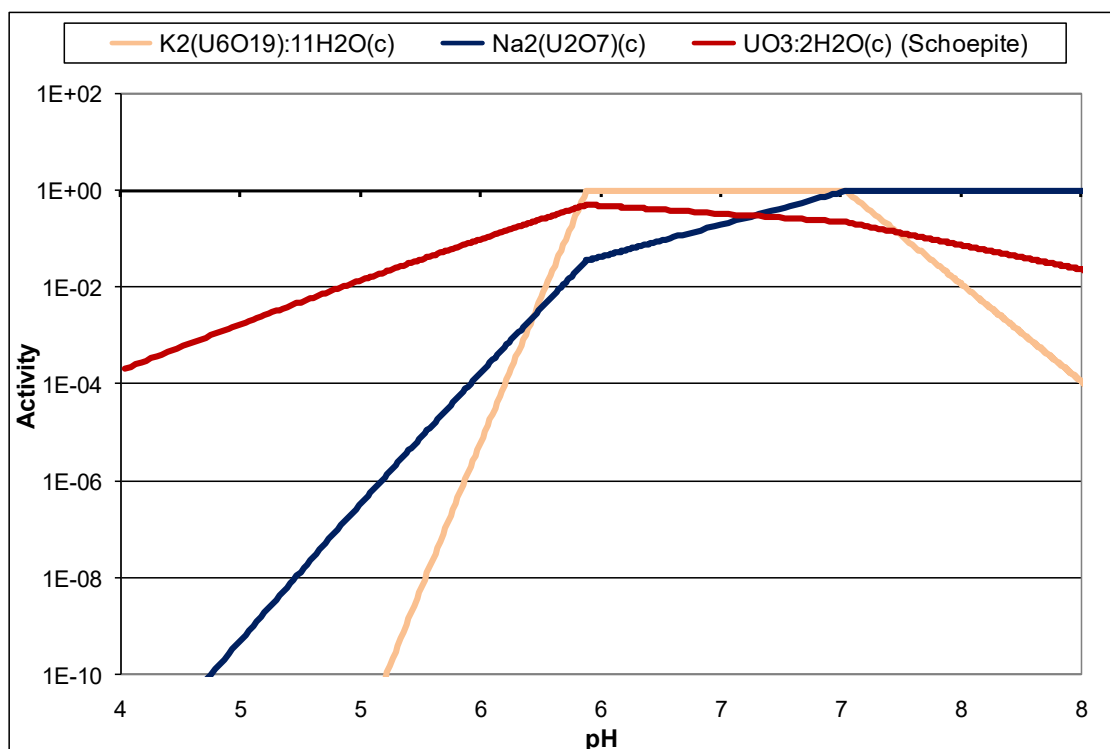


Fig. A1.18 Solid phase activities in the calculation of solubility of $U^{(VI)}$ in Q-Brine (without CO_2)

Solubility of $U^{(VI)}$ does not increase beyond pH ~ 7 as is the case in Gipshut-solution with CO_2 . This is due to the absence of carbonate.

Differences in the databases used might be the cause for the differing results between our calculations and those by INE. The phase $K_2(U^{(VI)}_6O_{19}) \cdot 11H_2O(c)$ (compreignacite), the formation of which was calculated by us, was not mentioned in /KIE 00/. On the other hand, there was no such phase like Na-Becquerelite in the database used for the calculations in this report.

A 2 Pitzer coefficients for actinides and Tc

The following table lists all Pitzer coefficients for actinides and Tc adopted from /ALT 04/.

Tab. A2.1 Pitzer coefficients for actinides and Tc adopted from /ALT 04/

Coefficient	Species	Value
beta0	(TcO)(OH)<+> (SO4)<2->	0.1
beta1	(TcO)(OH)<+> (SO4)<2->	1
cphi	(TcO)(OH)<+> (SO4)<2->	0
beta0	(TcO)(OH)<+> Cl<->	0.1
beta1	(TcO)(OH)<+> Cl<->	0.2
cphi	(TcO)(OH)<+> Cl<->	0
lambda	(TcO)(OH)2<0> (SO4)<2->	0
lambda	(TcO)(OH)2<0> Cl<->	0
beta0	(TcO)<2+> (SO4)<2->	0.2
beta1	(TcO)<2+> (SO4)<2->	3
beta2	(TcO)<2+> (SO4)<2->	-40
cphi	(TcO)<2+> (SO4)<2->	0
beta0	(TcO)<2+> Cl<->	0.3
beta1	(TcO)<2+> Cl<->	1.7
cphi	(TcO)<2+> Cl<->	0
psi	(TcO4)<-> (SO4)<2-> Na<+>	-0.003
psi	(TcO4)<-> (SO4)<2-> K<+>	0.002
psi	(TcO4)<-> (SO4)<2-> Mg<2+>	0
psi	(TcO4)<-> (SO4)<2-> Ca<2+>	-0.03
theta	(TcO4)<-> (SO4)<2->	0.179
psi	(TcO4)<-> Cl<-> Na<+>	-0.0085
psi	(TcO4)<-> Cl<-> K<+>	-0.011
psi	(TcO4)<-> Cl<-> Mg<2+>	-0.033
psi	(TcO4)<-> Cl<-> Ca<2+>	-0.0115
theta	(TcO4)<-> Cl<->	0.067
lambda	Ca<2+> (TcO)(OH)2<0>	0
beta0	Ca<2+> (TcO)(OH)3<->	0.3
beta1	Ca<2+> (TcO)(OH)3<->	1.7
cphi	Ca<2+> (TcO)(OH)3<->	0
beta0	Ca<2+> (TcO4)<->	0.2964
beta1	Ca<2+> (TcO4)<->	1.661
cphi	Ca<2+> (TcO4)<->	0
lambda	Ca<2+> Tc(CO3)(OH)2<0>	0
beta0	Ca<2+> Tc(CO3)(OH)3<->	0.3
beta1	Ca<2+> Tc(CO3)(OH)3<->	1.7
cphi	Ca<2+> Tc(CO3)(OH)3<->	0
beta0	Cs<+> (TcO4)<->	-0.1884
beta1	Cs<+> (TcO4)<->	-0.1588
cphi	Cs<+> (TcO4)<->	0
lambda	K<+> (TcO)(OH)2<0>	0
beta0	K<+> (TcO)(OH)3<->	0
beta1	K<+> (TcO)(OH)3<->	0.1
cphi	K<+> (TcO)(OH)3<->	0
beta0	K<+> (TcO4)<->	-0.0578

Coefficient	Species	Value
beta1	K<+> (TcO4)<->	0.006
cphi	K<+> (TcO4)<->	0
lambda	K<+> Tc(CO3)(OH)2<0>	0
beta0	K<+> Tc(CO3)(OH)3<->	0
beta1	K<+> Tc(CO3)(OH)3<->	0.3
cphi	K<+> Tc(CO3)(OH)3<->	0
lambda	Mg<2+> (TcO)(OH)2<0>	0
beta0	Mg<2+> (TcO)(OH)3<->	0.3
beta1	Mg<2+> (TcO)(OH)3<->	1.7
cphi	Mg<2+> (TcO)(OH)3<->	0
beta0	Mg<2+> (TcO4)<->	0.3138
beta1	Mg<2+> (TcO4)<->	1.84
cphi	Mg<2+> (TcO4)<->	0.0114
lambda	Mg<2+> Tc(CO3)(OH)2<0>	0
beta0	Mg<2+> Tc(CO3)(OH)3<->	0.3
beta1	Mg<2+> Tc(CO3)(OH)3<->	1.7
cphi	Mg<2+> Tc(CO3)(OH)3<->	0
lambda	Na<+> (TcO)(OH)2<0>	0
beta0	Na<+> (TcO)(OH)3<->	0
beta1	Na<+> (TcO)(OH)3<->	0.1
cphi	Na<+> (TcO)(OH)3<->	0
beta0	Na<+> (TcO4)<->	0.01111
beta1	Na<+> (TcO4)<->	0.1595
cphi	Na<+> (TcO4)<->	0.00236
psi	Na<+> Mg<2+> (TcO4)<->	-0.02
lambda	Na<+> Tc(CO3)(OH)2<0>	0
beta0	Na<+> Tc(CO3)(OH)3<->	0
beta1	Na<+> Tc(CO3)(OH)3<->	0.3
cphi	Na<+> Tc(CO3)(OH)3<->	0
lambda	Tc(CO3)(OH)2<0> (SO4)<2->	0
lambda	Tc(CO3)(OH)2<0> Cl<->	0
beta2	K<+> Th(CO3)4<4->	0
cphi	K<+> Th(CO3)4<4->	0
beta0	K<+> Th(CO3)5<6->	1.31
beta1	K<+> Th(CO3)5<6->	30
beta2	K<+> Th(CO3)5<6->	0
cphi	K<+> Th(CO3)5<6->	0
beta0	K<+> Th(OH)(CO3)4<5->	0
beta1	K<+> Th(OH)(CO3)4<5->	23
beta2	K<+> Th(OH)(CO3)4<5->	0
cphi	K<+> Th(OH)(CO3)4<5->	0
beta0	K<+> Th(OH)2(CO3)2<2->	0
beta1	K<+> Th(OH)2(CO3)2<2->	2
beta2	K<+> Th(OH)2(CO3)2<2->	0
cphi	K<+> Th(OH)2(CO3)2<2->	0
beta0	K<+> Th(OH)3(CO3)<->	0
beta1	K<+> Th(OH)3(CO3)<->	0.2
beta2	K<+> Th(OH)3(CO3)<->	0
cphi	K<+> Th(OH)3(CO3)<->	0
beta0	K<+> Th(OH)4(CO3)<2->	0
beta1	K<+> Th(OH)4(CO3)<2->	2

Coefficient	Species	Value
beta2	K<+> Th(OH)4(CO3)<2->	0
cphi	K<+> Th(OH)4(CO3)<2->	0
beta0	K<+> Th(OH)4<0>	0
beta0	Mg<2+> Th(OH)4<0>	0
beta2	Na<+> Th(CO3)4<4->	0
cphi	Na<+> Th(CO3)4<4->	0
beta0	Na<+> Th(CO3)5<6->	1.31
beta1	Na<+> Th(CO3)5<6->	30
beta2	Na<+> Th(CO3)5<6->	0
cphi	Na<+> Th(CO3)5<6->	0
beta0	Na<+> Th(OH)(CO3)4<5->	0
beta1	Na<+> Th(OH)(CO3)4<5->	23
beta2	Na<+> Th(OH)(CO3)4<5->	0
cphi	Na<+> Th(OH)(CO3)4<5->	0
beta0	Na<+> Th(OH)2(CO3)2<2->	0
beta1	Na<+> Th(OH)2(CO3)2<2->	2
beta2	Na<+> Th(OH)2(CO3)2<2->	0
cphi	Na<+> Th(OH)2(CO3)2<2->	0
beta0	Na<+> Th(OH)3(CO3)<->	0
beta1	Na<+> Th(OH)3(CO3)<->	0.2
beta2	Na<+> Th(OH)3(CO3)<->	0
cphi	Na<+> Th(OH)3(CO3)<->	0
beta0	Na<+> Th(OH)4(CO3)<2->	0
beta1	Na<+> Th(OH)4(CO3)<2->	2
beta2	Na<+> Th(OH)4(CO3)<2->	0
cphi	Na<+> Th(OH)4(CO3)<2->	0
beta0	Na<+> Th(OH)4<0>	0
psi	Th(CO3)5<6-> Cl<-> Na<+>	0.3
theta	Th(CO3)5<6-> Cl<->	1.8
beta0	Th(OH)<3+> Cl<->	0.6
beta1	Th(OH)<3+> Cl<->	5.9
beta2	Th(OH)<3+> Cl<->	0
cphi	Th(OH)<3+> Cl<->	0
beta0	Th(OH)2<2+> Cl<->	0.23
beta1	Th(OH)2<2+> Cl<->	1.93
beta2	Th(OH)2<2+> Cl<->	0
cphi	Th(OH)2<2+> Cl<->	0
beta0	Th(OH)3<+> Cl<->	0.08
beta1	Th(OH)3<+> Cl<->	0.39
beta2	Th(OH)3<+> Cl<->	0
cphi	Th(OH)3<+> Cl<->	0
beta0	Th(OH)4<0> Cl<->	0
beta0	Th<4+> Cl<->	1.014
beta1	Th<4+> Cl<->	13.33
beta2	Th<4+> Cl<->	0
cphi	Th<4+> Cl<->	-0.1034
lambda	(U+VI O2)(CO3)<0> Cl<->	0
beta0	(U+VI O2)(OH)<+> Cl<->	0.15
beta1	(U+VI O2)(OH)<+> Cl<->	0.3
beta2	(U+VI O2)(OH)<+> Cl<->	0
cphi	(U+VI O2)(OH)<+> Cl<->	0

Coefficient	Species	Value
lambda	(U +VI O2)(OH)2<0> (SO4)<2->	0
lambda	(U +VI O2)(OH)2<0> Cl<->	0
beta0	(U +VI O2)<2+> (SO4)<2->	0.322
beta1	(U +VI O2)<2+> (SO4)<2->	1.827
beta2	(U +VI O2)<2+> (SO4)<2->	0
cphi	(U +VI O2)<2+> (SO4)<2->	-0.0176
beta0	(U +VI O2)<2+> Cl<->	0.42735
beta1	(U +VI O2)<2+> Cl<->	1.644
beta2	(U +VI O2)<2+> Cl<->	0
cphi	(U +VI O2)<2+> Cl<->	-0.03686
psi	(U +VI O2)<2+> Na<+> Cl<->	0
psi	(U +VI O2)<2+> Na<+> Cl<->	0
theta	(U +VI O2)<2+> Na<+>	0.0231
theta	(U +VI O2)<2+> Na<+>	0
beta0	(U +VI O2)2(OH)2<2+> Cl<->	0.5
beta1	(U +VI O2)2(OH)2<2+> Cl<->	1.6
beta2	(U +VI O2)2(OH)2<2+> Cl<->	0
cphi	(U +VI O2)2(OH)2<2+> Cl<->	0
beta0	(U +VI O2)3(OH)4<2+> Cl<->	0.07
beta1	(U +VI O2)3(OH)4<2+> Cl<->	1.6
beta2	(U +VI O2)3(OH)4<2+> Cl<->	0
cphi	(U +VI O2)3(OH)4<2+> Cl<->	0
psi	(U +VI O2)3(OH)4<2+> Na<+> Cl<->	0
theta	(U +VI O2)3(OH)4<2+> Na<+>	0.05
beta0	(U +VI O2)3(OH)5<+> Cl<->	0.31
beta1	(U +VI O2)3(OH)5<+> Cl<->	0.3
beta2	(U +VI O2)3(OH)5<+> Cl<->	0
cphi	(U +VI O2)3(OH)5<+> Cl<->	0
psi	(U +VI O2)3(OH)5<+> Mg<2+> Cl<->	-0.08
theta	(U +VI O2)3(OH)5<+> Mg<2+>	0
beta0	(U +VI O2)4(OH)7<+> Cl<->	0.23
beta1	(U +VI O2)4(OH)7<+> Cl<->	0.3
beta2	(U +VI O2)4(OH)7<+> Cl<->	0
cphi	(U +VI O2)4(OH)7<+> Cl<->	0
beta0	K<+> (U +VI O2)(OH)2<0>	0
beta0	K<+> U +IV (CO3)4<4->	1
beta1	K<+> U +IV (CO3)4<4->	13
beta2	K<+> U +IV (CO3)4<4->	0
cphi	K<+> U +IV (CO3)4<4->	0
beta0	K<+> U +IV (CO3)5<6->	1.5
beta1	K<+> U +IV (CO3)5<6->	31.3
beta2	K<+> U +IV (CO3)5<6->	0
cphi	K<+> U +IV (CO3)5<6->	0
beta0	K<+> U +IV (OH)2(CO3)2<2->	0
beta1	K<+> U +IV (OH)2(CO3)2<2->	2
beta2	K<+> U +IV (OH)2(CO3)2<2->	0
cphi	K<+> U +IV (OH)2(CO3)2<2->	0
beta0	K<+> U +IV (OH)4(CO3)<2->	0
beta2	K<+> U +IV (OH)4(CO3)<2->	0
cphi	K<+> U +IV (OH)4(CO3)<2->	0
lambda	K<+> U +IV (OH)4<0>	0

Coefficient	Species	Value
lambda	Mg<2+> (U +VI O2)(OH)2<0>	0
beta0	Mg<2+> (U +VI O2)(OH)3<->	0.2
beta1	Mg<2+> (U +VI O2)(OH)3<->	1.6
beta2	Mg<2+> (U +VI O2)(OH)3<->	0
cphi	Mg<2+> (U +VI O2)(OH)3<->	0
beta0	Mg<2+> (U +VI O2)(OH)4<2->	0
beta1	Mg<2+> (U +VI O2)(OH)4<2->	3
beta2	Mg<2+> (U +VI O2)(OH)4<2->	-40
cphi	Mg<2+> (U +VI O2)(OH)4<2->	0
beta0	Mg<2+> (U +VI O2)3(OH)7<->	0.2
beta1	Mg<2+> (U +VI O2)3(OH)7<->	1.6
beta2	Mg<2+> (U +VI O2)3(OH)7<->	0
cphi	Mg<2+> (U +VI O2)3(OH)7<->	0
lambda	Mg<2+> U +IV (OH)4<0>	0
beta0	Na<+> (U +VI O2)(CO3)<0>	0
beta0	Na<+> (U +VI O2)(CO3)2<2->	-0.12
beta1	Na<+> (U +VI O2)(CO3)2<2->	2.5
beta2	Na<+> (U +VI O2)(CO3)2<2->	0
cphi	Na<+> (U +VI O2)(CO3)2<2->	0
beta0	Na<+> (U +VI O2)(CO3)3<4->	0.88
beta1	Na<+> (U +VI O2)(CO3)3<4->	11.8
beta2	Na<+> (U +VI O2)(CO3)3<4->	0
cphi	Na<+> (U +VI O2)(CO3)3<4->	0
lambda	Na<+> (U +VI O2)(OH)2<0>	0
beta0	Na<+> (U +VI O2)(OH)3<->	-0.24
beta1	Na<+> (U +VI O2)(OH)3<->	0.3
beta2	Na<+> (U +VI O2)(OH)3<->	0
cphi	Na<+> (U +VI O2)(OH)3<->	0
beta0	Na<+> (U +VI O2)(OH)4<2->	0.16
beta1	Na<+> (U +VI O2)(OH)4<2->	1.6
beta2	Na<+> (U +VI O2)(OH)4<2->	0
cphi	Na<+> (U +VI O2)(OH)4<2->	0
beta0	Na<+> (U +VI O2)3(OH)7<->	-0.24
beta1	Na<+> (U +VI O2)3(OH)7<->	0.3
beta2	Na<+> (U +VI O2)3(OH)7<->	0
cphi	Na<+> (U +VI O2)3(OH)7<->	0
beta0	Na<+> U +IV (CO3)4<4->	1
beta1	Na<+> U +IV (CO3)4<4->	13
beta2	Na<+> U +IV (CO3)4<4->	0
cphi	Na<+> U +IV (CO3)4<4->	0
beta0	Na<+> U +IV (CO3)5<6->	1.5
beta1	Na<+> U +IV (CO3)5<6->	31.3
beta2	Na<+> U +IV (CO3)5<6->	0
cphi	Na<+> U +IV (CO3)5<6->	0
beta0	Na<+> U +IV (OH)2(CO3)2<2->	0
beta1	Na<+> U +IV (OH)2(CO3)2<2->	2
beta2	Na<+> U +IV (OH)2(CO3)2<2->	0
cphi	Na<+> U +IV (OH)2(CO3)2<2->	0
beta0	Na<+> U +IV (OH)4(CO3)<2->	0
beta2	Na<+> U +IV (OH)4(CO3)<2->	0
cphi	Na<+> U +IV (OH)4(CO3)<2->	0

Coefficient	Species	Value
lambda	Na<+> U +IV (OH)4<0>	0
beta0	U +IV (OH)<3+> Cl<->	0.6
beta1	U +IV (OH)<3+> Cl<->	5.9
beta2	U +IV (OH)<3+> Cl<->	0
cphi	U +IV (OH)<3+> Cl<->	0
beta0	U +IV (OH)2<2+> Cl<->	0.23
beta1	U +IV (OH)2<2+> Cl<->	1.93
beta2	U +IV (OH)2<2+> Cl<->	0
cphi	U +IV (OH)2<2+> Cl<->	0
beta0	U +IV (OH)3<+> Cl<->	0.08
beta1	U +IV (OH)3<+> Cl<->	0.39
beta2	U +IV (OH)3<+> Cl<->	0
cphi	U +IV (OH)3<+> Cl<->	0
lambda	U +IV (OH)4<0> Cl<->	0
beta0	U +IV <4+> Cl<->	1.27
beta1	U +IV <4+> Cl<->	13.5
beta2	U +IV <4+> Cl<->	0
cphi	U +IV <4+> Cl<->	0
theta	(Np +V O2)(CO3)<-> Cl<->	-0.25
theta	(Np +V O2)(CO3)2<3-> Cl<->	-0.25
theta	(Np +V O2)(CO3)3<5-> (CO3)<2->	-0.83
theta	(Np +V O2)(CO3)3<5-> Cl<->	-0.25
lambda	(Np +V O2)(OH)<0> Cl<->	-0.19
theta	(Np +V O2)(OH)2<-> Cl<->	-0.24
theta	(Np +V O2)<+> Ca<2+>	0.05
beta0	(Np +V O2)<+> Cl<->	0.1415
beta1	(Np +V O2)<+> Cl<->	0.281
beta2	(Np +V O2)<+> Cl<->	0
cphi	(Np +V O2)<+> Cl<->	0
theta	(Np +V O2)<+> Mg<2+>	0.05
lambda	(Np +VI O2)(CO3)<0> Cl<->	0
lambda	(Np +VI O2)(CO3)<0> Cl<->	-0.25
beta0	(Np +VI O2)(OH)<+> Cl<->	0.15
beta1	(Np +VI O2)(OH)<+> Cl<->	0.3
beta2	(Np +VI O2)(OH)<+> Cl<->	0
cphi	(Np +VI O2)(OH)<+> Cl<->	0
lambda	(Np +VI O2)(OH)2<0> (SO4)<2->	0
lambda	(Np +VI O2)(OH)2<0> Cl<->	0
beta0	(Np +VI O2)<2+> Cl<->	0.4274
beta1	(Np +VI O2)<2+> Cl<->	1.644
beta2	(Np +VI O2)<2+> Cl<->	0
cphi	(Np +VI O2)<2+> Cl<->	-0.0368
beta0	(Np +VI O2)2(OH)2<2+> Cl<->	0.5
beta1	(Np +VI O2)2(OH)2<2+> Cl<->	1.6
beta2	(Np +VI O2)2(OH)2<2+> Cl<->	0
cphi	(Np +VI O2)2(OH)2<2+> Cl<->	0
beta0	(Np +VI O2)3(OH)5<+> Cl<->	0.31
beta1	(Np +VI O2)3(OH)5<+> Cl<->	0.3
beta2	(Np +VI O2)3(OH)5<+> Cl<->	0
cphi	(Np +VI O2)3(OH)5<+> Cl<->	0
beta0	K<+> (Np +V O2)(CO3)<->	0.1

Coefficient	Species	Value
beta1	K<+> (Np +V O2)(CO3)<->	0.34
beta2	K<+> (Np +V O2)(CO3)<->	0
cphi	K<+> (Np +V O2)(CO3)<->	0
beta0	K<+> (Np +V O2)(CO3)2<3->	0.48
beta1	K<+> (Np +V O2)(CO3)2<3->	4.4
beta2	K<+> (Np +V O2)(CO3)2<3->	0
cphi	K<+> (Np +V O2)(CO3)2<3->	0
beta0	K<+> (Np +V O2)(CO3)3<5->	1.8
beta1	K<+> (Np +V O2)(CO3)3<5->	22.7
beta2	K<+> (Np +V O2)(CO3)3<5->	-95.1
cphi	K<+> (Np +V O2)(CO3)3<5->	-0.219
beta0	K<+> (Np +VI O2)(OH)2<0>	0
beta1	K<+> (Np +VI O2)(OH)2<0>	
beta2	K<+> (Np +VI O2)(OH)2<0>	
cphi	K<+> (Np +VI O2)(OH)2<0>	
beta0	K<+> Np +IV (CO3)4<4->	1
beta1	K<+> Np +IV (CO3)4<4->	13
beta2	K<+> Np +IV (CO3)4<4->	0
cphi	K<+> Np +IV (CO3)4<4->	0
beta0	K<+> Np +IV (CO3)5<6->	1.5
beta1	K<+> Np +IV (CO3)5<6->	31.3
beta2	K<+> Np +IV (CO3)5<6->	0
cphi	K<+> Np +IV (CO3)5<6->	0
beta0	K<+> Np +IV (OH)2(CO3)2<2->	0
beta1	K<+> Np +IV (OH)2(CO3)2<2->	2
beta2	K<+> Np +IV (OH)2(CO3)2<2->	0
cphi	K<+> Np +IV (OH)2(CO3)2<2->	0
beta0	K<+> Np +IV (OH)3(CO3)<->	0
beta2	K<+> Np +IV (OH)3(CO3)<->	0
cphi	K<+> Np +IV (OH)3(CO3)<->	0
beta0	K<+> Np +IV (OH)4(CO3)<2->	0
beta1	K<+> Np +IV (OH)4(CO3)<2->	2
beta2	K<+> Np +IV (OH)4(CO3)<2->	0
cphi	K<+> Np +IV (OH)4(CO3)<2->	0
beta0	K<+> Np +IV (OH)4(CO3)2<4->	1
beta1	K<+> Np +IV (OH)4(CO3)2<4->	13
beta2	K<+> Np +IV (OH)4(CO3)2<4->	0
cphi	K<+> Np +IV (OH)4(CO3)2<4->	0
beta0	Mg<2+> (Np +V O2)(CO3)<->	0.4
beta1	Mg<2+> (Np +V O2)(CO3)<->	1.7
beta2	Mg<2+> (Np +V O2)(CO3)<->	0
cphi	Mg<2+> (Np +V O2)(CO3)<->	0
lambda	Mg<2+> (Np +V O2)(OH)<0>	0
beta0	Mg<2+> (Np +V O2)(OH)2<->	0.4
beta1	Mg<2+> (Np +V O2)(OH)2<->	1.7
beta2	Mg<2+> (Np +V O2)(OH)2<->	0
cphi	Mg<2+> (Np +V O2)(OH)2<->	0
lambda	Mg<2+> (Np +VI O2)(OH)2<0>	0
lambda	Mg<2+> Np +IV (OH)4<0>	0
beta0	Na<+> (Np +V O2)(CO3)<->	0.1
beta1	Na<+> (Np +V O2)(CO3)<->	0.34

Coefficient	Species	Value
beta2	Na<+> (Np +V O2)(CO3)<->	0
cphi	Na<+> (Np +V O2)(CO3)<->	0
beta0	Na<+> (Np +V O2)(CO3)2<3->	0.48
beta1	Na<+> (Np +V O2)(CO3)2<3->	4.4
beta2	Na<+> (Np +V O2)(CO3)2<3->	0
cphi	Na<+> (Np +V O2)(CO3)2<3->	0
beta0	Na<+> (Np +V O2)(CO3)3<5->	1.8
beta1	Na<+> (Np +V O2)(CO3)3<5->	22.7
beta2	Na<+> (Np +V O2)(CO3)3<5->	0
cphi	Na<+> (Np +V O2)(CO3)3<5->	0
lambda	Na<+> (Np +V O2)(OH)<0>	0
beta0	Na<+> (Np +V O2)(OH)2<->	0
beta1	Na<+> (Np +V O2)(OH)2<->	0
beta2	Na<+> (Np +V O2)(OH)2<->	0
cphi	Na<+> (Np +V O2)(OH)2<->	0
lambda	Na<+> (Np +VI O2)(CO3)<0>	0.05
beta0	Na<+> (Np +VI O2)(CO3)2<2->	0.212
beta1	Na<+> (Np +VI O2)(CO3)2<2->	2.5
beta2	Na<+> (Np +VI O2)(CO3)2<2->	0
cphi	Na<+> (Np +VI O2)(CO3)2<2->	0
beta0	Na<+> (Np +VI O2)(CO3)3<4->	1.25
beta1	Na<+> (Np +VI O2)(CO3)3<4->	11.6
beta2	Na<+> (Np +VI O2)(CO3)3<4->	0
cphi	Na<+> (Np +VI O2)(CO3)3<4->	0
lambda	Na<+> (Np +VI O2)(OH)2<0>	0
beta0	Na<+> Np +IV (CO3)4<4->	1
beta1	Na<+> Np +IV (CO3)4<4->	13
beta2	Na<+> Np +IV (CO3)4<4->	0
cphi	Na<+> Np +IV (CO3)4<4->	0
beta0	Na<+> Np +IV (CO3)5<6->	1.5
beta1	Na<+> Np +IV (CO3)5<6->	31.3
beta2	Na<+> Np +IV (CO3)5<6->	0
cphi	Na<+> Np +IV (CO3)5<6->	0
beta0	Na<+> Np +IV (OH)2(CO3)2<2->	0
beta1	Na<+> Np +IV (OH)2(CO3)2<2->	2
beta2	Na<+> Np +IV (OH)2(CO3)2<2->	0
cphi	Na<+> Np +IV (OH)2(CO3)2<2->	0
beta0	Na<+> Np +IV (OH)3(CO3)<->	0
beta2	Na<+> Np +IV (OH)3(CO3)<->	0
cphi	Na<+> Np +IV (OH)3(CO3)<->	0
beta0	Na<+> Np +IV (OH)4(CO3)<2->	0
beta1	Na<+> Np +IV (OH)4(CO3)<2->	2
beta2	Na<+> Np +IV (OH)4(CO3)<2->	0
cphi	Na<+> Np +IV (OH)4(CO3)<2->	0
beta0	Na<+> Np +IV (OH)4(CO3)2<4->	1
beta1	Na<+> Np +IV (OH)4(CO3)2<4->	13
beta2	Na<+> Np +IV (OH)4(CO3)2<4->	0
cphi	Na<+> Np +IV (OH)4(CO3)2<4->	0
lambda	Na<+> Np +IV (OH)4<0>	0
beta0	Np +IV (OH)<3+> Cl<->	0.6
beta1	Np +IV (OH)<3+> Cl<->	5.9

Coefficient	Species	Value
beta2	Np +IV (OH)<3+> Cl<->	0
cphi	Np +IV (OH)<3+> Cl<->	0
beta0	Np +IV (OH)2<2+> Cl<->	0.23
beta1	Np +IV (OH)2<2+> Cl<->	1.9
beta2	Np +IV (OH)2<2+> Cl<->	0
cphi	Np +IV (OH)2<2+> Cl<->	0
beta0	Np +IV (OH)3<+> Cl<->	0.08
beta1	Np +IV (OH)3<+> Cl<->	0.39
beta2	Np +IV (OH)3<+> Cl<->	0
cphi	Np +IV (OH)3<+> Cl<->	0
beta0	Np +IV (OH)4<0> Cl<->	0
beta0	Np +IV <4+> Cl<->	1.32
beta1	Np +IV <4+> Cl<->	13.5
beta2	Np +IV <4+> Cl<->	0
cphi	Np +IV <4+> Cl<->	0
theta	(Pu +V O2)(CO3)<-> Cl<->	-0.21
theta	(Pu +V O2)(CO3)3<5-> (CO3)<2->	-0.83
theta	(Pu +V O2)(CO3)3<5-> Cl<->	-0.26
lambda	(Pu +V O2)(OH)<0> Cl<->	0
theta	(Pu +V O2)<+> Ca<2+>	0.05
beta0	(Pu +V O2)<+> Cl<->	0.1415
beta1	(Pu +V O2)<+> Cl<->	0.281
beta2	(Pu +V O2)<+> Cl<->	0
cphi	(Pu +V O2)<+> Cl<->	0
theta	(Pu +V O2)<+> Mg<2+>	0.05
lambda	(Pu +V O2)(CO3)<0> Cl<->	0
beta0	(Pu +V O2)(OH)<+> Cl<->	0.15
beta1	(Pu +V O2)(OH)<+> Cl<->	0.3
beta2	(Pu +V O2)(OH)<+> Cl<->	0
cphi	(Pu +V O2)(OH)<+> Cl<->	0
lambda	(Pu +V O2)(OH)2<0> (SO4)<2->	0
lambda	(Pu +V O2)(OH)2<0> Cl<->	0
beta0	(Pu +V O2)<2+> Cl<->	0.42735
beta1	(Pu +V O2)<2+> Cl<->	1.644
beta2	(Pu +V O2)<2+> Cl<->	0
cphi	(Pu +V O2)<2+> Cl<->	-0.03686
beta0	(Pu +V O2)2(OH)2<2+> Cl<->	0.5
beta1	(Pu +V O2)2(OH)2<2+> Cl<->	1.6
beta2	(Pu +V O2)2(OH)2<2+> Cl<->	0
cphi	(Pu +V O2)2(OH)2<2+> Cl<->	0
beta0	(Pu +V O2)3(OH)5<+> Cl<->	0.31
beta1	(Pu +V O2)3(OH)5<+> Cl<->	0.3
beta2	(Pu +V O2)3(OH)5<+> Cl<->	0
cphi	(Pu +V O2)3(OH)5<+> Cl<->	0
beta0	K<+> (Pu +V O2)(CO3)<->	0.1
beta1	K<+> (Pu +V O2)(CO3)<->	0.34
beta2	K<+> (Pu +V O2)(CO3)<->	0
cphi	K<+> (Pu +V O2)(CO3)<->	0
beta2	K<+> (Pu +V O2)(CO3)2<3->	0
cphi	K<+> (Pu +V O2)(CO3)2<3->	0
beta0	K<+> (Pu +V O2)(CO3)3<5->	1.8

Coefficient	Species	Value
beta1	K<+> (Pu +V O2)(CO3)3<5->	22.7
beta2	K<+> (Pu +V O2)(CO3)3<5->	-95.1
cphi	K<+> (Pu +V O2)(CO3)3<5->	-0.219
lambda	K<+> (Pu +V O2)(OH)2<0>	0
beta0	K<+> Pu +IV (CO3)4<4->	1
beta1	K<+> Pu +IV (CO3)4<4->	13
beta2	K<+> Pu +IV (CO3)4<4->	0
cphi	K<+> Pu +IV (CO3)4<4->	0
beta0	K<+> Pu +IV (CO3)5<6->	1.5
beta1	K<+> Pu +IV (CO3)5<6->	31.3
beta2	K<+> Pu +IV (CO3)5<6->	0
cphi	K<+> Pu +IV (CO3)5<6->	0
beta0	K<+> Pu +IV (OH)2(CO3)2<2->	0
beta1	K<+> Pu +IV (OH)2(CO3)2<2->	2
beta2	K<+> Pu +IV (OH)2(CO3)2<2->	0
cphi	K<+> Pu +IV (OH)2(CO3)2<2->	0
beta0	K<+> Pu +IV (OH)4(CO3)<2->	0
beta1	K<+> Pu +IV (OH)4(CO3)<2->	2
beta2	K<+> Pu +IV (OH)4(CO3)<2->	0
cphi	K<+> Pu +IV (OH)4(CO3)<2->	0
beta0	K<+> Pu +IV (OH)4(CO3)2<4->	1
beta1	K<+> Pu +IV (OH)4(CO3)2<4->	13
beta2	K<+> Pu +IV (OH)4(CO3)2<4->	0
cphi	K<+> Pu +IV (OH)4(CO3)2<4->	0
beta0	Mg<2+> (Pu +V O2)(CO3)<->	0.4
beta1	Mg<2+> (Pu +V O2)(CO3)<->	1.7
beta2	Mg<2+> (Pu +V O2)(CO3)<->	0
cphi	Mg<2+> (Pu +V O2)(CO3)<->	0
lambda	Mg<2+> (Pu +V O2)(OH)<0>	0
beta2	Mg<2+> (Pu +V O2)(OH)2<->	0
cphi	Mg<2+> (Pu +V O2)(OH)2<->	0
lambda	Mg<2+> (Pu +VI O2)(OH)2<0>	0
lambda	Mg<2+> Pu +III (OH)3<0>	0
lambda	Mg<2+> Pu +IV (OH)4<0>	0
beta0	Na<+> (Pu +V O2)(CO3)<->	0.1
beta1	Na<+> (Pu +V O2)(CO3)<->	0.34
beta2	Na<+> (Pu +V O2)(CO3)<->	0
cphi	Na<+> (Pu +V O2)(CO3)<->	0
beta2	Na<+> (Pu +V O2)(CO3)2<3->	0
cphi	Na<+> (Pu +V O2)(CO3)2<3->	0
beta0	Na<+> (Pu +V O2)(CO3)3<5->	1.8
beta1	Na<+> (Pu +V O2)(CO3)3<5->	22.7
beta2	Na<+> (Pu +V O2)(CO3)3<5->	0
cphi	Na<+> (Pu +V O2)(CO3)3<5->	0
lambda	Na<+> (Pu +V O2)(OH)<0>	0
beta1	Na<+> (Pu +V O2)(OH)2<->	0
beta2	Na<+> (Pu +V O2)(OH)2<->	0
cphi	Na<+> (Pu +V O2)(OH)2<->	0
lambda	Na<+> (Pu +VI O2)(CO3)<0>	0
beta0	Na<+> (Pu +VI O2)(CO3)2<2->	0.212
beta1	Na<+> (Pu +VI O2)(CO3)2<2->	2.5

Coefficient	Species	Value
beta2	Na<+> (Pu +VI O2)(CO3)2<2->	0
cphi	Na<+> (Pu +VI O2)(CO3)2<2->	0
beta0	Na<+> (Pu +VI O2)(CO3)3<4->	1.25
beta1	Na<+> (Pu +VI O2)(CO3)3<4->	11.6
beta2	Na<+> (Pu +VI O2)(CO3)3<4->	0
cphi	Na<+> (Pu +VI O2)(CO3)3<4->	0
lambda	Na<+> (Pu +VI O2)(OH)2<0>	0
beta2	Na<+> Pu +III (CO3)2<->	0
beta2	Na<+> Pu +III (CO3)3<3->	0
beta2	Na<+> Pu +III (CO3)4<5->	0
lambda	Na<+> Pu +III (OH)3<0>	0
beta0	Na<+> Pu +IV (CO3)4<4->	1
beta1	Na<+> Pu +IV (CO3)4<4->	13
beta2	Na<+> Pu +IV (CO3)4<4->	0
cphi	Na<+> Pu +IV (CO3)4<4->	0
beta0	Na<+> Pu +IV (CO3)5<6->	1.5
beta1	Na<+> Pu +IV (CO3)5<6->	31.3
beta2	Na<+> Pu +IV (CO3)5<6->	0
cphi	Na<+> Pu +IV (CO3)5<6->	0
beta0	Na<+> Pu +IV (OH)2(CO3)2<2->	0
beta1	Na<+> Pu +IV (OH)2(CO3)2<2->	2
beta2	Na<+> Pu +IV (OH)2(CO3)2<2->	0
cphi	Na<+> Pu +IV (OH)2(CO3)2<2->	0
beta0	Na<+> Pu +IV (OH)4(CO3)<2->	0
beta1	Na<+> Pu +IV (OH)4(CO3)<2->	2
beta2	Na<+> Pu +IV (OH)4(CO3)<2->	0
cphi	Na<+> Pu +IV (OH)4(CO3)<2->	0
beta0	Na<+> Pu +IV (OH)4(CO3)2<4->	1
beta1	Na<+> Pu +IV (OH)4(CO3)2<4->	13
beta2	Na<+> Pu +IV (OH)4(CO3)2<4->	0
cphi	Na<+> Pu +IV (OH)4(CO3)2<4->	0
lambda	Na<+> Pu +IV (OH)4<0>	0
beta0	Pu +III (OH)<2+> Cl<->	0.055
beta1	Pu +III (OH)<2+> Cl<->	1.81
beta2	Pu +III (OH)<2+> Cl<->	0
cphi	Pu +III (OH)<2+> Cl<->	0
beta2	Pu +III (OH)2<+> Cl<->	0
cphi	Pu +III (OH)2<+> Cl<->	0
lambda	Pu +III (OH)3<0> Cl<->	0
theta	Pu +III <3+> Ca<2+>	0.2
beta0	Pu +III <3+> Cl<->	0.5856
beta1	Pu +III <3+> Cl<->	5.6
beta2	Pu +III <3+> Cl<->	0
cphi	Pu +III <3+> Cl<->	-0.019
theta	Pu +III <3+> K<+>	0.1
theta	Pu +III <3+> Mg<2+>	0.2
theta	Pu +III <3+> Na<+>	0.1
beta2	Pu +III Cl<2+> Cl<->	0
beta2	Pu +III Cl2<+> Cl<->	0
beta0	Pu +IV (OH)<3+> Cl<->	0.6
beta1	Pu +IV (OH)<3+> Cl<->	5.9

Coefficient	Species	Value
beta2	Pu +IV (OH)<3+> Cl<->	0
cphi	Pu +IV (OH)<3+> Cl<->	0
beta0	Pu +IV (OH)2<2+> Cl<->	0.23
beta1	Pu +IV (OH)2<2+> Cl<->	1.9
beta2	Pu +IV (OH)2<2+> Cl<->	0
cphi	Pu +IV (OH)2<2+> Cl<->	0
beta0	Pu +IV (OH)3<+> Cl<->	0.08
beta1	Pu +IV (OH)3<+> Cl<->	0.39
beta2	Pu +IV (OH)3<+> Cl<->	0
cphi	Pu +IV (OH)3<+> Cl<->	0
lambda	Pu +IV (OH)4<0> Cl<->	0
beta0	Pu +IV <4+> Cl<->	1.32
beta1	Pu +IV <4+> Cl<->	13.5
beta2	Pu +IV <4+> Cl<->	0
cphi	Pu +IV <4+> Cl<->	0
beta2	PuCO3<+> Cl<->	0
theta	(Am +V O2)(CO3)<-> Cl<->	-0.21
theta	(Am +V O2)(CO3)2<3-> Cl<->	-0.26
theta	(Am +V O2)(CO3)3<5-> (CO3)<2->	-0.83
theta	(Am +V O2)(CO3)3<5-> Cl<->	-0.26
lambda	(Am +V O2)(OH)<0> Cl<->	0
theta	(Am +V O2)<+> Ca<2+>	0.05
beta0	(Am +V O2)<+> Cl<->	0.1415
beta1	(Am +V O2)<+> Cl<->	0.281
beta2	(Am +V O2)<+> Cl<->	0
cphi	(Am +V O2)<+> Cl<->	0
theta	(Am +V O2)<+> Mg<2+>	0.05
beta0	Am +III (CO3)<+> Cl<->	-0.072
beta1	Am +III (CO3)<+> Cl<->	0.403
beta2	Am +III (CO3)<+> Cl<->	0
cphi	Am +III (CO3)<+> Cl<->	0.0388
beta0	Am +III (OH)<2+> Cl<->	0.055
beta1	Am +III (OH)<2+> Cl<->	1.81
beta2	Am +III (OH)<2+> Cl<->	0
cphi	Am +III (OH)<2+> Cl<->	0
beta0	Am +III (OH)2<+> Cl<->	-0.414
beta1	Am +III (OH)2<+> Cl<->	0
beta2	Am +III (OH)2<+> Cl<->	0
cphi	Am +III (OH)2<+> Cl<->	0
lambda	Am +III (OH)3<0> Cl<->	-0.2
beta0	Am +III <3+> (SO4)<2->	1.792
beta1	Am +III <3+> (SO4)<2->	15.044
beta2	Am +III <3+> (SO4)<2->	0
cphi	Am +III <3+> (SO4)<2->	-0.6
theta	Am +III <3+> Ca<2+>	0.2
beta0	Am +III <3+> Cl<->	0.5856
beta1	Am +III <3+> Cl<->	5.6
beta2	Am +III <3+> Cl<->	0
cphi	Am +III <3+> Cl<->	-0.016
theta	Am +III <3+> K<+>	0.1
theta	Am +III <3+> Mg<2+>	0.2

Coefficient	Species	Value
theta	Am +III <3+> Na<+>	0.1
theta	Am +III Cl<2+> Ca<2+>	-0.014
beta0	Am +III Cl<2+> Cl<->	0.593
beta1	Am +III Cl<2+> Cl<->	3.15
beta2	Am +III Cl<2+> Cl<->	0
cphi	Am +III Cl<2+> Cl<->	-0.006
theta	Am +III Cl<2+> Mg<2+>	-0.014
theta	Am +III Cl2<+> Ca<2+>	-0.196
beta0	Am +III Cl2<+> Cl<->	0.516
beta1	Am +III Cl2<+> Cl<->	1.75
beta2	Am +III Cl2<+> Cl<->	0
cphi	Am +III Cl2<+> Cl<->	0.01
theta	Am +III Cl2<+> Mg<2+>	-0.196
beta0	K<+> (Am +V O2)(CO3)<->	0.1
beta1	K<+> (Am +V O2)(CO3)<->	0.34
beta2	K<+> (Am +V O2)(CO3)<->	0
cphi	K<+> (Am +V O2)(CO3)<->	0
beta0	K<+> (Am +V O2)(CO3)2<3->	0.48
beta1	K<+> (Am +V O2)(CO3)2<3->	4.4
beta2	K<+> (Am +V O2)(CO3)2<3->	0
cphi	K<+> (Am +V O2)(CO3)2<3->	0
beta0	K<+> (Am +V O2)(CO3)3<5->	1.8
beta1	K<+> (Am +V O2)(CO3)3<5->	22.7
beta2	K<+> (Am +V O2)(CO3)3<5->	-95.1
cphi	K<+> (Am +V O2)(CO3)3<5->	-0.219
beta0	Mg<2+> (Am +V O2)(CO3)<->	0.4
beta1	Mg<2+> (Am +V O2)(CO3)<->	1.7
beta2	Mg<2+> (Am +V O2)(CO3)<->	0
cphi	Mg<2+> (Am +V O2)(CO3)<->	0
lambda	Mg<2+> (Am +V O2)(OH)<0>	0
beta2	Mg<2+> (Am +V O2)(OH)2<->	0
cphi	Mg<2+> (Am +V O2)(OH)2<->	0
beta0	Na<+> (Am +V O2)(CO3)<->	0.1
beta1	Na<+> (Am +V O2)(CO3)<->	0.34
beta2	Na<+> (Am +V O2)(CO3)<->	0
cphi	Na<+> (Am +V O2)(CO3)<->	0
beta0	Na<+> (Am +V O2)(CO3)2<3->	0.48
beta1	Na<+> (Am +V O2)(CO3)2<3->	4.4
beta2	Na<+> (Am +V O2)(CO3)2<3->	0
cphi	Na<+> (Am +V O2)(CO3)2<3->	0
beta0	Na<+> (Am +V O2)(CO3)3<5->	1.8
beta1	Na<+> (Am +V O2)(CO3)3<5->	22.7
beta2	Na<+> (Am +V O2)(CO3)3<5->	0
cphi	Na<+> (Am +V O2)(CO3)3<5->	0
lambda	Na<+> (Am +V O2)(OH)<0>	0
beta1	Na<+> (Am +V O2)(OH)2<->	0
beta2	Na<+> (Am +V O2)(OH)2<->	0
cphi	Na<+> (Am +V O2)(OH)2<->	0
beta0	Na<+> Am +III (CO3)2<->	-0.24
beta1	Na<+> Am +III (CO3)2<->	0.224
beta2	Na<+> Am +III (CO3)2<->	0

Coefficient	Species	Value
cphi	Na<+> Am +III (CO3)2<->	0.0284
beta0	Na<+> Am +III (CO3)3<3->	0.125
beta1	Na<+> Am +III (CO3)3<3->	4.73
beta2	Na<+> Am +III (CO3)3<3->	0
cphi	Na<+> Am +III (CO3)3<3->	0.0007
beta2	Na<+> Am +III (CO3)4<5->	0
lambda	Na<+> Am +III (OH)3<0>	0
beta0	Cm(CO3)<+> Cl<->	-0.072
beta1	Cm(CO3)<+> Cl<->	0.403
beta2	Cm(CO3)<+> Cl<->	0
cphi	Cm(CO3)<+> Cl<->	0.0388
beta0	Cm(OH)<2+> Cl<->	0.055
beta1	Cm(OH)<2+> Cl<->	1.81
beta2	Cm(OH)<2+> Cl<->	0
cphi	Cm(OH)<2+> Cl<->	0
beta0	Cm(OH)2<+> Cl<->	-0.414
beta1	Cm(OH)2<+> Cl<->	0
beta2	Cm(OH)2<+> Cl<->	0
cphi	Cm(OH)2<+> Cl<->	0
lambda	Cm(OH)3<0> Cl<->	0
beta0	Cm(SO4)<+> Cl<->	-0.091
beta1	Cm(SO4)<+> Cl<->	-0.39
beta2	Cm(SO4)<+> Cl<->	0
cphi	Cm(SO4)<+> Cl<->	0.048
beta0	Cm<3+> (SO4)<2->	1.792
beta1	Cm<3+> (SO4)<2->	15.044
beta2	Cm<3+> (SO4)<2->	0
cphi	Cm<3+> (SO4)<2->	-0.6
theta	Cm<3+> Ca<2+>	0.2
beta0	Cm<3+> Cl<->	0.5856
beta1	Cm<3+> Cl<->	5.6
beta2	Cm<3+> Cl<->	0
cphi	Cm<3+> Cl<->	-0.016
theta	Cm<3+> K<+>	0.1
theta	Cm<3+> Mg<2+>	0.2
theta	Cm<3+> Na<+>	0.1
theta	CmCl<2+> Ca<2+>	-0.014
beta0	CmCl<2+> Cl<->	0.593
beta1	CmCl<2+> Cl<->	3.15
beta2	CmCl<2+> Cl<->	0
cphi	CmCl<2+> Cl<->	-0.006
theta	CmCl<2+> Mg<2+>	-0.014
theta	CmCl2<+> Ca<2+>	-0.196
beta0	CmCl2<+> Cl<->	0.516
beta1	CmCl2<+> Cl<->	1.75
beta2	CmCl2<+> Cl<->	0
cphi	CmCl2<+> Cl<->	0.01
theta	CmCl2<+> Mg<2+>	-0.196
beta0	Na<+> Cm(CO3)2<->	-0.24
beta1	Na<+> Cm(CO3)2<->	0.224
beta2	Na<+> Cm(CO3)2<->	0

Coefficient	Species	Value
cphi	Na<+> Cm(CO3)2<->	0.0284
beta0	Na<+> Cm(CO3)3<3->	0.125
beta1	Na<+> Cm(CO3)3<3->	4.73
beta2	Na<+> Cm(CO3)3<3->	0
cphi	Na<+> Cm(CO3)3<3->	0.0007
beta0	Na<+> Cm(CO3)4<5->	2.022
beta1	Na<+> Cm(CO3)4<5->	19.22
beta2	Na<+> Cm(CO3)4<5->	0
cphi	Na<+> Cm(CO3)4<5->	-0.305
lambda	Na<+> Cm(OH)3<0>	0
beta0	Na<+> Cm(SO4)2<->	-0.354
beta1	Na<+> Cm(SO4)2<->	-0.4
beta2	Na<+> Cm(SO4)2<->	0
cphi	Na<+> Cm(SO4)2<->	0.051

List of Figures

- Fig. 3.1 Schematic concept for the evolution of solutions intruding into the emplacement area of a repository for heat-generating waste in salt
- Fig. 3.2 The five-component system NaCl-KCl-MgCl₂-Na₂SO₄-H₂O at 25 °C and 1 bar at NaCl saturation /BRA 71/
- Fig. A1.1 C-speciation in Gipshut-solution: top = p(CO₂) = 0.1 bar (GRS), centre = p(CO₂) = 0.01 bar (GRS) and bottom = /KIE 00/
- Fig. A1.2 C-speciation in Q-Brine: top = p(CO₂) = 0.01 bar (GRS), centre = p(CO₂) = 0.1 bar (GRS) and bottom = /KIE 00/
- Fig. A1.3 Solubility of Am^(+III) in Gipshut-solution with p(CO₂) = 0 bar, top = this report (GRS) and bottom = /KIE 00/
- Fig. A1.4 Solubility of Am^(+III) in Gipshut-solution with p(CO₂) = 0.0003 bar, top = this report (GRS) and bottom = /KIE 00/
- Fig. A1.5 Solubility of Am^(+III) in Q-brine with p(CO₂) = 0 bar, top = this report (GRS) and bottom = /KIE 00. Fig. 18/
- Fig. A1.6 Solubility of Np^(+V) in Gipshut-solution with p(CO₂) = 0 bar and (Np^(+V)O₂)(OH)(am,aged) as solubility limiting phase, top = this report (GRS) and bottom = /KIE 00/
- Fig. A1.7 Solubility of Np^(+V) in Gipshut-solution with p(CO₂) = 0 bar and Np^(+V)₂O₅(c) as solubility limiting phase (compare with result from the INE-report as given in the bottom of Fig. 7.8 /KIE 00/)
- Fig. A1.8 Solubility of Np^(+V) in Gipshut-solution with p(CO₂) = 0.0003 bar and (Np^(+V)O₂)(OH)(am,aged) as solubility limiting phase, top = this report (GRS) and bottom = /KIE 00/
- Fig. A1.9 Np^(+V) in Gipshut-solution with p(CO₂) = 0.0003 bar and (Np^(+V)O₂)(OH)(am,aged) as solubility limiting phase: solid phase activities, top = oceanic carbonates included and bottom = oceanic carbonates eliminated
- Fig. A1.10 Solubility of Np^(+V) in Gipshut-solution with p(CO₂) = 0.0003 bar and Np^(+V)₂O₅(c) as solubility limiting phase (compare with result from the INE-report as given in the bottom of Fig. 7.9 /KIE 00/)
- Fig. A1.11 Solid phase activities in the system Np^(+V) in Gipshut-solution with p(CO₂) = 0.0003 bar and Np^(+V)₂O₅(c) as solubility limiting phase (oceanic carbonates eliminated)

- Fig. A1.12 Solubility of $\text{Np}^{(+IV)}$ in Gipshut-solution with $p(\text{CO}_2) = 0.0003$ bar and $\text{Np}^{(+IV)}(\text{OH})_4(\text{am})$ as solubility limiting phase, top = this report (GRS) and bottom = /KIE 00/
- Fig. A1.13 Solubility of $\text{Pu}^{(+IV)}$ in 0.5 M NaCl-solution at various CO_2 -partial pressures and $\text{Pu}^{(+IV)}(\text{OH})_4(\text{am})$ as solubility limiting phase, top = this report (GRS) and bottom = /KIE 00/
- Fig. A1.14 Solubility of $\text{U}^{(+VI)}$ in Gipshut-solution with $p(\text{CO}_2) = 0.0003$ bar, top = this report (GRS) and bottom = /KIE 00/
- Fig. A1.15 Solubility of $\text{U}^{(+VI)}$ in Gipshut-solution with $p(\text{CO}_2) = 0.0003$ bar; U|+VI|-sulphato-complexes were eliminated
- Fig. A1.16 Solid phase activities in the calculation of solubility of $\text{U}^{(+VI)}$ in Gipshut-solution with $p(\text{CO}_2) = 0.0003$ bar
- Fig. A1.17 Solubility of $\text{U}^{(+VI)}$ in Q-Brine (without CO_2), top = this report (GRS) and bottom = /KIE 00/
- Fig. A1.18 Solid phase activities in the calculation of solubility of $\text{U}^{(+VI)}$ in Q-Brine (without CO_2)

List of Tables

Tab. 3.1	Priority classes of fission and activation products according to /HOS 85/
Tab. 3.2	Considered actinides and decay products according to /HOS 85/
Tab. 3.3	Stable crystallizing salts in the hexary oceanic salt system; after /BRA 71/ and /EUG 80/
Tab. 3.4	Selected components in container materials for HLW and Pollux cask in wt.-% /KTA 88/
Tab. 3.5	Jänecke coordinates of invariant points (IP) in the halite saturated six-component system Na-K-Mg-Ca-SO ₄ -Cl-H ₂ O at 25°C and 1 bar /EUG 80/
Tab. 3.6	Capabilities and features of the described geochemical codes
Tab. 4.1	Principal pattern of considered systems
Tab. 4.2	Composition of R7T7 glass matrix /GRA 99/
Tab. 4.3	Chemical composition of spent fuel as used for the calculations – The element content is referred to 1 kg of waste
Tab. 4.4	pH and E _H values calculated with ChemApp for the considered systems, representing the basis for the solubility calculations; values in brackets represent systems with metallic iron
Tab. 5.1	Solubility data for C at different geochemical conditions derived from previous studies
Tab. 5.2	Solubility data for Mo at different geochemical conditions
Tab. 5.3	Solubility data for Ni at different geochemical conditions
Tab. 5.4	Solubility data for Nb at different geochemical conditions
Tab. 5.5	Solubility data for Pd at different geochemical conditions
Tab. 5.6	Solubility data for Sm at different geochemical conditions
Tab. 5.7	Solubility data for Se at different geochemical conditions
Tab. 5.8	Solubility data for Sr at different geochemical conditions

Tab. 5.9	Solubility data for Tc at different geochemical conditions
Tab. 5.10	Solubility data for Sn at different geochemical conditions
Tab. 5.11	Solubility data for Zr at different geochemical conditions
Tab. 5.12	Solubility data for Am at different geochemical conditions derived from previous studies
Tab. 5.13	Solubility data for Np at different geochemical conditions derived from previous studies
Tab. 5.14	Solubility data for Pa at different geochemical conditions derived from previous studies
Tab. 5.15	Solubility data for Pu at different geochemical conditions
Tab. 5.16	Solubility data for Ra at different geochemical conditions
Tab. 5.17	Solubility data for Th at different geochemical conditions derived from previous studies
Tab. 5.18	Solubility data for U at different geochemical conditions derived from previous studies
Tab. 6.1	Proposed solubility determining solid phase, calculated solubility limit, relevance for long term Safety (LTS), uncertainty and R&D needs for elements with relevant radionuclides (see text for explanation)
Tab. A1.1	Comparison of three model solutions as given from INE /KIE 00/, and calculated for this report with CHEMAPP (CA) and EQ3/6, with CA: pH and density calculated – Concentration unit: mol (1000 mol H ₂ O) ⁻¹
Tab. A1.2	Gipshut-solution with CO ₂
Tab. A1.3	Q-brine with CO ₂
Tab. A1.4	Comparison of solubility constants used in /KIE 00/ and this report
Tab. A1.5	Solubility of Americium in Gipshut-solution
Tab. A1.6	Solubility of Americium in Q-Brine-solution
Tab. A1.7	Solubility of Neptunium(+V) in Gipshut-solution

Tab. A1.8 Solubility of Neptunium(+IV) in Gipsht-solution

Tab. A1.9 Solubility of Plutonium(+IV) in Gipsht-solution

Tab. A1.10 Solubility of Uranium(+VI) with Gipsht-solution

Tab. A1.11 Solubility of Uranium(+VI) in Q-Brine-solution without CO₂

Tab. A2.1 Pitzer coefficients for actinides and Tc adopted from /ALT 04/

**Gesellschaft für Anlagen-
und Reaktorsicherheit
(GRS) gGmbH**

Schwertnergasse 1
50667 Köln
Telefon +49 221 2068-0
Telefax +49 221 2068-888

Boltzmannstraße 14
85748 Garching b. München
Telefon +49 89 32004-0
Telefax +49 89 32004-300

Kurfürstendamm 200
10719 Berlin
Telefon +49 30 88589-0
Telefax +49 30 88589-111

Theodor-Heuss-Straße 4
38122 Braunschweig
Telefon +49 531 8012-0
Telefax +49 531 8012-200

www.grs.de